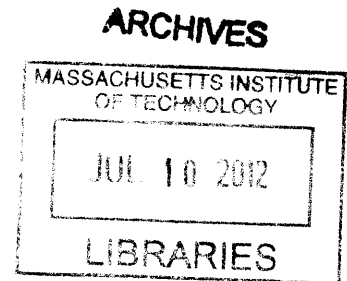


# Space Suit Simulator for Partial Gravity Extravehicular Activity Experimentation and Training

by

Andrea L. Gilkey

B.S. in Biological Systems Engineering  
University of Nebraska-Lincoln, 2010



Submitted to the Department of Aeronautics and Astronautics  
in Partial Fulfillment of the Requirements for the Degree of  
Master of Science in Aeronautics and Astronautics  
at the  
MASSACHUSETTS INSTITUTE OF TECHNOLOGY  
June 2012

©2012 Massachusetts Institute of Technology. All rights reserved.

Author: .....  
Department of Aeronautics and Astronautics  
May 24, 2012

Certified by: .....  
Dava J. Newman, Ph.D.  
Professor, MacVicar Faculty Fellow  
Department of Aeronautics and Astronautics  
Thesis Supervisor

Accepted by: .....  
Eytan H. Modiano  
Professor of Aeronautics and Astronautics  
Chair, Graduate Program Committee



# **Space Suit Simulator for Partial Gravity Extravehicular Activity Experimentation and Training**

by

Andrea L. Gilkey

Submitted to the Department of Aeronautics and Astronautics, May 24, 2012, in partial fulfillment of the requirements for the degree of Master of Science in Aeronautics and Astronautics

## **Abstract**

During human space exploration, mobility is extremely limited when working inside a pressurized space suit. Astronauts perform extensive training on Earth to become accustomed to space suit-imposed high joint torques and limited range of motion. Space suit experimentation is difficult for researchers because the current suit is expensive, bulky, heavy, hard to don/doff, and in very short supply. The main objective of this thesis is to develop a wearable space suit simulator (S3) exoskeleton that can mimic the joint torques and reduced mobility of various pressurized space suit designs. A space suit simulator exoskeleton is a novel method for simulating joint torques while offering a lightweight, portable, and easily accessible design.

This thesis describes early work towards development of the S3 exoskeleton. A space suit joint database was developed, which includes joint torque and angle range of motion information for multiple pressurized space suits, degrees of freedom, and pressurization levels. The space suit joint database was used to set the joint torque and angle range of motion requirements for the S3 exoskeleton.

Additionally, various actuators that have been used in previous exoskeleton designs were compared according to weight and bulk characteristics to select actuators for the S3 exoskeleton. The conceptual designs of the S3 knee and hip components are presented. Finally, the S3 computer simulation is described, which allows users to input the geometries and locations of the S3 exoskeleton components. The computer simulation outputs the space suit hysteresis curves to compare S3 joint design performance to actual space suit performance. Feasible design solutions for the S3 exoskeleton joints can be determined from designs that minimize the root-mean-square error of the hysteresis curves.

Thesis Supervisor: Dava J. Newman

Title: Professor of Aeronautics and Astronautics



## Acknowledgements

First, I would like to thank my advisors, Professor Dava Newman and Dr. Jessica Duda. Thank you for giving me the incredible opportunity to study at MIT and to work with Aurora Flight Sciences these past two years. Thank you for your guidance and encouragement on the space suit simulator project, and for supporting me personally and professionally. Thank you, Professor Jeff Hoffman, for your invaluable insights on the S3 project, and for meeting with me while Dava was on sabbatical.

I would like to thank the S3 team at Aurora: Roedolph Opperman, Charlie De Vivero, and Morris Vanegas. I am honored to have had the opportunity to work with such a talented and fun group. Thank you to Professor Grant Schaffner at the University of Cincinnati and the folks at NASA JSC for S3 feedback and space suit simulator knowledge. Thank you, Kelly Gilkey and Gail Perusek at NASA GRC, for your S3 suggestions and support.

Thank you, Sally Chapman and Quentin Alexander, for your help with all of my logistical and administrative questions. Thank you to all faculty and staff in the Man Vehicle Lab for your advice and support.

Thank you to all of the students in the MVL, I have learned a great deal from you and I have also thoroughly enjoyed my time here because of you. Thank you to my friends for family lunches and weekend get-togethers. Finally, I would like to thank my family for their unending support and encouragement.



## Table of Contents

Abstract .....	3
Acknowledgements .....	5
Table of Contents .....	7
List of Figures .....	9
List of Tables .....	11
List of Acronyms .....	13
<b>Chapter 1: Introduction .....</b>	<b>15</b>
1.1 Motivation .....	15
1.2 Objectives .....	17
1.3 Road Map.....	19
<b>Chapter 2: Background .....</b>	<b>21</b>
2.1 Overview .....	21
2.2 Space Suit Joint Torque and Mobility Testing .....	21
2.2.1 Empty Pressurized Suit Testing.....	22
2.2.2 Human-in-the-Suit Testing .....	24
2.2.3 Robot Space Suit Testing .....	26
2.3 Space Suit Simulators.....	28
2.3.1 Analog Space Suits .....	28
2.3.2 Prototype Space Suits .....	29
2.4 Exoskeleton Review.....	32
2.4.1 Hydraulic Actuators.....	32
2.4.2 Pneumatic Actuators.....	33
2.4.3 Magnetorheological (MR) Fluid Actuators .....	33
2.4.4 Electric Actuators.....	34
2.5 Summary.....	35
<b>Chapter 3: Space Suit Simulator.....</b>	<b>37</b>
3.1 Overview .....	37
3.2 Space Suit Joint Database.....	37
3.2.1 Joint Convention .....	37
3.2.2 Space Suit Joint Database Methods .....	41
3.2.3 Range of Motion and Torque Requirements.....	42
3.3 Actuator Selection .....	43
3.4 Conceptual Design .....	49
3.5 Summary .....	57
<b>Chapter 4: Space Suit Simulator (S3) Computer Simulation .....</b>	<b>59</b>
4.1 S3 Simulation Introduction and Capabilities .....	59
4.2 Example Space Suit Simulation.....	67
4.3 Implementation of S3 Knee Design.....	70
4.4 S3 Knee Joint Design Results .....	73
4.5 Summary.....	90

<b>Chapter 5: Conclusions .....</b>	<b>93</b>
5.1 Overview .....	93
5.2 Space Suit Joint Database.....	94
5.3 Actuator Comparison .....	94
5.4 Conceptual Design .....	95
5.5 Computer Simulation .....	96
5.6 Moving Forward.....	97
5.6.1 Key Challenges.....	97
5.6.2 Recommendations for Improvement.....	98
5.6.3 Directions for Future Research .....	99
5.7 Final Conclusions .....	100
<b>Bibliography.....</b>	<b>103</b>
<b>Appendix A: Space Suit Joint Database .....</b>	<b>107</b>
<b>Appendix B: S3 Designs Implemented in Computer Simulator .....</b>	<b>117</b>



## List of Figures

### Chapter 1

Figure 1.1 Photo of the hatch of the Voskhod 2 taken at Russia's Energia Spaceflight Museum [Courtesy of Gui Trotti].....	16
---	----

### Chapter 2

Figure 2.1 (a) MIT space suit test rig, shown with the EMU arm specimen resting, and (b) flexed to 90 deg [Holschuh et al., 2009] .....	23
Figure 2.2 Torque vs. angle for the EMU elbow, shoulder, and knee [Dionne, 1991] .....	23
Figure 2.3 Primus RS <sup>(TM)</sup> collecting unpressurized ACES elbow torque data [Matty & Aitchison, 2009]....	25
Figure 2.4 (a) LIDO Multi-Joint II isokinetic dynamometer bench drawing and (b) elbow flexion/extension setup [Morgan et al., 1996] .....	26
Figure 2.5 (a) Robot Space Suit Tester (RSST), (b) RSST with EMU installed [Schmidt et al., 2001] .....	27
Figure 2.6 Knee flexion joint of the space suit simulator [Newman et al., 2007] .....	29
Figure 2.7 Mark III suit [www.nasa.gov] .....	30
Figure 2.8 I-suit [Graziosi & Lee, 2003] .....	31
Figure 2.9 David Clark Company D-suit [Thomas & McMann, 2006] .....	32
Figure 2.10 Series elastic actuator [Pratt et al., 2002] .....	34
Figure 2.11 Honda exoskeleton legs [Ikeuchi et al., 2009] .....	35

### Chapter 3

Figure 3.1 Spatial coordinate system used for all data and analysis [Winter, 1990] .....	38
Figure 3.2 Shoulder flexion joint convention from (a) Industry [Ripps et al., 2011], (b) NASA [Morgan et al., 1996], (c) Academia [Schmidt et al., 2001], (d) Human biomechanics [NASA-STD-3000, 1994] .....	39
Figure 3.3 Space Suit Simulator (S3) Joint Convention.....	40
Figure 3.4 A snapshot of the space suit joint database depicting minimum and maximum knee and elbow torques achieved for various pressurized space suits.....	42
Figure 3.5 Qualitative comparison of actuators, (a) Series elastic actuators (actuator length 45.5 cm (18 in), diameter 5.8 cm (2.3 in)) [Pratt et al., 2004], (b) Electric motors (exoskeleton height from ground to shoulders 1600 mm (63 in)) [Suzuki et al., 2007], (c) MR fluid actuator [Chen et al., 2010], (d) Hydraulic actuator (fits soldiers with heights between 1.6 m and 1.9 m (5 ft 4 in and 6 ft 2 in)) [Lockheed Martin, 2008], (e) Pneumatic actuator [Ferris et al., 2005] .....	47
Figure 3.6 (a) NASA GRC eZLS, (b) NASA JSC ARGOS [www.nasa.gov] .....	48
Figure 3.7 (a) Festo Airic's Arm robotic arm (dimensions when deployed 85 x 85 x 65 cm), (b) Festo fluidic muscle actuators (from left, 40 mm diameter, 20 mm diameter, 10 mm diameter) [www.festo.com].....	49
Figure 3.8 Aurora Flight Sciences Phase I S3 Knee Prototype [Duda, 2010].....	50
Figure 3.9 Knee torque versus angle curve for a robotic space suit testing method (in blue) [Schmidt et al., 2001] and an empty pressurized suit testing method (in red) [Dionne, 1991] .....	51
Figure 3.10 S3 knee prototype torque testing setup [Duda, 2010] .....	52
Figure 3.11 Aurora Flight Sciences S3 knee prototype torque vs. angle curve [Duda, 2010].....	53

Figure 3.12 S3 knee joint design [drawing by Roedolph Opperman, Aurora Flight Sciences].....	54
Figure 3.13 Hip conceptual designs (a) No exoskeleton frame, (b) Uses an exoskeleton based on the Berkeley Lower Body Exoskeleton (BLEEX) design [Zoss et al., 2006] with pneumatic actuators shown in blue.....	56

**Chapter 4**

Figure 4.1 S3 computer simulator inputs and outputs.....	60
Figure 4.2 S3 computer simulator GUI.....	61
Figure 4.3 S3 computer simulator with the knee angle pushbuttons and the joint elements dropdown menu indicated.....	62
Figure 4.4 Additional user inputs for S3 computer simulator.....	63
Figure 4.5 S3 computer simulator outputs.....	64
Figure 4.6 Graph depicting relationship between tension force, percent contraction, and supply pressure for a 10 mm (0.4 in) diameter fluidic muscle actuator [www.festo.com].....	65
Figure 4.7 The leg modeled as a two link system with the forces and moments indicated on each component.....	67
Figure 4.8 Front actuator inputs to example design for 50% female anthropometry.....	68
Figure 4.9 Back actuator inputs to example design for 50% female anthropometry.....	69
Figure 4.10 Torque vs. angle curve of example simulation compared with Schmidt et al., 2001.....	70
Figure 4.11 The circle representing the greave rotates with the lower leg as the knee flexion (kf) angle increases.....	71
Figure 4.12 Knee torque versus angle curve of a pressurized EMU space suit [Schmidt et al., 2001].....	72
Figure 4.13 Knee torque versus angle curve of baseline design compared against Schmidt 2001 data ...	75
Figure 4.14 Knee torque versus angle curve of design 2 compared against Schmidt 2001 data.....	76
Figure 4.15 Knee torque versus angle curve of design 3 compared against Schmidt 2001 data.....	77
Figure 4.16 Designs 2 and 3 compared with baseline design 1 and Schmidt data.....	78
Figure 4.17 S3 Knee Design Comparisons.....	82
Figure 4.18 (a) Front actuator length comparison given short (200 mm or 7.9 in) back actuator, (b) Front actuator length comparison given long (495 mm or 19.5 in) back actuators.....	85
Figure 4.19 Back actuator length comparison given short (300 mm or 11.8 in) front actuator length.....	85
Figure 4.20 Back actuator length comparison given medium (350 mm or 13.8 in) front actuator length.....	86
Figure 4.21 Back actuator length comparison given long (495 mm or 19.5 in) front actuator.....	87

## List of Tables

### Chapter 3

Table 3.1 S3 angle range of motion and torque requirements.....	43
---	----

### Chapter 4

Table 4.1 Baseline design implemented in the S3 computer simulator.....	74
Table 4.2 Nominal lengths and diameters of front and back actuators for designs 4-7 .....	79
Table 4.3 Front and back actuator combinations .....	83
Table 4.4 Comparison of the designs implemented in the S3 knee simulator .....	89

### Appendix B

Table B.1 Example simulation design to accommodate 50% female anthropometry .....	117
Table B.2 Baseline design 1 to accommodate 95% male anthropometry .....	117
Table B.3 Design 2 with a longer back actuator than baseline design 1 .....	118
Table B.4 Design 3 with shorter front and back actuators than baseline design 1.....	118
Table B.5 Design 4 with a small back actuator diameter and a short front actuator nominal length .....	118
Table B.6 Design 5 with a large back actuator diameter and a short front actuator nominal length.....	119
Table B.7 Design 6 with a small back actuator diameter and a long front actuator nominal length.....	119
Table B.8 Design 7 with a large back actuator diameter and a long front actuator nominal length .....	119
Table B.9 Combo 1 with a short back actuator nominal length and a short front actuator length.....	120
Table B.10 Combo 2 with a short back actuator nominal length and a medium front actuator length ..	120
Table B.11 Combo 3 with a short back actuator nominal length and a long front actuator length .....	120
Table B.12 Combo 4 with a long back actuator nominal length and a short front actuator length .....	121
Table B.13 Combo 5 with a long back actuator nominal length and a medium front actuator length....	121
Table B.14 Combo 6 with a long back actuator nominal length and a long front actuator length.....	121



## Acronyms

3D	= three-dimensional
ABF	= Anthropometry and Biomechanics Facility
ACES	= Advanced Crew Escape Suit
BLEEX	= Berkeley lower extremity exoskeleton
DOF	= degrees of freedom
EM-ACES	= Enhanced Mobility-Advanced Crew Escape Suit
EMG	= electromyography
EMU	= Extravehicular Mobility Unit
EVA	= extravehicular activity
eZLS	= enhanced Zero-gravity Locomotion Simulator
HAL	= Hybrid Assistive Limb
GRC	= Glenn Research Center
GUI	= graphical user interface
HULC	= human universal load carrier
ILC	= International Latex Corporation
ISS	= International Space Station
IVA	= intravehicular activity
JSC	= Johnson Space Center
LEA	= launch, entry, and abort
MIT	= Massachusetts Institute of Technology
MK-III	= Mark-III
MR	= magnetorheological
NASA	= National Aeronautics and Space Administration
PLSS	= Portable Life Support System
PPA	= Pilot Protective Assembly
RMSE	= root-mean-square error
ROM	= range of motion
RSST	= robot space suit tester
S3	= space suit simulator
SEA	= series elastic actuators

✓

## 1.1 Motivation

Widely acknowledged in the literature is the fact that pressurized space suits impose high joint torques on crew members, which results in reduced mobility [Holschuh et al., 2009; Bethke, 2005; Schmidt, 2001; Kosmo & Ross, 1998]. The first spacewalk demonstrated the reduced mobility caused by working in a pressurized space suit. The first human to conduct a spacewalk was Russian cosmonaut Alexei Leonov, in 1965. He was outside his spacecraft, the Voskhod 2 (Figure 1.1), for just over twelve minutes. By the end of the spacewalk, Leonov's suit had inflated in the vacuum of space and he could not re-enter the airlock. Leonov relieved some of the suit's pressure to regain mobility, but he was barely able to get back inside the capsule [Portree & Trevino, 1997].

Although mobility in pressurized space suits has improved since the 1960s, it is still much less than shirt-sleeve mobility and requires additional research. Researchers both at academic institutions and in industry have studied this altered mobility, as well as the metabolic energy expended when working in a pressurized space suit [Carr & Newman, 2005; Morgan et al., 1996]. Studying the joint torques imposed by the suits and the resulting reduced mobility is also important when astronauts are training on Earth, to try and mitigate potential injuries caused by the suit, and to identify areas where future space suit designs can improve upon the current designs.

Using a National Aeronautics and Space Administration (NASA) space suit for research is difficult, especially for academic use. The current space suits are expensive, bulky, difficult to transport, in limited supply, and not easily accessible. According to a 1994 study by the space suit manufacturers, International Latex Corporation (ILC) Dover, at the time there were only approximately fifty space suits available for actual extravehicular activity (EVA) and training, and each cost \$2 million to manufacture, not including the cost of the life support system backpack [ILC Dover, 1994].

A solution to the problem of utilizing expensive and not easily accessible space suits is to develop a space suit simulator (S3) exoskeleton. A space suit simulator exoskeleton can be used by space suit researchers to conduct EVA experimentation and training. This thesis describes the work performed to develop a space suit simulator exoskeleton that can mimic the angle range of motion and joint torque properties of several pressurized space suits.



**Figure 1.1 Photo of the hatch of the Voskhod 2 taken at Russia's Energia Spaceflight Museum [Courtesy of Gui Trotti]**

The S3 exoskeleton project draws from three main areas of research: space suit simulators, joint torque testing, and exoskeleton design. Previously developed analogue and prototype space suits have accurately mimicked the bulk of a pressurized space suit [Braden & Akin, 2004], however work on simulating the joint torques of a pressurized space suit has been minimal. Researchers at the Massachusetts Institute of Technology (MIT) were able to develop an extravehicular mobility unit (EMU) knee space suit simulator that simulated the knee torques of a pressurized space suit; however, resistance to knee flexion was only passively controlled with springs [Carr & Newman, 2008]. Researchers at ATA Engineering (San Diego, CA) also developed an EMU knee space suit simulator, which was tested with the MIT robot space suit tester [Newman et al., 2007]. This simulator modeled the hysteresis of the EMU knee joint, however it also used passive resistance to motion with springs. While simulators have been developed that mimic the torque properties of a pressurized space suit, only passive resistance to motion has been explored. A space suit simulator using active control would allow for more precise mapping of space suit joint torques to joint angles.

To measure joint torque of a pressurized space suit, one of three joint torque testing methods are typically used: empty pressurized suit testing, human-in-the-suit testing, and robot space suit testing. Space suit joint torques are determined during empty pressurized suit testing by moving the suit limbs through their full range of motion. While this method does not include the volume and pressure effects seen with a person in the suit [Holschuh et al., 2009], the torque measurements are assured to



be due to the torques imposed by the suit alone. The human-in-the-suit testing method accounts for the volume and pressure effects seen with a person in the suit. While human-in-the-suit testing allows for more accurate measurements of joint torque, there is difficulty in cancelling out gravity and determining the joint torque effects due to the pressurized suit alone. Both empty pressurized suit testing and human-in-the-suit testing methods output the torque required to move the space suit component externally through its range of motion (ROM), instead of the joint torque felt internally at the point of rotation. In the robot suit testing method, a robot is outfitted with a pressurized space suit. As the robot moves through its angle ROM, the internal joint torque at the point of rotation is measured with strain gauges. Because the robot suit testing method includes an anthropometric body in the suit, the volume and pressure effects of having a person in the suit are included in the torque calculation, providing a more accurate determination of joint torque.

Exoskeleton designs developed for military or biomedical applications have utilized both passive elastics to achieve desired joint torques and also actuators to actively control resistance to motion. Actuators that allow for active control have the ability to more accurately mimic joint torques.

The S3 exoskeleton will allow for active control of space suit joint torques. This tool will allow space suit researchers to perform their experiments while accurately mimicking space suit joint torques. The space suit simulator exoskeleton will provide researchers with an inexpensive, readily accessible, and easily transportable tool with which to conduct space suit research. The S3 will improve upon the current state of the art in space suit simulators by actively controlling resistance to motion, and by providing the ability to mimic multiple pressurized space suits with one exoskeleton design.

## **1.2 Objectives**

The goal of the project is to develop a space suit simulator (S3) exoskeleton that mimics the mechanical properties, namely, the angle range of motion and joint torques, of multiple pressurized space suits. The joint torques of each pressurized space suit will be implemented in the S3 through software control. Therefore, the exoskeleton hardware components will be the same for each simulated space suit. The space suit simulator will be designed to be compatible with equipment used at NASA Glenn Research Center and NASA Johnson Space Center for partial gravity experimentation and training. This thesis describes the early stages of exoskeleton design. The specific aims of this thesis are:

- 1) Generate a space suit joint database and use the database to specify the S3 range of motion and torque requirements.

- 2) Qualitatively compare and select actuators used in previous exoskeleton designs to actively resist joint motion for the S3 exoskeleton.
- 3) Develop the conceptual design of the S3 exoskeleton.
- 4) Advance a computer S3 simulation in order to implement the S3 joint concepts and determine feasible design solutions.

In order to generate a space suit joint database, joint torque and angle range of motion information must be gathered. There are three primary methods used to measure space suit joint torque: empty pressurized space suit testing, human-in-the-suit testing, and robot space suit testing. Joint torque data has been measured for several pressurized space suits at NASA centers, in industry, and at universities. Joint torque data will be compiled for several pressurized space suits and several degrees of freedom for each space suit. Joint torque data gathered using all three joint torque testing methods will be included in the space suit joint database. The angle range of motion information will be gathered primarily from biomechanics reference guides, which include shirt-sleeve range of motion. Unsuit range of motion will be included in the space suit joint database so that the S3 exoskeleton will be able to accommodate any future space suit designs that have greater mobility than the current space suits. Once the joint torque and range of motion data is compiled, the information will be used to set the requirement bounds for the S3 joint torques and angle ROM.

Actuators that have been used in previous exoskeleton designs will be compared qualitatively according to weight and bulk characteristics. The objectives of the S3 exoskeleton design are to minimize weight and bulk while providing the necessary joint torques. An exoskeleton that is low in weight will be easier to transport and will minimize the weight the subject wearing the exoskeleton will have to offset. An exoskeleton that is low in bulk will be more easily integrated with specialized space suit research equipment at NASA centers and academic institutions. The actuators that allow for active control of resistance to motion while minimizing the weight and bulk characteristics of the S3 exoskeleton design will be selected.

The selected actuators will be incorporated into the S3 conceptual design. A design concept will be selected that once again minimizes the weight and bulk characteristics of the exoskeleton, but also allows for the space suit joint torques to be mimicked without creating any out of plane torques. Integration considerations will be made between the S3 exoskeleton design and the space suit research equipment at NASA Glenn Research Center and NASA Johnson Space Center. Additionally, safety of the subject will be of utmost importance during all design considerations.

The S3 computer simulation will allow the user to input the S3 exoskeleton joint design concept. Users will be able to input the dimensions of various exoskeleton components along with their locations relative to the joint point of rotation. The simulation will allow the user to move the limbs through their full range of motion and the simulator will output the joint torque over the range of motion. Feasible design solutions will be selected after several design iterations have been implemented in the simulation. Designs will be compared according to performance in reducing the error from the joint torque hysteresis curves used as the standards.

By completing the above objectives, the early framework will be set for the development of a space suit simulator exoskeleton that can mimic the joint torque and angle range of motion properties of a pressurized space suit. This early framework is essential in creating a tool that can be used by space suit researchers for experimentation.

### **1.3 Road Map**

This introductory chapter describes the motivation and objectives of the space suit simulator project while outlining the following chapters of this thesis. The thesis begins with an introduction to the need of a space suit simulator and current limitations of using actual pressurized space suits for extravehicular activity (EVA) experimentation and training.

Chapter 2 describes a review of the literature regarding several aspects of the space suit simulator project. First, methods for space suit joint torque and mobility testing that have been used in the past are described. A variety of pressurized space suit testing methods have been employed: empty pressurized suit testing, human-in-the-suit testing, and humanoid robot space suit testing. Next, analog and prototype space suits that have been used for EVA experimentation and training are discussed. Finally, various actuation methods that have been used in exoskeleton design for active control of joints are described.

Chapter 3 details the methods used to meet each of the objectives described above, along with the results. A space suit joint database was compiled consisting of joint torque versus angle curves for several pressurized space suits, joint degrees of freedom, and joint torque testing methods. The S3 joint convention, range of motion, and torque requirements were set based on the findings gathered in the space suit joint database. Qualitative characteristics of actuators used in previous exoskeleton designs for active control of joints are compared in order to select the actuation method for the S3 exoskeleton. Finally, the design process and conceptual design of the joints of the S3 exoskeleton is detailed.

In chapter 4, the improvement of a space suit simulator computer simulation is described, which discusses the process of making the simulator 3D capable and incorporating the conceptual design of the S3 exoskeleton knee into the simulation to be used to determine feasible design solutions of the S3 knee. Several design iterations of the S3 knee are implemented in the S3 computer simulator. The joint torques are plotted against the knee angles and feasible design solutions are selected based on the results.

Chapter 5 provides a discussion of the S3 results. First, the creation of the space suit joint database is described, along with the method used to determine the minimum and maximum bounds for the joint torque and angle ROM requirements for the S3 exoskeleton. The description of the qualitative comparisons of actuators that have been used for active control in exoskeleton designs follows. Next, the design process for development of the S3 conceptual knee and hip designs is discussed. The results of the S3 computer simulation are examined, along with a discussion of the feasible design solutions. The chapter continues with key challenges for the S3 project, along with future plans and recommendations.

## 2.1 Overview

During space exploration, mobility is extremely limited when working inside a pressurized space suit. Astronauts perform extensive training on Earth to become accustomed to space suit-imposed high joint torques and limited range of motion (ROM). Space suit researchers attempt to quantify suit performance by studying metabolic energy expenditure, fatigue, and joint torques while working in the suit. However, the current NASA space suit, or Extravehicular Mobility Unit (EMU), is expensive, bulky, heavy (125 kg including the Portable Life Support System [Thomas & McMann, 2006]), in limited supply, and hard to don and doff, which makes it difficult for researchers to use for extensive experimentation.

A wearable, full-body space suit simulator exoskeleton that can mimic the joint torques and reduced mobility of several pressurized suits provides a novel method for simulating joint torques while offering a lightweight, portable, and easily accessible design for experimentation and training. In order to mimic the joint torques of pressurized space suits, joint torque testing methods that have been used in the past are reviewed. In addition, space suit simulators, consisting of analog and prototype suits, have been developed for extravehicular activity (EVA) experimentation and training. However, these simulators tend to be bulky in order to mimic the volume inside the simulated space suit, and oftentimes the suits cannot be used in partial gravity simulation environments, such as partial weight suspension systems, because of their bulk. An exoskeleton concept can be used to simulate the joint torque properties of a pressurized space suit while maintaining compatibility with partial weight suspension systems. Exoskeletons have been developed for several university, biomedical, and military projects, and can be passively or actively controlled. A review of the exoskeleton literature further informs the development of the space suit simulator exoskeleton.

## 2.2 Space Suit Joint Torque and Mobility Testing

Research has shown that working in a pressurized space suit imposes high torques on the astronaut's joints and results in reduced mobility and increased fatigue. A pressure suit of average size has over 1.9 m<sup>2</sup> (3000 in<sup>2</sup>) of internal surface area and at least 21 kPa (3 psi) pressure are needed to support life; therefore, even minimum pressure can make fabric pressure suits potentially immobile without mobility joints designed into the suit [Thomas & McMann, 2006]. Morgan et al. found that average EMU suited strength decreased by up to 42% compared to unsuited strength [Morgan et al.,

1996]. Because the astronaut's mobility and strength is altered in the space suit, research is needed to study the changes in joint torques and angle ROM. There are three general methods used for determining space suit imposed joint torques and reduced mobility: empty pressurized suit testing, human-in-the-suit testing, and robot space suit testing.

### **2.2.1 Empty Pressurized Suit Testing**

Space suit joint torques can be determined by moving empty pressurized suits through the full range of motion for each degree of freedom. Although the joint torques of an empty pressurized suit will not include the same volume and pressure effects as would be seen with a person in the suit [Holschuh et al., 2009], empty pressurized suit torque measurements are assured to be due to torques imposed by the suit alone and represent a starting point in quantifying space suit joint stiffness.

Hypobaric testing is one method that has been used to determine the joint torque of a space suit component. Researchers at the Massachusetts Institute of Technology (MIT) quantified the elbow torque of an Extravehicular Mobility Unit (EMU) space suit using a hypobaric testing method [Holschuh et al., 2009]. The space suit arm segment was incorporated into a hypobaric chamber, while allowing the arm segment to be externally rotated through its ROM (Figure 2.1). The hypobaric chamber was reduced to -30 kPa (-4.35 psi) gauge pressure, creating a pressure differential between the suit component and the chamber equal to the pressure differential of a pressurized suit in space.

Hamilton Sundstrand researchers measured the joint torque and angle relationship of the EMU by using an empty pressurized space suit testing method [Dionne, 1991]. To bend the joints, torques were applied to the outside of the suit and resulting angular displacements were measured. Torque vs. angle curves of the EMU shoulder, elbow, and knee joints are shown in Figure 2.2.

In a study performed at the National Aeronautics and Space Administration (NASA) Johnson Space Center (JSC), researchers quantified the joint torque of the EMU using a modified fish scale method [Matty & Aitchison, 2009]. The modified fish scale method consisted of a load cell connected to a suit component, and a pulling mechanism, which was manipulated by the experimenter. The load cell measured the force required to move the suit component through its ROM. The joint angle was collected by videos and photos of the suit in front of a grid with a known scale. All suit components were tested in gravity neutral positions. Advantages of this method are its simplicity and flexibility in setting up the testing, while eliminating the difficulties associated with removing gravity and human subject influence during data analysis. Disadvantages include the possibility for human error and difficulty with repeatability.

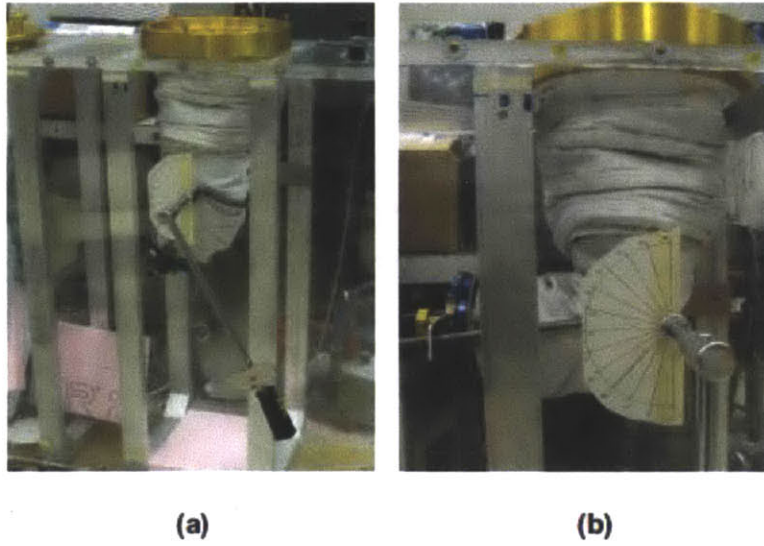


Figure 2.1 (a) MIT space suit test rig, shown with the EMU arm specimen resting, and (b) flexed to 90 deg [Holschuh et al., 2009]

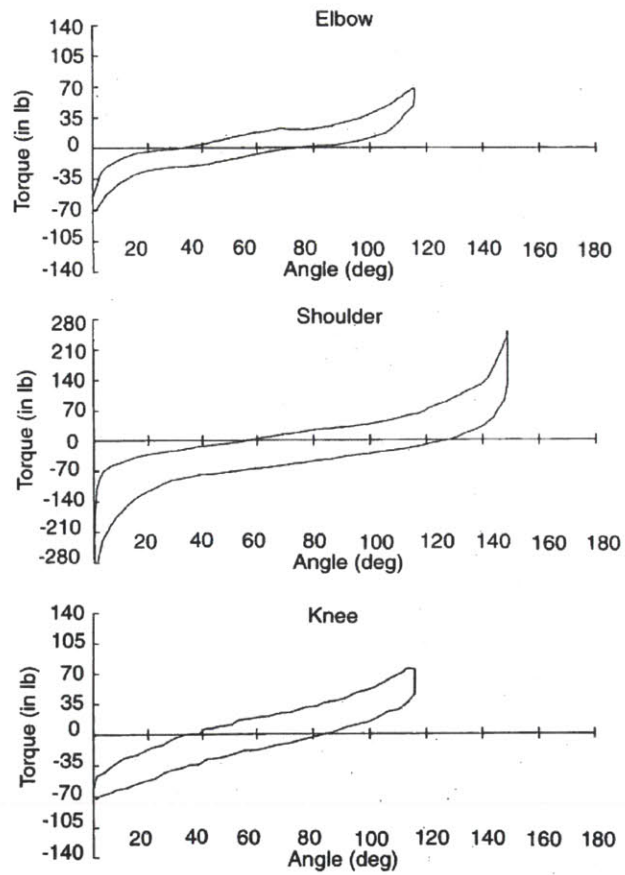


Figure 2.2 Torque vs. angle for the EMU elbow, shoulder, and knee [Dionne, 1991]

Using the modified fish scale method, NASA researchers have collected ROM and joint torque data for six pressurized suits and 16 degrees of freedom (DOF) [Matty, 2010]. The six space suits studied were the EMU, the current International Space Station (ISS) extravehicular activity (EVA) suit; the Advanced Crew Escape Suit (ACES), the suit worn during launch and entry on the Space Shuttle; the I-suit, an all-soft advanced suit used for EVA mobility field studies; the D-suit, an advanced pressure prototype space suit; the Enhanced Mobility (EM)-ACES, a prototype space suit with improved mobility over the ACES; and the Mark III (MK-III), a space suit demonstrator. DOFs measured for each space suit include:

- Shoulder flexion/extension
- Shoulder adduction/abduction
- Shoulder medial/lateral
- Shoulder extension/internal rotation
- Elbow flexion/extension
- Torso rotation
- Torso flexion/extension
- Hip flexion/extension
- Hip adduction/abduction
- Hip extension/internal rotation
- Knee flexion/extension
- Ankle flexion/extension
- Ankle extension/internal rotation
- Wrist flexion/extension
- Wrist adduction/abduction
- Wrist pronation/supination

Although there are difficulties with repeatability and a greater possibility of human error when using an empty pressurized suit testing method, the experimental procedure is relatively simple. Additionally, the empty pressurized suit testing method has the most comprehensive data thus far with analysis completed for six pressurized space suits and 16 DOF. However, empty pressurized suit torque data does not include some of the volume and pressure effects that would be seen with a person inside the pressurized suit, which is why the torque values are less in empty pressurized suit testing. Therefore, another method used to determine space suit joint torques, which incorporates the volume and pressure effects seen when a person is inside the suit, is the human-in-the-suit testing method.

### ***2.2.2 Human-in-the-Suit Testing***

Joint torques of space suits can more rigorously be determined with a person in the suit. In general, joint torque measurements are greater for suited experiments as opposed to empty pressurized



suits. Specifically, the wearer of the suit affects pressure and volume measurements, which may contribute to the larger torques reported.

Researchers in the Anthropometry and Biomechanics Facility (ABF) at NASA JSC collected joint torque data with a Primus RS™ system (Figure 2.3)(BTE Technologies, Ontario, Canada), which manipulates the limb through its ROM while recording the force required to move the limb [Matty & Aitchison 2009]. The ABF collected data for 10 DOF from each of 5 space suits. There are several limitations to using this method to determine joint torques of a space suit, including: oscillations in some joints during rotation due to the design of the suit components, not allowing the Primus RS™ to move the joints in a clean single axis; difficulty cancelling out gravity and person-in-the-suit effects on torque measurements; measuring joint torques at ROM extremes; and experiment repeatability. Due to the limitations of this testing method, it is no longer used at NASA.

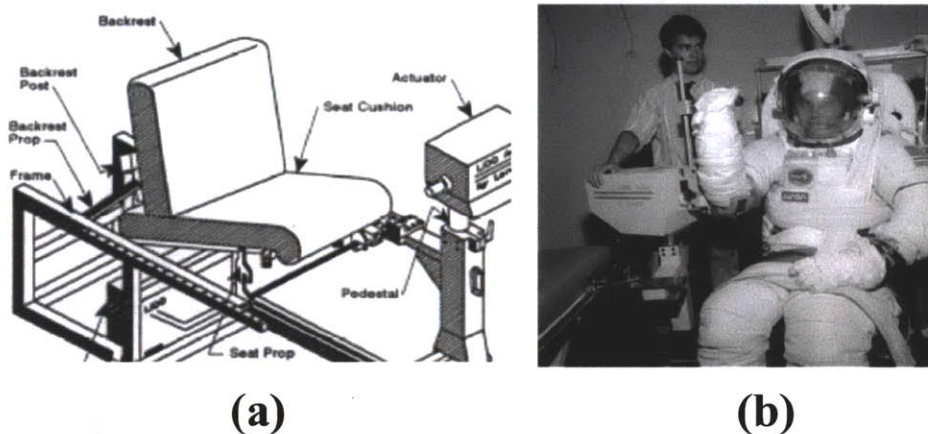


**Figure 2.3 Primus RS™ collecting unpressurized ACES elbow torque data [Matty & Aitchison, 2009]**

Researchers at NASA JSC have conducted human-in-the-suit testing by measuring subject strength when unsuited and suited in a pressurized EMU [Morgan et al., 1996]. Six DOFs were included in the study. A LIDO Multi-Joint II testing unit (Loredam Biomedical, Inc., West Sacramento, Calif.), which consists of an isokinetic dynamometer and a computer, was used to determine strength measurements (Figure 2.4). The system also includes a gravity compensation feature, which is able to subtract the weight of the suit, apparatus, and test subject limbs from the total torque measurement. The subject's limb was constrained to a single DOF and the testing apparatus moved the subject's limb through the ROM as comfort threshold feedback was given by the subject. One limitation of this suit testing method is that strength measurements were collected in a seated posture, which is not the natural posture of

EVA astronauts. Further, ROM measurements were restricted for some of the DOF due to interference with the hardware components.

The human-in-the-suit testing method includes the pressure and volume effects seen in a pressurized space suit when a person is in the suit, which may provide a more accurate assessment of joint torque than empty pressurized space suit testing methods. However, the human-in-the-suit testing method is not without limitations. A major limitation with using the human-in-the-suit testing method is that it is difficult to determine the joint torque effects of the pressurized suit alone. Even if subjects are told to relax and let the testing apparatus move the subject's limb through its ROM, it is impossible to know if the subject is aiding the testing apparatus in the motion, and if they are it is difficult to determine how much torque the subject is contributing by aiding in that motion. Further, a disadvantage of both the empty pressurized suit and human-in-the-suit testing methods is that both methods output the torque required to move the pressurized space suit component externally through its ROM, instead of the joint torque felt internally at the point of rotation. Robot space suit testing provides a method to determine joint torques internally.



**Figure 2.4 (a) LIDO Multi-Joint II isokinetic dynamometer bench drawing and (b) elbow flexion/extension setup [Morgan et al., 1996]**

### **2.2.3 Robot Space Suit Testing**

A third way to determine joint torques of a pressurized space suit is to outfit a humanoid robot with the suit. MIT's robot space suit tester (RSST) is an anthropometric humanoid robot, that can move through 12 DOF with hydraulic actuators on the right side of the body, while the left side can be passively repositioned by the experimenter (Figure 2.5). RSST was built for NASA by SARCOS (Salt Lake City, Utah). NASA later donated the RSST to MIT for space suit testing research.



**Figure 2.5 (a) Robot Space Suit Tester (RSST), (b) RSST with EMU installed [Schmidt et al., 2001]**

The major advantage of determining joint torques with the robot method is that researchers can determine the internal joint torque with strain gauges located at the point of rotation, while other methods calculate the external torque, or the torque required to move the limb about its point of rotation. Problems with using the robot method include difficulty in donning the suit on the robot and the possibility of hydraulic leaks, which makes the possibility of using one-of-a-kind NASA suits on the robot unlikely.

Researchers at MIT compiled a joint torque-angle database for the EMU space suit, using realistic EVA motions. Joint angle trajectories produced by humans in the pressurized EMU were measured with a Multitrax (Adaptive Optics Associates, Cambridge, MA) motion capture system. The angle trajectories were used as robot commands once RSST was outfitted with the pressurized EMU. RSST measured torque and angle for 11 DOF and 9 complex motions [Schmidt et al., 2001].

From the data collected with RSST, three models were developed relating the joint torques to joint angles for each DOF. The first model, the Preisach model, used coefficients to reproduce the torque-angle relationships collected during robot testing. The beam model treated the inflated cylinder suit limb as a beam with a fabric wall that stretches, maintaining a constant internal volume. The membrane model treated the fabric as an inextensible membrane, so when the limb was bent, there were deformations of the cross-sectional area and a change in the internal volume. The joint torque-angle data gathered with RSST matched the membrane model closely, indicating space suit joint mobility is sensitive to internal pressure and joint geometry [Schmidt et al., 2001; Frazer et al., 2002]. The model was applied to EVA operations in a work envelope analysis. The EMU joint torque model

results were also used to propose improvements to the current space suit and to promote new designs for future space suits [Schmidt et al., 2001].

MIT's RSST has also been used to characterize mobility of military pressure suits. MIT researchers quantified mobility characteristics of the S1034 Pilot Protective Assembly (PPA), which is a pressure suit worn by U2 pilots [Meyen et al., 2011]. Joint torques were collected for 4 DOF when the suit was unpressurized, pressurized to 5.5 kPa (0.8 psi) to represent the Constellation Program specified vent pressure, and pressurized to 20.7 kPa (3 psi) to represent emergency pressure.

Although the joint torque data available using the robot space suit testing method is not as comprehensive as the data gathered with the empty pressurized suit testing method, robot space suit testing does provide joint torques internally at the point of rotation while including the pressure and volume effects seen with an anthropometric robot in the suit. By reviewing the data gathered using the various space suit testing methods, a detailed joint torque database was compiled in order to create a space suit simulator that incorporates actual pressurized space suit joint torques. Space suit simulators can mimic actual space suit properties without the added cost, bulk, and access difficulty.

## **2.3 Space Suit Simulators**

Space suit simulators, consisting of analog and prototype suits, have been developed by researchers both at NASA JSC and at various academic institutions, such as MIT and the University of Maryland. These suits are developed and tested to allow researchers to conduct EVA experimentation and training.

### **2.3.1 Analog Space Suits**

Analog space suits have been developed to enable space suit researchers to do EVA experimentation when they do not have access to NASA space suits. Researchers at the University of Maryland have developed a series of pressure suit simulators, designed to be used in their on-campus neutral buoyancy pool for EVA experiments. The next analog suit, the MX-3, will be modular, allowing for suit components to be easily changed out depending on the experiment task. Suit components include arm and leg joints, passive and active sizing systems, and hard or soft torso assemblies [Braden & Akin, 2004].

Researchers at MIT developed an EMU knee space suit simulator, using two non-linear fiberglass springs to simulate the torques seen at the knee in a pressurized space suit [Carr & Newman, 2008]. The exoskeleton leg had pin adaptors that attached to the person at the hip and ankle and when subjects bent their knees, the joint torque at the knee matched the torques seen in a pressurized EMU knee.

Although the torque measurements at the knee corresponded to those of an EMU, the springs could only passively control the resistance to knee flexion, therefore only one pressurized space suit could be simulated with the given exoskeleton springs.

Researchers at MIT later conducted robot testing of an EMU knee space suit simulator developed by engineers at ATA Engineering (San Diego, CA) to more accurately match the torques seen in a pressurized EMU (Figure 2.6) [Newman et al., 2007]. This analog knee was adjustable in terms of friction, angle ROM, and stiffness. The friction was altered by loosening or tightening screws connecting portions of the upper and lower brace, the angle ROM could be changed by altering the location of hard stops, and the stiffness could be accomplished by changing the spring at its pre-load. Through experimental testing and statistical analysis they found that it was possible to closely model the hysteresis of the EMU knee joint. This space suit simulator, along with the previous knee simulator, passively provided resistance to motion by using a spring.

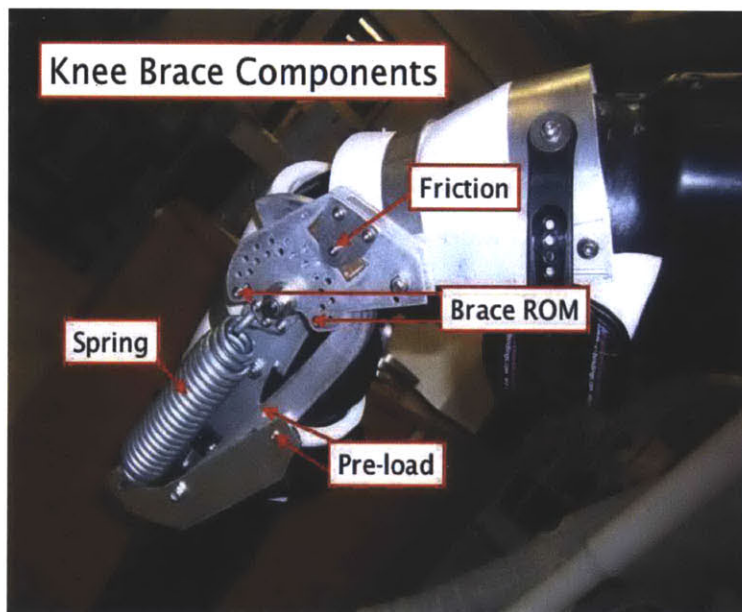


Figure 2.6 Knee flexion joint of the space suit simulator [Newman et al., 2007]

### 2.3.2 Prototype Space Suits

Prototype space suits have been developed to test advanced space suit designs that may improve the mobility characteristics of the current suits. The Mark-III prototype suit was built in conjunction with ILC Dover as a partly hard, partly soft suit. MK-III was designed to be a zero-prebreathe suit. This advanced suit prototype is a rear-entry suit, with modular components to accommodate users of varying sizes. The MK-III is 65% metal, weighs 59 kg (130 lbs) without the Portable Life Support

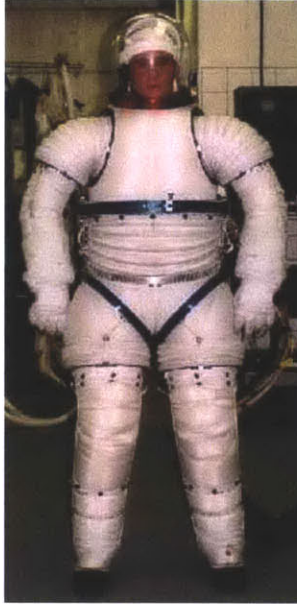
System (PLSS), and can be pressurized to about 55 kPa (8 psi). To improve the mobility of the current space suit, the MK-III was designed with rolling convolute joints at the waist and shoulder, and a 3-bearing hard component hip, while including fabric flat pattern arm and leg components (Figure 2.7) [Kozloski, 1994; [www.nasa.gov](http://www.nasa.gov)].



**Figure 2.7 Mark III suit [[www.nasa.gov](http://www.nasa.gov)]**

In an experiment performed at NASA JSC, researchers studied the mobility characteristics of the MK-III prototype space suit while flying in the KC-135 aircraft at simulated lunar and Martian gravity environments [Kosmo & Ross, 1998]. The person in the MK-III suit was able to perform all mobility test tasks except rolling from a supine to prone position. The MK-III also allowed the subject to kneel and retrieve an object from the ground.

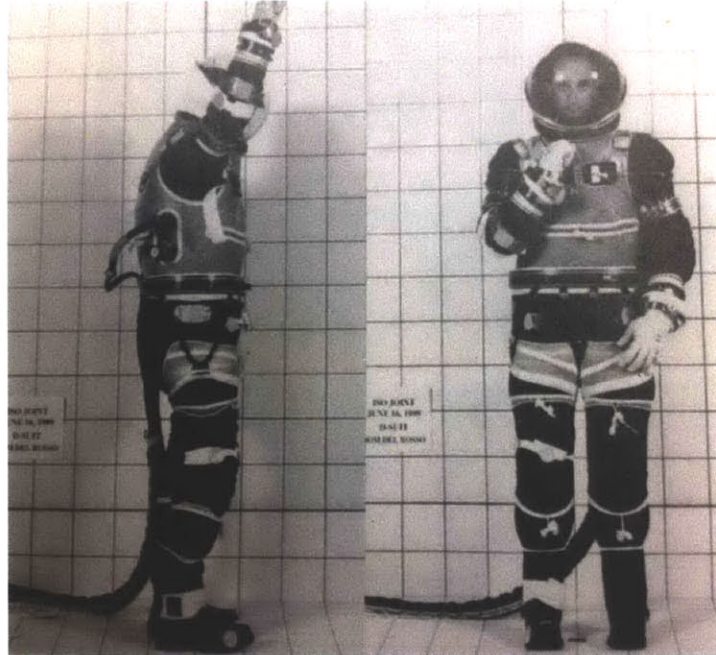
In the late 1990's, ILC Dover was awarded a NASA contract to develop the I-suit, a test bed suit for evaluating future multi-role EVAs, when astronauts may have to communicate with robot teams on a planetary surface. The I-suit was an advanced, all soft multi-bearing EVA suit. Because future planetary EVAs would require astronauts to fulfill multiple roles, improved mobility was one of the major goals of the I-suit design. The suit was an all soft, waist entry suit, with a convoluted shoulder joint, scye bearing, and arm bearing. The hip was a 2-bearing design with an integral single axis convoluted mobility joint (Figure 2.8) [Graziosi & Lee, 2003].



**Figure 2.8 I-suit [Graziosi & Lee, 2003]**

In conjunction with the I-suit development, NASA also awarded a soft suit contract to the David Clark Company (Worcester, MA). The suit, which was designated the D-suit, improved upon an advanced Apollo fabric suit concept. The D-suit was a mid-entry suit with arm bearings and a Link-net restraint system at the chest (Figure 2.9). Shoulder mobility was aided by a metallic cable restraint system. The arm components included convolute mobility joints with webbing axial restraints. The D-suit was lightweight at 10 kg (22 lbs) [Thomas & McMann, 2006].

A test and evaluation space suit, the Demonstrator Suit, was developed by researchers at the David Clark Company. The suit was designed to be able to be used during launch, entry, and abort (LEA), intravehicular activity (IVA), and contingency EVA. In its evaluation, the Demonstrator Suit was characterized by its physical characteristics, its functional performance, and its human factors abilities [Ripps et al., 2011]. The suit was designed to operate at 33 kPa (4.8 psi), weigh less than 18 kg (40 lbs), allow for rapid self donning and doffing, and comply with spacecraft seating dimensions and harnesses. The researchers found that the suit performed well with regard to suit mobility due to a cable assist shoulder joint, a convolute waist/hip, and convolute knees/elbows. Eight of eleven degrees of freedom met the range of motion requirements set forth for the Demonstrator Suit. For example, the requirement for the shoulder flexion degree of freedom was to achieve 55 degrees of flexion, and one subject was able to achieve 125 degrees of flexion [Ripps et al., 2011]. The upper arm bearings aided in improving shoulder and arm mobility, but added mass and slight discomfort.



**Figure 2.9 David Clark Company D-suit [Thomas & McMann, 2006]**

Although analog and prototype space suits more closely simulate the reach capability, operational envelope, and bulk characteristics of a pressurized space suit, they do not accurately simulate the joint torque properties. In order to determine the energy output associated with working in a pressurized space suit, joint torques must be precisely simulated. A space suit simulator exoskeleton with the ability to actively control mobility could be used to simulate the joint torques and angle ROM of a pressurized space suit.

## **2.4 Exoskeleton Review**

Significant exoskeleton design research has been accomplished at several academic institutions for biomedical and military applications to help people suffering from spinal cord injury or cerebral palsy and to aid soldiers in carrying heavy equipment. Researchers use materials to either passively achieve desired joint torques or they actively control movement with actuators, such as hydraulics, pneumatics, magnetorheological (MR) fluids, or electric actuators. The active control that can be achieved with exoskeleton actuators will allow for accurate implementation of space suit joint torques in the space suit simulator.

### **2.4.1 Hydraulic Actuators**

Researchers at the University of California-Berkeley developed a lower body exoskeleton to offload up to 34 kg (75 lbs) of a soldier's payload backpack [Zoss et al., 2006]. The lower body



exoskeleton has 7 DOF per leg, 4 of which are powered by bi-directional linear hydraulic actuators. The actuators were selected because they were lightweight, low bulk, and could achieve high torques. Passive joints were controlled by impedances due to steel springs and elastomers. The lower body exoskeleton was designed to match human joint angles and torques for a typical walking cycle, as measured in clinical gait analysis data [Chu et al., 2005].

Researchers at the Berkeley Robotics and Human Engineering Laboratory continued to develop the Berkeley lower body exoskeleton to a version known as the Human Universal Load Carrier (HULC). The group entered into an exclusive licensing agreement with Lockheed Martin in 2009. The HULC was developed in order to augment soldier strength and endurance. HULC transfers the loads carried by soldiers to the ground. HULC is an improvement over the previous Berkeley exoskeleton because it is untethered and powered by batteries, and carries up to 91 kg (200 lbs) of supplies without hindering soldier mobility [Lockheed Martin, 2008].

#### **2.4.2 Pneumatic Actuators**

Researchers at the University of Michigan have developed an ankle-foot orthosis powered by pneumatic actuators and controlled by electromyography (EMG) input commands [Ferris et al., 2005]. There were two pneumatic actuators on the orthosis, one on the front of the ankle, and one on the back of the ankle. When nerve signals on the front of the leg were activated the pneumatic actuator on the front was pressurized, causing it to contract and aid in ankle dorsiflexion. When EMG signals to the calf muscle were activated, pressure was supplied to the posterior pneumatic actuator, causing it to contract and aid in plantar flexion. The ankle orthosis was able to achieve torques of up to 70 Nm in plantar flexion, and 38 Nm in dorsiflexion. For a space suit comparison, EMU ankle torques measured with MIT's robot space suit tester were 2 Nm in plantar flexion, and 7 Nm in dorsiflexion [Schmidt, 2001].

#### **2.4.3 Magnetorheological (MR) Fluid Actuators**

At the Chinese University of Hong Kong, researchers in the Smart Materials and Structures Laboratory designed and tested a MR fluid actuator in an assistive knee brace [Chen & Liao, 2010]. The assistive knee brace was designed to assist the elderly with mobility problems by acting as a brake or clutch to prevent stumbles or falls. The MR actuator was able to achieve torques needed for daily human activities.

Researchers in the Biomechatronics Group at MIT and the orthopedic company Ossur have developed the Rheo Knee, a MR fluid prosthetic knee that controls damping by changing the strength of the magnetic field through MR fluid. The Rheo Knee was tested at a rehabilitation hospital with trans-

femoral amputee subjects to investigate if MR fluid technology decreases metabolic expenditure compared to hydraulically actuated prosthetics [Thakkar 2002]. The researchers found that there was a significant metabolic improvement when using the Rheo Knee, as opposed to the hydraulically actuated C-LEG.

#### 2.4.4 Electric Actuators

Electric actuators used in exoskeleton design include electric motors and series elastic actuators (SEA). SEAs utilize motors in series with springs to create force output. A diagram of a SEA is shown in Figure 2.10. The motors drive the ball nut forward or backward and the ball nut flange compresses springs which push on the spring retaining plate, which is attached to output plungers, causing force in the direction of the ball nut motion [Pratt et al., 2002].

Researchers at MIT improved an ankle foot orthosis by adding a SEA to control the impedance of the orthotic joint throughout the walking cycle to treat patients with drop foot [Blaya 2003]. The SEA weighted 11.6 N (2.6 lb) and the overall orthosis weighed 30.2 N (6.8 lb). Kinetic and kinematic gait data was collected on subjects with drop foot wearing the active ankle foot orthosis. During a five step trial for one subject wearing the orthotic, the mean number of occurrences of slap foot was reduced from an average of two occurrences per five steps with zero impedance to an average of no occurrences per five steps with constant and variable impedance. Researchers found the actively controlling joint impedance reduced the occurrence of foot slap, which occurs during drop foot gait.

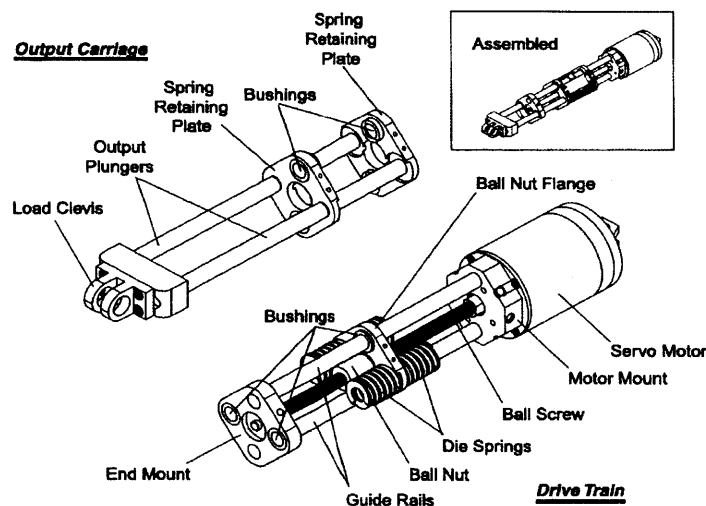


Figure 2.10 Series elastic actuator [Pratt et al., 2002]

A company called Yobotics (Cambridge, MA) developed a prototype knee orthotic, called RoboKnee, actuated by SEA [Pratt et al., 2004]. The RoboKnee exoskeleton offloads the weight of a

backpack and provides most of the energy needed to work against gravity. Subjects were able to climb stairs and perform deep knee bends while wearing RoboKnee.

Exoskeletons that use electric motors for actuation have also been developed. Honda researchers developed exoskeleton legs to assist the elderly with walking and partially support their bodyweight [Ikeuchi et al., 2009]. The exoskeleton legs fit on the inner side of the user's legs and connect at a seat that can support the bodyweight of the subject (Figure 2.11). The legs are actuated by electric motors, which help reduce the load on the leg muscles and reduce the energy expenditure when climbing stairs or doing squats.



**Figure 2.11 Honda exoskeleton legs [Ikeuchi et al., 2009]**

The Hybrid Assistive Limb (HAL) exoskeleton developed by researchers at the University of Tsukuba utilizes electric motors to actuate the hip and knee [Suzuki et al., 2007]. HAL was initially designed to measure electrical signals on the subject's skin to control the force applied to the exoskeleton to aid subjects in walking or carrying heavy loads. Researchers at the University of Tsukuba developed an algorithm to estimate human intentions instead of relying on electrical signals so that HAL could be used with paraplegic patients. Using the algorithm, HAL was able to support a paraplegia patient's walk.

## **2.5 Summary**

Current pressurized space suits limit mobility and are fatiguing to work in for long periods of time. Space suit researchers at NASA, academic institutions, and in industry attempt to quantify the mobility and energy expenditure of astronaut's wearing a pressurized space suit in order to learn the capabilities of the current suits and design future generation suits that improve mobility and minimize joint torques. A space suit simulator exoskeleton with the ability to mimic the joint torque and angle

ROM properties of several pressurized space suits could be a useful tool for space suit researchers and space suit designers working on the development of next-generation suits.

The most extensive space suit joint torque data has been collected with empty pressurized space suit testing methods. While empty suit testing methods are simple, there is the probability of human error during testing and repeatability is difficult. Joint torque measurements from person-in-the-suit testing methods include the volume and pressure effects associated with having a person in the suit, but it is difficult to quantify the torque due to the suit bending alone. Both empty pressurized suit and person-in-the-suit testing methods output the external torque required to move the pressurized limb through its range of motion, instead of the internal joint torque. The robot space suit testing method utilizes an anthropometric humanoid robot donning a pressurized space suit to calculate the joint torque internally with strain gauges at the point of rotation of the joints.

Analog and prototype space suits have been developed for EVA experimentation and training. Although analog suits mimic the bulk of a pressurized space suit, they do not closely match the joint torques and mobility characteristics of pressurized suits. A space suit simulator exoskeleton that actively controls joint torque and angle ROM could be used by space suit researchers and designers to study the current suits and develop future suit concepts.

Exoskeletons have been used for military and biomedical applications. Exoskeletons can be controlled passively using elastics and springs, or actively with hydraulics, pneumatics, MR fluids, and electric actuators. There are advantages and disadvantages to both passively and actively controlled exoskeletons, however active control could achieve a more accurate joint torque measurement given the joint angle.

The contribution of this thesis is to discuss preliminary work in collaboration with Aurora Flight Sciences and MIT on the development of a space suit simulator exoskeleton that mimics the joint torque properties of several pressurized space suits. First, a joint-torque database was compiled including torque-angle curves for multiple pressurized space suits and space suit testing methods. Next, a review and comparison of actuators that have been used in exoskeleton design for active control of joints is discussed, along with the conceptual design of space suit simulator including the selected actuators. Finally, a space suit computer simulator was developed to calculate joint torques with feasible space suit simulator knee designs as the leg moves through its range of motion.

## 3.1 Overview

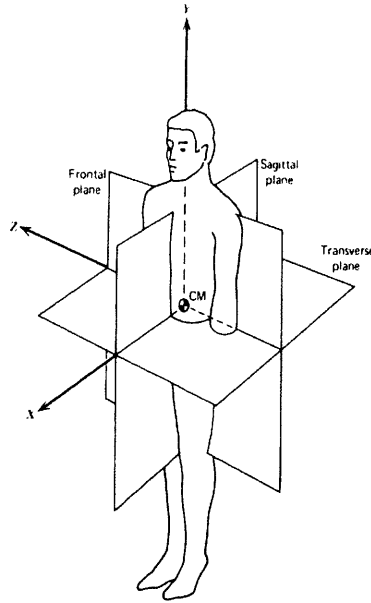
A space suit simulator exoskeleton that can mimic the joint torque properties of several pressurized space suits would be a useful tool for space suit researchers and designers as a low-cost and easily accessible alternative to space suit research. The first step in this research effort was to compile joint torque data from several sources to combine into a space suit joint database to set the overall angle range of motion and torque requirements for the space suit simulator (S3). After the overall torque requirements were determined, actuators that have been used for active control in previous exoskeleton designs were compared qualitatively in order to select the actuation device to be implemented in the space suit simulator. Finally, various lower body exoskeleton design concepts were discussed.

The following sections outline the methods used to generate a space suit joint database and set angle range of motion and torque requirements, qualitatively compare and select actuators that have been used for active control in previous exoskeleton designs, and develop conceptual designs of the space suit simulator knee and hip.

## 3.2 Space Suit Joint Database

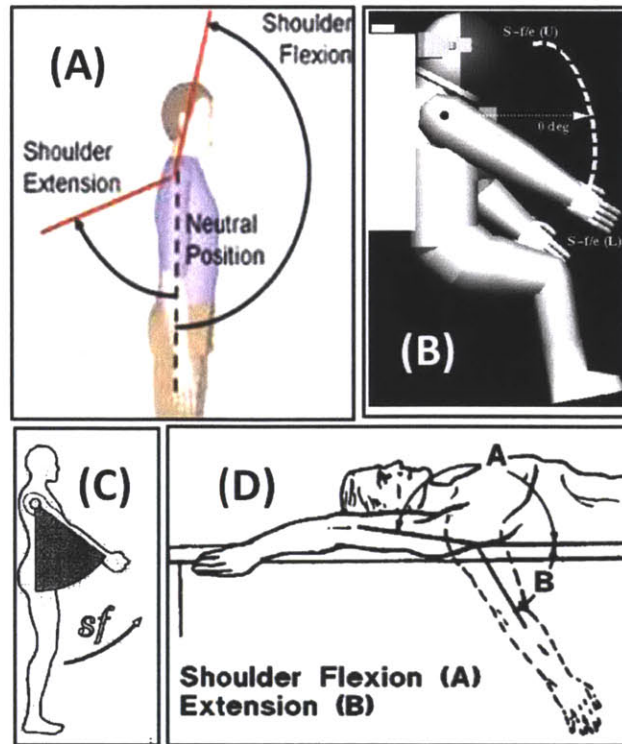
### 3.2.1 Joint Convention

A space suit joint database was created in order to compile space suit angle range of motion and joint torque data to be used to determine overall angle and torque requirements for the space suit simulator. Before developing the space suit joint database, a standard joint convention was selected. The human body coordinate system used in the human biomechanics field is used for all data and analysis in this thesis and is described by Figure 3.1 [Winter, 1990].



**Figure 3.1 Spatial coordinate system used for all data and analysis [Winter, 1990]**

There is disagreement in the literature as to the neutral position of the limbs, and which direction indicates a positive angle, and which a negative angle. Joint conventions were compared in the fields of human biomechanics and space suit research. Within space suit research, human body joint conventions vary between NASA centers, industry, and academia. An example is shown in Figure 3.2. Figure 3.2 (a) is the joint convention for shoulder flexion for a study by the David Clark Company [Ripps et al., 2011]. In this study, the neutral position is when the arm is vertically down, flexion is when the arm moves forward and up and indicates the positive direction, and extension is when the arm moves backward and up, indicating the negative direction. Figure 3.2 (b) is the joint convention for a NASA study where the subject is seated and the neutral position is when the arm is out straight in front of the subject and perpendicular to the floor, and the positive direction is when the arm moves up above the neutral point, and the negative direction is when the arm moves down below the neutral point [Morgan et al., 1996]. Figure 3.2 (c) is the joint convention for an MIT study, which follows the same convention as the David Clark Company in (a) [Schmidt et al., 2001]. Figure 3.2 (d) is the joint convention used in a human biomechanics reference guide, where the subject is lying down, and the neutral position is when the arm is pointing toward the subject's feet, with flexion indicating a positive angle, and extension indicating a negative angle, similar to (a) and (c) [NASA-STD-3000, 1994].



**Figure 3.2** Shoulder flexion joint convention from (a) Industry [Ripps et al., 2011], (b) NASA [Morgan et al., 1996], (c) Academia [Schmidt et al., 2001], (d) Human biomechanics [NASA-STD-3000, 1994]

As Figure 3.2 depicts, human body joint conventions vary between resources and research methods, and selecting and indicating the conventions to be used for each study is important. The joint conventions that were most commonly used for each degree of freedom were selected, along with the location of the neutral point, or the location of zero degrees. The S3 joint convention that was chosen is shown below in Figure 3.3 for nine degrees of freedom. The blue limb represents the reference body. The red limb movement with respect to the blue limb indicates the positive direction. For example, the positive direction for hip flexion is when the leg moves forward and up from a straight leg pointing vertically downward. These joint conventions will be used for all data and analysis in this thesis.

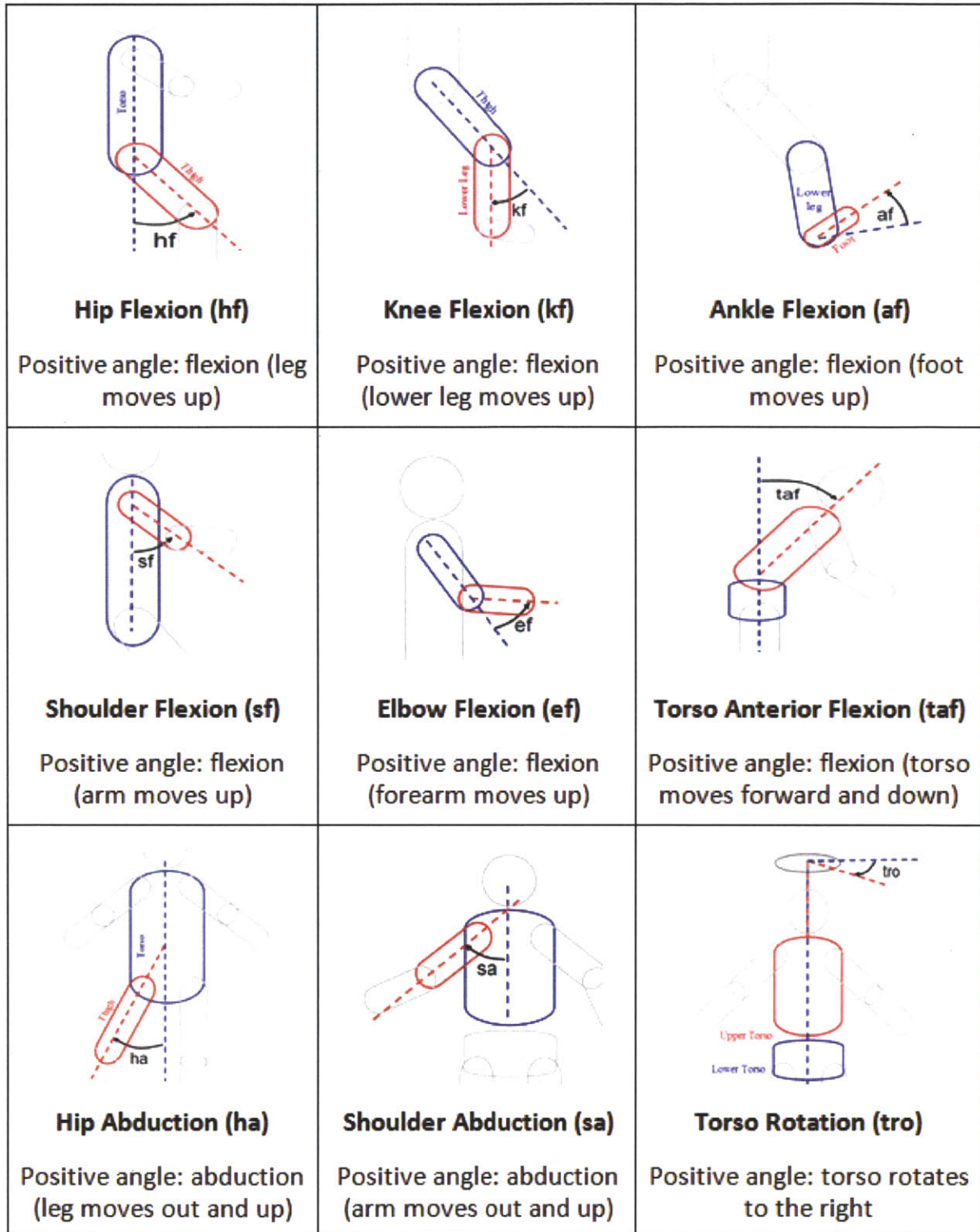


Figure 3.3 Space Suit Simulator (S3) Joint Convention



### **3.2.2 Space Suit Joint Database Methods**

Angle and torque data was collected for several pressurized space suits and degrees of freedom for each suit. Torque and angle information was collected from multiple sources that used varying methods to measure joint torque. One method used to measure joint torque was externally manipulating empty pressurized space suits through their range of motion for each degree of freedom. A second method was to measure the torque required to move components of a pressurized suit through their range of motion when a person was in the suit. Finally, a robot space suit tester was used to measure the torques required internally at each joint to move the pressurized suit through the limb range of motion.

The database consists of torque versus angle data for six pressurized space suits and fifteen degrees of freedom. For each degree of freedom, a visual depiction indicating the positive direction is included, along with the minimum and maximum torques and angle range of motion each suit is able to achieve. The pressurization level of the space suit is also indicated because torque versus angle data was taken when suits were pressurized to different levels. When the information is available, the torque versus angle curves are also included in the database for each degree of freedom. Stirling fit polynomial torque equations to the torque versus angle curves produced by experimental data taken with the MIT robot space suit tester donning an EMU space suit [Stirling, 2008], which are also included in the space suit joint database. Angle range of motion data was also collected in unsuited human experiments and is depicted and included in the database. Full human range of motion data was included because if future space suits allow for greater range of motion, the S3 could accommodate up to shirt-sleeve mobility. Finally, the overall S3 joint range of motion and torque minimum and maximum requirements were selected based on the information gathered in the database.

A representation of a portion of the space suit joint database is shown below in Figure 3.4. As shown, the knee degree of freedom is indicated, including a visual depiction of the reference body and the lower leg limb moving in the positive direction with respect to the blue body. The knee flexion abbreviation is included, along with the minimum and maximum torque each suit pressurized to the indicated level could achieve. Another tab in the database included the information for angle range of motion for each suit, pressurization level, and degree of freedom. The entire space suit joint database is included in Appendix A.



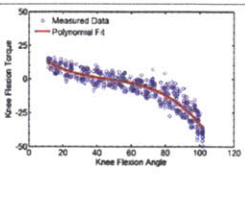
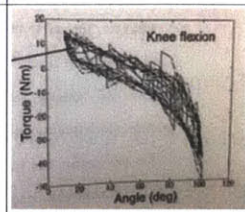

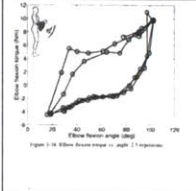
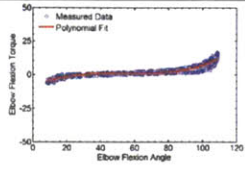
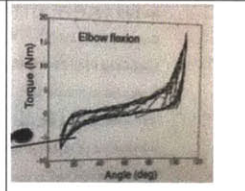

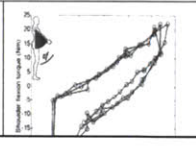
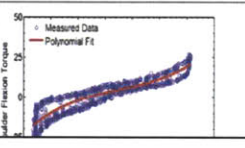
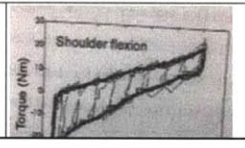
	Visual Depiction*	Abbreviation	Human Suited [1]		Torque Limitations			
			Minimum (Nm)	Maximum (Nm)	EMU Robot Suited [1] (Nm)	EMU Robot Suited [5] (Nm)	EMU Robot Suited [6] (Nm)	Polynomial Fit
KNEE		kf	-10	25				$\tau = -1.5 \times 10^{-4} \theta^3 +$
ELBOW		ef	-7	15				$\tau = 6.8 \times 10^{-5} \theta^3 -$
Shoulder Flexion		sf	-25	23				$\tau = 4.4 \times 10^{-5} \theta^3 - 0$

Figure 3.4 A snapshot of the space suit joint database depicting minimum and maximum knee and elbow torques achieved for various pressurized space suits

### 3.2.3 Range of Motion and Torque Requirements

The space suit joint database was utilized to determine the minimum and maximum angle range of motion and torque requirements for each degree of freedom for the S3. For angle range of motion, the minimum and maximum range of motion people could achieve for each degree of freedom was presented in the joint database. The angle range of motion data was collected from human biomechanics references [NASA-STD-3000, 1994; MIL-HDBK-759C, 1995; HF-STD-001, 2003; Openshaw, 2006; Soames, 2003]. In these reference guides, subjects were unsuited and in a shirt-sleeve environment. The S3 angle requirements were based off unsuited testing methods in order to accommodate future space suit designs with greater mobility.

To determine minimum and maximum joint torque requirements for each degree of freedom, the greatest negative torque measured with space suit testing methods was used, along with the greatest positive torque measured. Torque is positive or negative depending on the direction of limb motion relative to the neutral point of the space suit. The joint convention images indicate the positive direction. Negative torque is the magnitude of the torque in the negative direction with respect to the space suit's neutral point.

The overall angle range of motion and torque requirements for the S3 are shown below in Table 3.1. The minimum angle the S3 will be able to achieve for each degree of freedom is listed in the first

column, while the maximum angle is listed in the second column. The angle data was gathered from human biomechanics reference guides. The third column indicates the minimum torque the S3 will achieve for each degree of freedom, while the last column designates the maximum torque each degree of freedom will be able to achieve. The torque requirements were set based on space suit testing methods. Torque measurements for the torso lateral flexion and ankle inversion degrees of freedom were not included in the space suit joint torque testing literature, while angle range of motion data was included. If the angle and torque requirements listed in Table 3.1 are met, each pressurized space suit simulated in the S3 will have range of motion and torque values lying within the ranges indicated in the table.

**Table 3.1 S3 angle range of motion and torque requirements**

<b>Joint</b>	<b>Minimum Angle (deg)</b>	<b>Maximum Angle (deg)</b>	<b>Minimum Torque (N-m)</b>	<b>Maximum Torque (N-m)</b>
<b>Knee Flexion/Extension (KF)</b>	0	146	-40	32
<b>Elbow Flexion/Extension (EF)</b>	0	166	-18	15
<b>Shoulder Flexion/Extension (SF)</b>	-88	217	-25	32
<b>Shoulder Abduction/Adduction (SA)</b>	-25	110	-32	36
<b>Humerus Rotation (HR)</b>	-131	97	-15	24
<b>Shoulder Interior/Exterior Transverse Rotation (SI)</b>	-151	57	-23	32
<b>Hip Flexion/Extension (HF)</b>	-20	148	-41	72
<b>Hip Abduction/Adduction (HA)</b>	-30	45	-52	165
<b>Thigh Rotation (TR)</b>	-49	45	-4	3
<b>Torso Anterior Flexion/Extension (TAF)</b>	-30	55	-34	72
<b>Torso Lateral Flexion (TLF)</b>	-30	30	N/A	N/A
<b>Torso Rotation (TRO)</b>	-46	46	-7	11
<b>Ankle Flexion/Extension (AF)</b>	-91	42	-15	9
<b>Ankle Inversion (AI)</b>	-33	30	N/A	N/A
<b>Ankle Rotation (AR)</b>	-47	55	-1	1

### 3.3 Actuator Selection

A space suit simulator exoskeleton that actively controls resistance to motion is desirable over an exoskeleton with passive materials because active control allows for more precise mapping of joint torques to angles. Exoskeletons have been developed in the biomedical and military fields utilizing a

variety of actuation methods specific to the objectives of the exoskeleton. In order to select the actuators to be used for the S3 project, an extensive literature review of exoskeleton design and actuation methods was conducted. The four actuation methods compared were hydraulic actuators, pneumatic actuators, magnetorheological (MR) fluid actuators, and electric actuators.

The Berkeley Lower Extremity Exoskeleton (BLEEX) was developed to help soldiers offload the weight of up to a 75 kg (165 lb) backpack [Zoss et al., 2006]. Using 19 mm (0.75 in) bore bi-directional linear hydraulic actuators, BLEEX was able to achieve up to 130 Nm (96 ft-lb) of torque. Because linear hydraulic actuators can be bi-directional, hydraulic actuators are beneficial over other actuation methods. For each degree of freedom, one actuator could provide torque resistance in two directions, as opposed to only one direction for some actuation devices. Therefore, an exoskeleton design utilizing hydraulic actuators would be low bulk because only one actuator would be required per degree of freedom. A disadvantage to using hydraulic actuators is that they require hydraulic fluid. If a hydraulic leak were to occur, it could be uncomfortable for the human subject.

Pneumatic actuators have been used in exoskeleton devices as well. An ankle-foot orthosis was developed by researchers at the University of Michigan [Ferris et al., 2005]. Since pneumatic actuators are unidirectional, two actuators were used in the orthosis, one to aid in ankle plantar flexion, and the other to aid in ankle dorsiflexion. The actuators used in the orthosis were 16 cm (6.3 in) in length, and were able to achieve 38 Nm (28 ft-lb) of peak torque. Pneumatic actuators are lightweight and have the ability to mimic spring-like properties well. The ability to mimic spring-like properties is ideal for the S3 project, because pressurized space suit limbs exhibit spring-like properties. A disadvantage to using a pneumatic actuator is that pneumatics are only unidirectional, requiring two actuators per degree of freedom, increasing the bulk of an exoskeleton design.

Magnetorheological (MR) fluid actuators have been used in exoskeleton design to actively control resistance to motion. MR fluids are suspensions of tiny polarized particles whose rheological properties change when a magnetic field is present. When a magnetic field is applied to the fluid, the magnetic particles line up along the direction of the magnetic field. Resistance to motion increases as the magnetic field increases. Researchers at the Chinese University of Hong Kong proposed using MR fluids for an assistive knee brace which would aid the elderly in walking [Chen, 2010]. The researchers developed the actuator and found it could provide the torques needed for normal activity. MR fluid actuators can quickly change resistance with a change in the magnetic field, and they can achieve high

torques. While MR fluid actuators simulate damper-like properties well, they cannot simulate spring-like qualities well, which are a major characteristic of current gas-pressurized space suit joints.

Researchers have used electric motors in exoskeleton designs. At Honda, exoskeleton legs were developed to assist operators with walking and to partially support their bodyweight [Ikeuchi, 2009]. The electric motor used in the Honda exoskeleton legs added mass. Researchers at Yobotics (Cambridge, MA) developed RoboKnee, a prototype knee orthotic, which uses series elastic actuators to aid the user in carrying a heavy load [Pratt et al., 2004]. Electric actuators have the ability to achieve high torques, but the motors add mass and bulk.

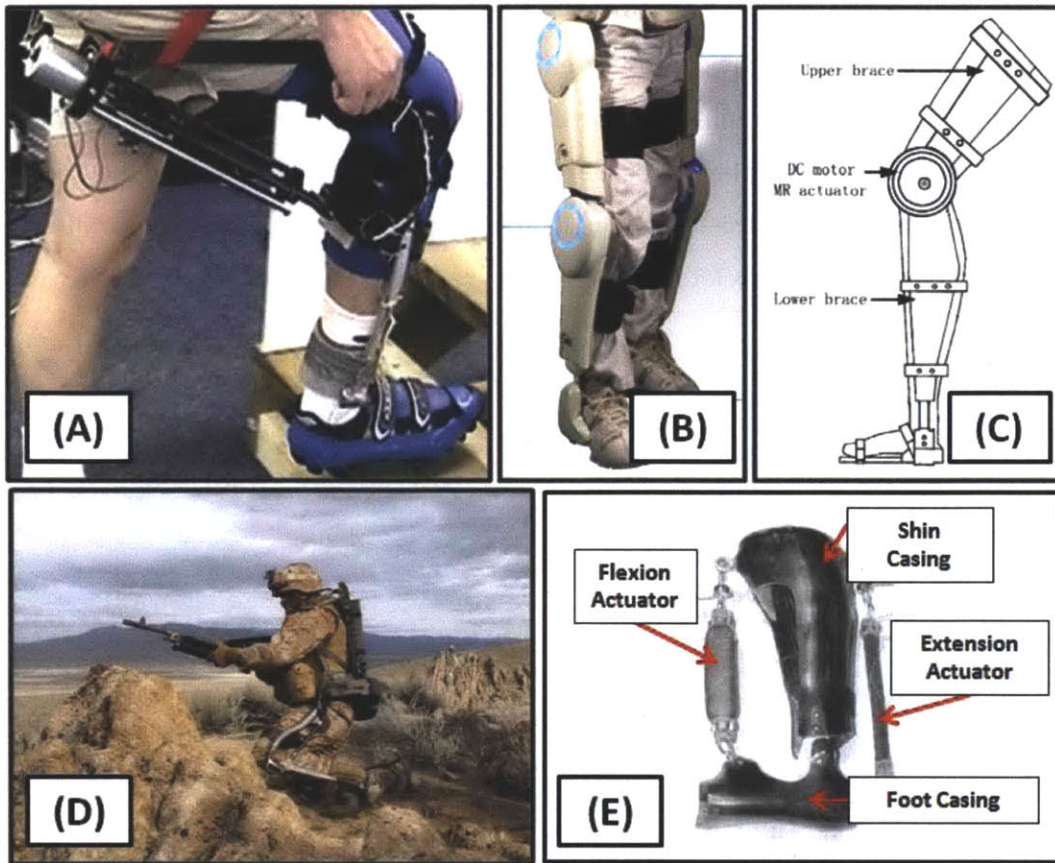
All of the actuators reviewed were able to achieve the maximum forces and speeds needed for the S3 exoskeleton as defined in the S3 torque requirements table. The weight and bulk characteristics of hydraulic, pneumatic, MR fluid, and electric actuators were compared qualitatively. Gross estimates of the weights of the actuator types used in previous exoskeleton designs were determined.

Hydraulic actuators produced by Lehigh Fluid Power (Lambertville, NJ) weigh 3.42 kg (7.55 lbs) for a 3.81 cm (1.5 inch) bore size ([www.lehighfluidpower.com](http://www.lehighfluidpower.com)). Pneumatic actuators, also known as fluidic muscles, developed by Festo (Brussels, Belgium), weigh 0.14 kg (0.3 lbs) for a 1 m (3.28 ft) long actuator with a 10 mm (0.40 in) diameter ([www.festo.com](http://www.festo.com)), which are much longer than the lengths needed for a lower body exoskeleton. The Rheo Knee, a prosthetic knee that uses an MR fluid actuator, weighs 1.52 kg (3.35 lbs) ([www.ossur.com](http://www.ossur.com)). The developers of the RoboKnee used series elastic actuators that weigh 1.13 kg (2.5 lbs) for an 45.7 cm (18 in) long actuator [Pratt et al., 2004], however, the weight of the output carriage the SEA fits in is not included, which consists of metal output plungers, spring retaining plates, and bushings, which would increase the weight and bulk. Researchers at the University of Tsukuba developed the Hybrid Assistive Limb (HAL) exoskeleton, which uses electric motors to actuate the hip and knee [Suzuki et al., 2007]. The lower body of HAL weighs 15 kg (33 lbs), which consists of four electric motors, bio-electric signal sensors, and plastic shin and thigh sheaths. Based on gross estimates of actuator weights from previous exoskeleton designs, the pneumatic actuators appear to weigh less than hydraulic, MR fluid, and electric actuators.

Qualitative comparisons of the bulk characteristics of actuators were conducted visually with the actuators used in previous exoskeleton designs. A qualitative comparison of actuators used in exoskeleton design is shown in Figure 3.5. Figure 3.5 (a) depicts the RoboKnee, with a series elastic actuator (SEA) used for knee actuation [Pratt et al., 2004]. The SEA is large, extending from the middle of the calf to behind the buttocks, in order to provide actuation for one degree of freedom. The SEA length

is 45.5 cm (18 in) and diameter is 5.8 cm (2.3 in). If multiple degrees of freedom were incorporated using SEAs, the exoskeleton would be very bulky and there would potentially be problems with actuator interference. Figure 3.5 (b) is the Hybrid Assistive Limb (HAL) exoskeleton, which uses electric motors for actuation [Suzuki et al., 2007]. Two degrees of freedom are actuated on each leg, one for knee flexion/extension, and one for hip flexion/extension. Each electric actuator is about the size of the diameter of the leg, which alone is not bulky, however the exoskeleton structure required to support the electric motors is bulky. The full height from the ground to the subject's shoulders of the exoskeleton is 1600 mm (63 in). Figure 3.5 (c) depicts a diagram of an assistive knee brace which uses a MR fluid actuator to provide resistance to knee flexion, which could aid disabled or elderly people with mobility problems [Chen et al., 2010]. The actuator is similar in size to the electric motors used in the HAL design, and the exoskeleton structure required to support the actuator is also bulky. Figure 3.5 (d) is Lockheed Martin's Human Universal Load Carrier (HULC) exoskeleton, which offloads the weight of a heavy backpack [Lockheed Martin, 2008]. The exoskeleton actuates the hip and knee joints, using one hydraulic actuator per degree of freedom. The bi-directional hydraulic actuators are small in size and the structure supporting the actuators is also low in bulk. The HULC fits soldiers with heights between 1.6 m and 1.9 m (5 ft 4 in and 6 ft 2 in). Figure 3.5 (e) is an ankle-foot orthosis that uses pneumatic actuators to actuate the ankle in flexion and extension [Ferris et al., 2005]. Two actuators are needed per degree of freedom with pneumatic actuators which adds bulk, but because the actuators are in front of and behind the leg, they would not cause interference with actuators on the opposite leg or with actuators used for additional degrees of freedom. Additionally, because of the low weight of pneumatic actuators, the exoskeleton structure that supports the actuators would not have to be as high strength as the structure of the MR fluid and electric motor exoskeletons, which reduces weight and bulk of the overall exoskeleton using pneumatic actuators.

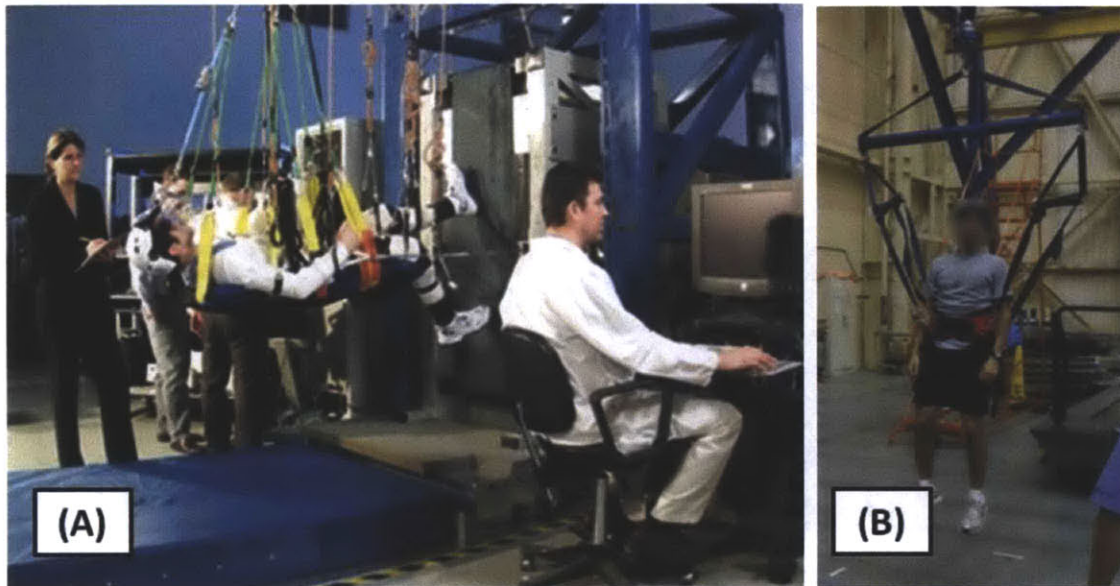
Based on visual comparisons of the bulk characteristics of exoskeletons that use various actuation devices, the hydraulic actuators use the least bulk. However, the bulk of an exoskeleton utilizing a pneumatic actuator would be less than those which use electric motors or MR fluid actuators because of the low weight of the pneumatic actuators, which results in a smaller exoskeleton structure.



**Figure 3.5 Qualitative comparison of actuators, (a) Series elastic actuators (actuator length 45.5 cm (18 in), diameter 5.8 cm (2.3 in)) [Pratt et al., 2004], (b) Electric motors (exoskeleton height from ground to shoulders 1600 mm (63 in)) [Suzuki et al., 2007], (c) MR fluid actuator [Chen et al., 2010], (d) Hydraulic actuator (fits soldiers with heights between 1.6 m and 1.9 m (5 ft 4 in and 6 ft 2 in)) [Lockheed Martin, 2008], (e) Pneumatic actuator [Ferris et al., 2005]**

Low weight and bulk characteristics of the S3 exoskeleton are ideal. An exoskeleton that is low weight and bulk can be easily packaged and transported to space suit researchers. Also, the subjects wearing the S3 will have to offset some of the weight of the exoskeleton when performing complex tasks such as kneeling, therefore a low weight exoskeleton will minimize the weight the subject has to offload. The S3 can support some of its own weight if the exoskeleton is grounded. A low bulk system is desired for the S3 for several reasons. The torques at the leg degrees of freedom will be affected greatly by the moment of inertia effects of a high weight, bulky system, therefore a low bulk exoskeleton is desired in order to minimize the moment of inertia effects of the exoskeleton components. Finally, the S3 exoskeleton will interface with specialized space suit testing equipment at NASA JSC and NASA Glenn Research Center (GRC). Space suit researchers at NASA GRC use the enhanced Zero-gravity Locomotion Simulator (eZLS), a vertical treadmill, to simulate locomotion in a partial gravity environment, as would

be seen on the moon or Mars (Figure 3.6 (a)). At NASA JSC, researchers use the Active Response Gravity Offload System (ARGOS) for the same purpose as eZLS by suspending subjects from a gantry crane system, offloading a portion of the subject's weight during dynamic motion (Figure 3.6 (b)). The subject comes in contact with several components of the eZLS and ARGOS during testing, and the S3 exoskeleton cannot interfere with the test equipment. In order to minimize interference with space suit testing equipment, a low bulk exoskeleton is needed.



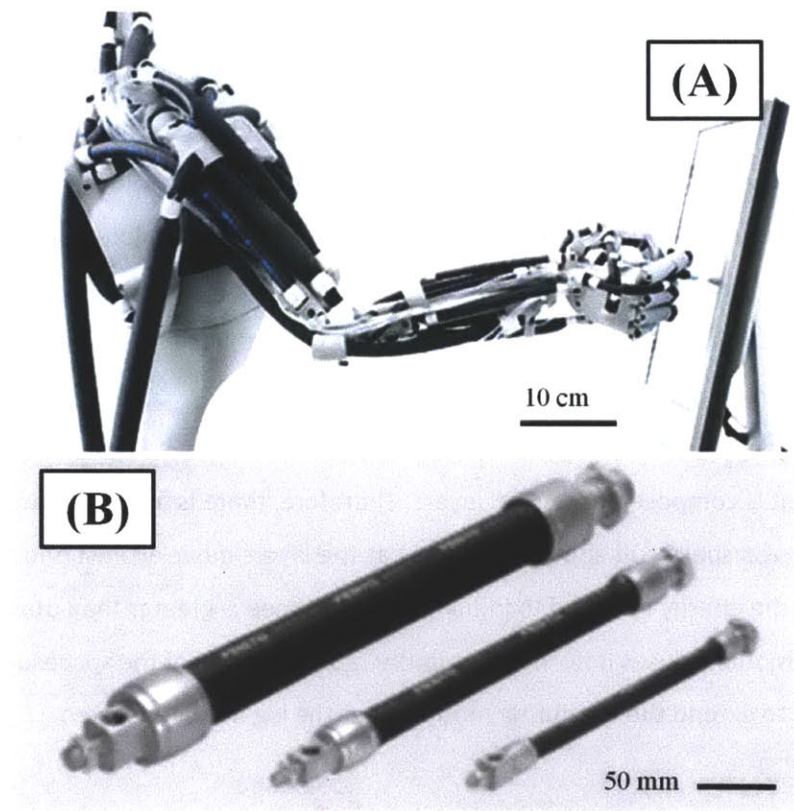
**Figure 3.6 (a) NASA GRC eZLS, (b) NASA JSC ARGOS [www.nasa.gov]**

When comparing the weight and bulk characteristics of the actuators, pneumatic and hydraulic actuators are advantageous because they provide the lowest weight and bulk, respectively. Pneumatic actuators were selected because they are more flexible and can bend around corners, such as joints, they mimic spring-like properties well, and they require air instead of a hydraulic fluid.

Pneumatic actuators have been used in robot applications. Festo (Brussels, Belgium) produces a pneumatic actuator called a fluidic muscle ([www.festo.com](http://www.festo.com)) that has been used by Festo in projects such as the bionic AirArm, which assists the human in workshop manufacture or rehabilitation, the Aqua ray, which is a robotic manta ray that performs oceanography without disturbing the natural environment, and the Airmotion ride, which is a seat used in driving and flight simulators. Fluidic muscles are hollow elastomer cylinders embedded with high strength, heat resistant aramid fibers. As the actuator fills with air, the diameter increases, decreasing the length of the actuator, which increases force output at the endpoints. The fluidic muscles are also flexible, lightweight, and can be custom



ordered by length and diameter. The Festo fluidic muscle actuators were selected for the S3 application (Figure 3.7).



**Figure 3.7 (a) Festo Airic's Arm robotic arm (dimensions when deployed 85 x 85 x 65 cm), (b) Festo fluidic muscle actuators (from left, 40 mm diameter, 20 mm diameter, 10 mm diameter) [www.festo.com]**

### 3.4 Conceptual Design

After the fluidic muscle pneumatic actuators were selected, the conceptual design was developed. The conceptual design for the S3 was based off a previous version, developed by Aurora Flight Sciences Research and Development Center (Cambridge, MA) in collaboration with MIT. In 2009, the Aurora team designed, built, and tested a space suit simulator knee prototype, in order to assess the feasibility of using actively controlled actuators to mimic the joint torque properties of a pressurized space suit [Duda, 2010]. The knee prototype is shown in Figure 3.8. The researchers purchased a commercial off-the-shelf knee brace, built a spool for the actuators to wrap around, and added extenders to the knee brace to attach to the actuators. The actuators selected were pneumatic actuators. During knee flexion, the pneumatic actuator on the front of the leg, which is shown in red on the inset in the lower left of Figure 3.8, pressurizes to resist the flexion motion, and when the knee

extends, the pneumatic actuator on the back of the leg, shown in blue on the inset, pressurizes to resist extension motion.

The expected torque output felt at the knee point of rotation follows a hysteretic pattern as the leg moves through its range of motion. The torque versus angle curves of the knee of a pressurized EMU suit are shown in Figure 3.9 and demonstrate this hysteresis behavior [Schmidt et al., 2001; Dionne 1991]. Schmidt's data was gathered using the robotic space suit tester at MIT, while Dionne's data was collected using an empty pressurized suit testing method. During knee flexion, when the knee angle increases, the torque output also increases. During extension, when the knee angle decreases, the torque output also decreases, but the torque required to extend the leg is less than the torque required to flex the leg due to space suit hysteresis.

The reason a pressurized space suit exhibits a hysteretic torque behavior is two-fold. A pressurized space suit is composed of several layers. Therefore, there is friction between the many layers of the pressurized space suit and energy is lost as the layers move against one another. Also, during knee flexion, the energy required to initially bend the knee is greater than during extension because the flexion motion causes deformations in the fabric material of the spacesuit; therefore, it requires less energy to extend the leg during motion after the leg has been flexed.

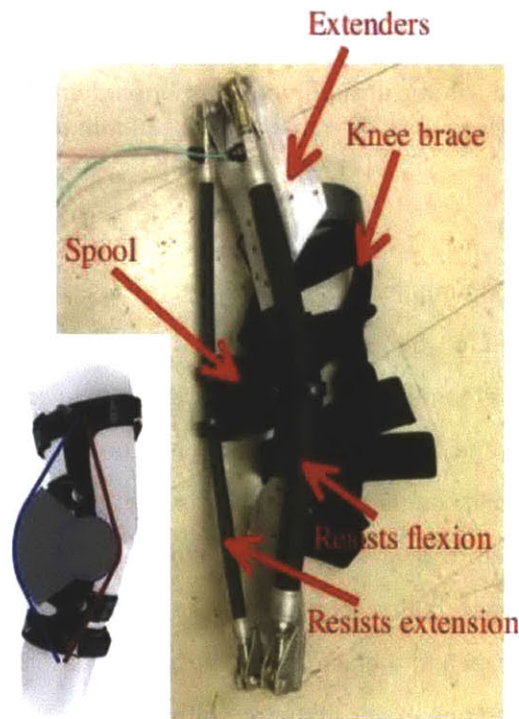
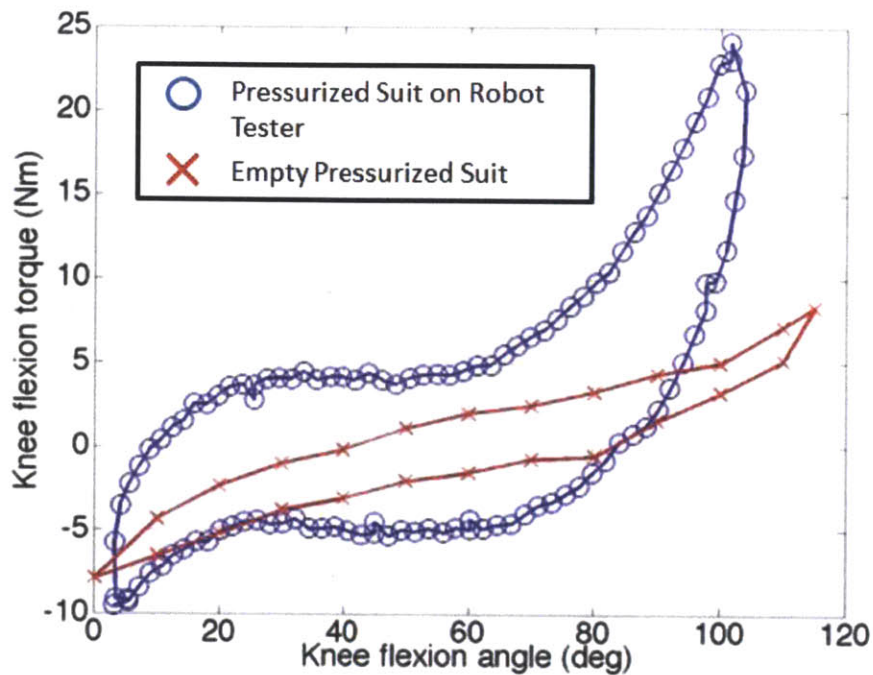


Figure 3.8 Aurora Flight Sciences Phase I S3 Knee Prototype [Duda, 2010]

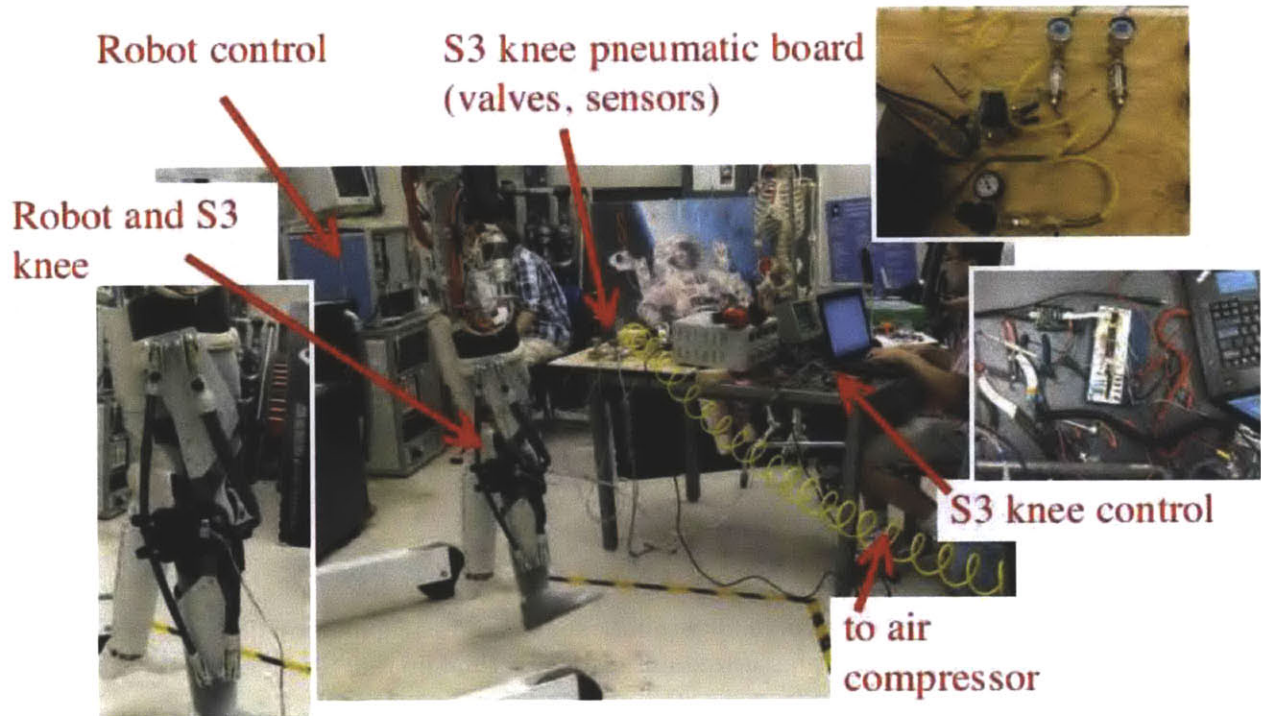


**Figure 3.9 Knee torque versus angle curve for a robotic space suit testing method (in blue) [Schmidt et al., 2001] and an empty pressurized suit testing method (in red) [Dionne, 1991]**

The S3 knee prototype was designed to accommodate 95% male anthropometry so that it could be tested on MIT's robot space suit tester (RSST). The knee simulator was installed on the RSST and the robot was commanded through 90 degrees of flexion and extension. The test setup is shown below in Figure 3.10. The left inset depicts the S3 knee installed on the robot leg. The upper right inset shows the S3 knee pneumatic board which included the solenoid valves that allowed the compressed air to pressurize the pneumatic actuators, and the sensors that indicated the pressure in each actuator. The lower right inset is the S3 controller, which supplied a pre-specified pressure to each pneumatic actuator at a given knee angle. The knee angle was measured with a potentiometer located on the spool of the S3 knee prototype. Finally, an air compressor supplied air to the solenoid valves.

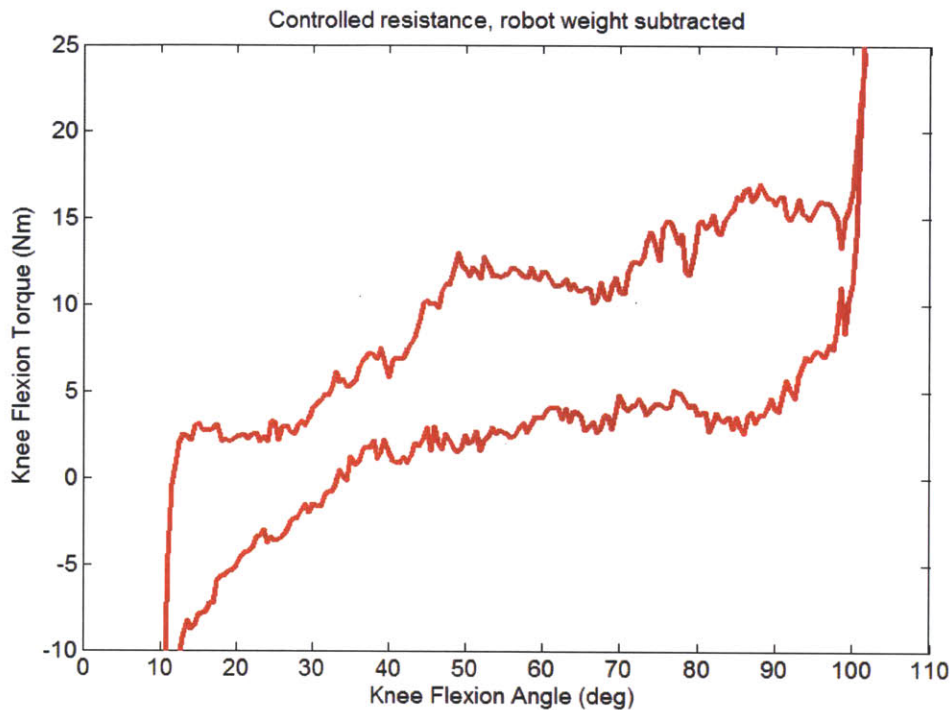
The knee torque was measured as the knee moved through 90 degrees of flexion and extension. The resulting graph is shown in Figure 3.11. As can be seen in the figure, data recorded for the S3 knee was able to approximately match Schmidt's data and achieve a similar torque versus angle relationship. Schmidt's torque values ranged from -10 Nm to 25 Nm, while the S3 knee torque values ranged from -11 Nm to 25 Nm. Schmidt's angle range of motion was from 3 degrees to 103 degrees, while the S3's angle range of motion was from 10 degrees to 100 degrees. The S3 knee was therefore able to approximately match the torque versus angle curve of a pressurized EMU space suit using the same space suit testing

method as Schmidt. The researchers concluded that it was feasible for an actively controlled exoskeleton to mimic the joint torque properties of a pressurized space suit.



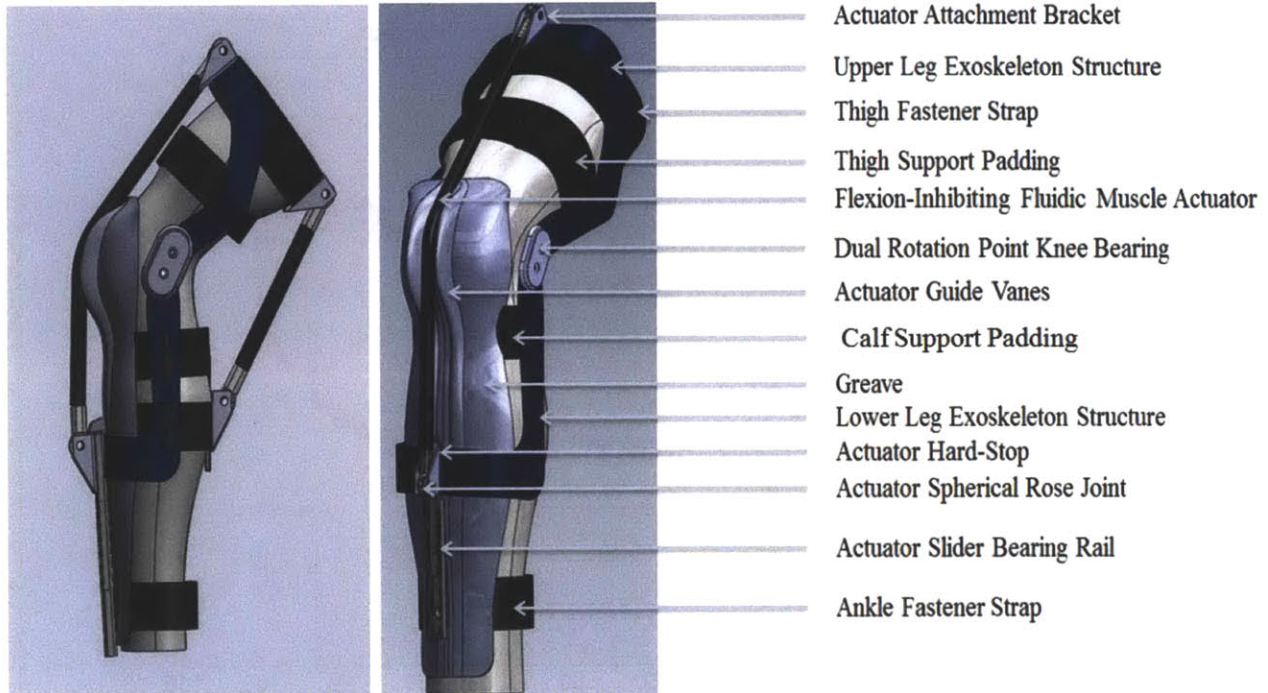
**Figure 3.10 S3 knee prototype torque testing setup [Duda, 2010]**

After successfully demonstrating the feasibility of using an actively controlled exoskeleton to mimic space suit torque behaviors, the group proposed designing the S3 lower body exoskeleton, which will have the ability to mimic the space suit torque properties for multiple lower body degrees of freedom. Improving upon the design of the first S3 knee prototype, a new knee design was developed, along with a hip flexion and extension degree of freedom, a hip abduction and adduction degree of freedom, and a third joint degree of freedom.



**Figure 3.11 Aurora Flight Sciences S3 knee prototype torque vs. angle curve [Duda, 2010]**

The detailed drawing of the new S3 knee design is depicted in Figure 3.12. There are two pneumatic actuators attached to the exoskeleton, one that runs along the front of the leg and over the knee, and another that runs behind the leg. The actuators attach to the exoskeleton at the actuator attachment bracket. The leg exoskeleton structure is depicted in blue. The uppermost black strap is the thigh fastener strap which attaches the exoskeleton to the subject by wrapping around the subject's upper thigh. There is an additional thigh strap that adds support and includes padding along the subject's thigh. The actuator that runs over the knee is the fluidic muscle actuator that inhibits flexion motion by pressurizing during leg flexion. The dual rotation point knee bearing allows the exoskeleton to bend at the knee point of rotation. The actuator guide vanes keep the actuator confined to the front of the leg. The calf padding adds support and additional padding for the subject. The groove structure is a hard surface that conforms to the subject's leg and provides knee and shin protection from the pressurized actuator. The groove also includes the actuator guide vanes. At the actuator attachment bracket on the lower part of the leg there is a hard-stop, which will not allow the actuator to move past the point of the attachment bracket. The hard-stop at one end will allow the actuator to move along a slider rail when the actuator is not pressurized. Likewise, the actuator on the back of the leg will also move along a slider at the lower endpoint of the actuator when the leg is bent to large angles of flexion or when the back actuator is not pressurized.



**Figure 3.12 S3 knee joint design [drawing by Roedolph Opperman, Aurora Flight Sciences]**

The sliding rails were included in the S3 knee design in order to prevent actuator buckling. The first S3 knee prototype design did not include sliding rails, which caused the actuators to buckle when the actuators were not pressurized. After several buckling cycles, the actuator fatigue could be accelerated, possibly leading to actuator failure. Therefore, the enhanced S3 knee design includes sliding rails and hard-stops to allow the actuator to slide along the rails when not pressurized.

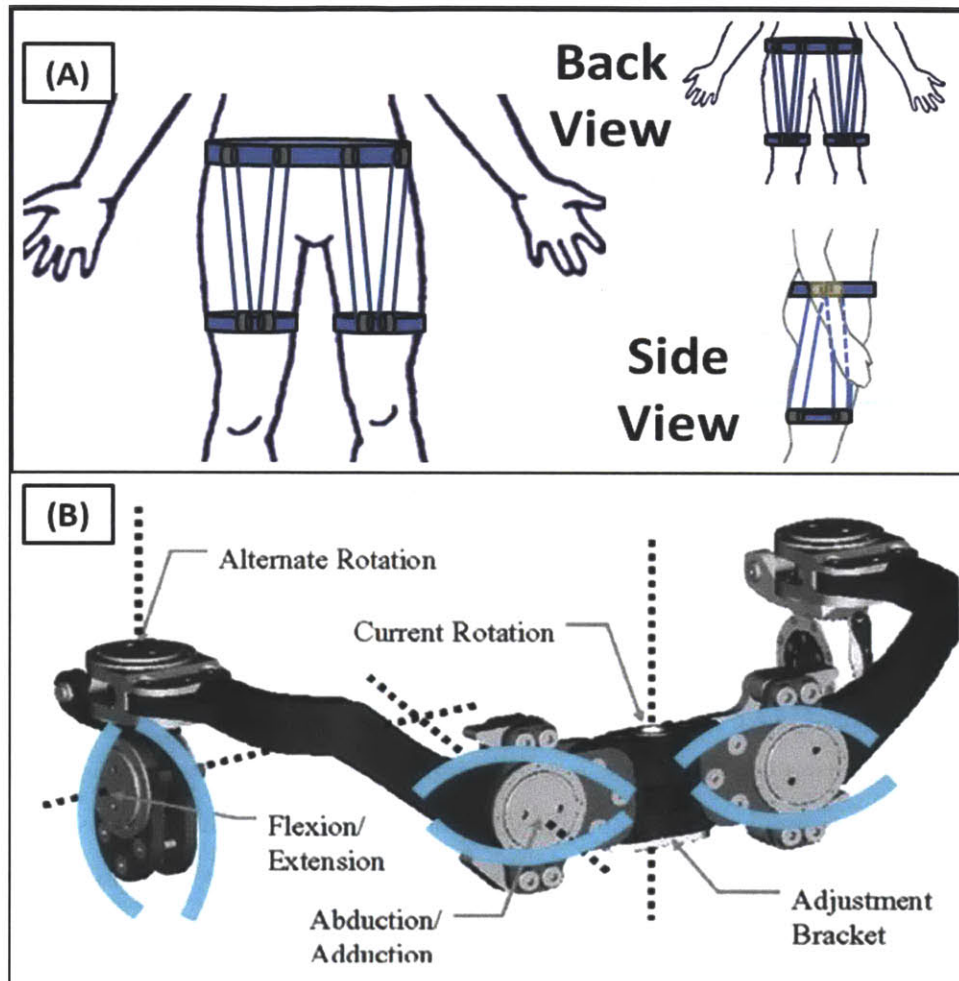
The exoskeleton design places the actuators directly in front of and behind the leg. In the first S3 knee prototype design, the actuators were offset laterally so that they attached to the outer side of the subject's leg. This caused out of plane torques and the exoskeleton was pulled outward away from the leg during large knee flexion angles. For this reason, the actuators in the enhanced knee design were placed directly in front of and behind the leg to eliminate any out of plane torques as the leg moves through its range of motion.

A second joint that will be implemented in the S3 project is the hip, particularly the flexion and extension degree of freedom, and the abduction and adduction degree of freedom. The hip joint is in the conceptual design phase and two conceptual designs have been developed. The first conceptual design is shown in Figure 3.13 (a). This design has four pneumatic actuators on the front of the body, and an additional four on the back of the body. The point of rotation of the hip is between each of the two actuators on each leg. The location of the actuators will allow for active control of two degrees of

freedom, flexion/extension, and abduction/adduction, in a single design. During hip flexion, when the leg moves up and in front of the subject, the two actuators on the back of the leg will pressurize to resist that motion. The opposite is true when the person extends their leg. When the subject abducts their leg, or moves it out and away from the body, the actuators close to the midline of the body, one actuator on the front of the leg and one actuator on the back of the leg, will pressurize to resist the abduction motion.

The conceptual design shown in Figure 3.13 (a) does not use an exoskeleton frame. Therefore, while the design is simple, lightweight, and able to provide torque resistance for two degrees of freedom, the actuator will pressurize against the subject's leg, which may cause subject discomfort. Also, because the actuators will not be connected to a hard surface, but a flexible one, hip torque calculations may be difficult to compute.

Figure 3.13 (b) depicts a left dorsal side view of an alternative hip design concept, based on the Berkeley Lower Body Exoskeleton (BLEEX) design [Zoss et al., 2006]. The Berkeley design, shown in grey, allows for active control of two degrees of freedom, but also allows for passive movement of hip rotation. The vertical dotted line labeled as "current rotation" falls directly at the midline of the subject's lower back, just above the hips, and allows for hip rotation. Alternatively, passive hip rotation could be allowed at each leg, indicated by the "alternate rotation" label. Two circular points of rotation on the dorsal side of the subject allow for hip abduction and adduction, and are labeled "abduction/adduction" in the picture. Finally, circular points of rotation labeled "flexion/extension" allow for hip flexion and extension movement. The Berkeley researchers selected the locations of the abduction/adduction and flexion/extension points of rotation so that they would both rotate in line with the human's natural hip point of rotation, which is shown at the intersection of the abduction/adduction and flexion/extension dotted lines.



**Figure 3.13 Hip conceptual designs (a) No exoskeleton frame, (b) Uses an exoskeleton based on the Berkeley Lower Body Exoskeleton (BLEEX) design [Zoss et al., 2006] with pneumatic actuators shown in blue**

The S3 hip design would include two pneumatic actuators per actively controlled degree of freedom, which wrap around the degree of freedom points of rotation. For example, to resist hip abduction, the actuator on the bottom of the abduction/adduction point of rotation would pressurize, and to resist hip adduction, the actuator on the top of the abduction/adduction point of rotation would pressurize. Likewise, to resist hip flexion motion, the actuator on the back of the flexion/extension point of rotation would pressurize, while the actuator on the front would pressurize to resist hip extension. Therefore, this alternative hip conceptual design would also allow for two actively controlled hip degrees of freedom movement in one design, and would also include an exoskeleton structure to support the pressurized pneumatic actuators. While this design would provide more subject comfort and allow for quantifiable torques due to its hard structure, it is a much more complex design.



### 3.5 Summary

The first step in the S3 research effort was to create a space suit joint database, which was a compilation of human range of motion and space suit joint torque data from several resources. The space suit joint database was created and used to set the overall angle range of motion and torque bounds for the S3. Once the angle and torque bounds were set, actuators that could be used for active control were compared qualitatively to select actuators to be used on the S3. Actuators were desired that had low weight and low bulk characteristics while having the ability to achieve the desired torques for each degree of freedom. A low weight, low bulk exoskeleton design is desired to improve ease of packaging and transportation, to minimize the weight subjects have to offset, and to provide compatibility with space suit testing equipment at NASA centers. Upon qualitative comparisons between hydraulic, pneumatic, MR fluid, and electric actuators, the pneumatic actuators were selected for use in the S3 design. Pneumatic actuators have desirable low weight characteristics, and have the ability to mimic the spring-like properties of pressurized space suits. The design of the S3 knee included two pneumatic actuators, both along the midline of the leg, one in front of the leg and one behind the leg. A greave design was included, which provided protection for the knee and shank from the pressurized actuator. Finally, two conceptual hip designs were presented, one including an exoskeleton structure, and the other without. The advantages and disadvantages of each hip design were discussed. The conceptual knee design presented will be implemented in a S3 computer simulation described in Chapter 4, which will help determine feasible design solutions regarding the dimensions of the exoskeleton components and the pneumatic actuators.



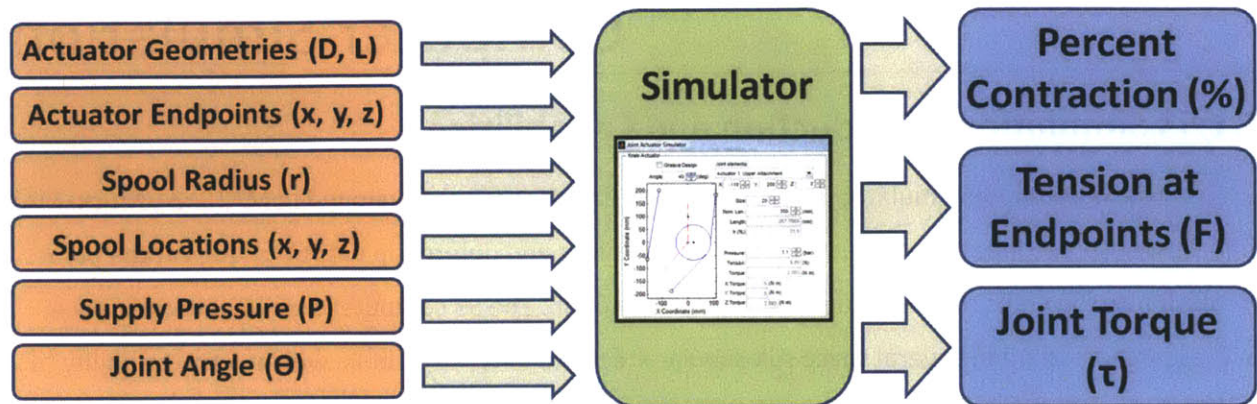
## 4.1 S3 Simulation Introduction and Capabilities

The S3 computer simulator is a graphical user interface (GUI) developed in MATLAB (Natick, MA) that allows users to input space suit simulator joint designs and determine output torques at the point of rotation as the limbs move through their range of motion. The S3 computer simulator allows space suit researchers to trade several space suit simulator designs in terms of bulk, weight, and the ability to match torque versus angle curves of actual pressurized space suits. The goal of the S3 project is to develop a low bulk and lightweight design that accurately mimics joint torque properties of pressurized space suits, to be used as an alternative to NASA pressurized suits for space suit research.

The motivation for creating a computer simulation was to provide an iterative design capability to determine feasible design solutions that closely match the torque versus angle curves of actual pressurized space suits, while minimizing weight and bulk. The computer simulator can be used as a design tool to determine a set of actuator geometries and endpoint locations that are feasible for the S3 design. Along with specifying actuator geometries and endpoint locations, users can choose the necessary supply pressure for the actuators to achieve the desired torques at the point of rotation about the joint. The simulator can help determine which supply pressures achieve the desired torques at specified joint angles, which is critical information for the design of the S3 controller.

Figure 4.1 is a flowchart showing inputs and outputs from the MATLAB computer simulator. The user can specify the diameter and lengths of the actuators, the location of both the upper and lower endpoints of each of the actuators, the geometry and locations of the spools that the actuators wrap around, the pressure to supply to the actuators, and finally the joint angle. Any of the inputs to the simulator can be changed while the GUI is running. Given the specified inputs, the simulator will then calculate the percent contraction of each of the actuators, the tension at the endpoints of each of the actuators, and the joint torque at the specified joint angle, supply pressure, and actuator information. The input process can be repeated as the user moves the limb through its range of motion, and the percent contraction of the actuators, the tensions at the endpoints of the actuators, and the joint torque will be updated accordingly. The user can then compare the torque versus angle information

gathered for each design to actual pressurized space suit data. The designs with the least error from the actual pressurized space suit data will be further investigated for potential use in the S3 design.



**Figure 4.1 S3 computer simulator inputs and outputs**

The initial S3 computer simulator was created at Aurora Flight Sciences and consisted of a 2D visual depiction of the S3 knee design that calculated the magnitude of the torque at the knee with two actuators wrapped around spools. Figure 4.2 is a view of the current S3 computer simulator GUI, which has been enhanced and expanded by the author to include three-dimensional (3D) knee torque in the x, y, and z directions, along with additional features that allow the S3 knee conceptual design to be implemented. The graphic is a conceptual S3 knee design, depicted in the sagittal plane. The red dotted lines represent the midline of the limbs of the human subject. The red dotted lines in the knee simulator graphic represent the midline of the upper leg and the lower leg. The location of the bend in the red dotted lines is the point of rotation of the joint, in this case the knee. The large blue circle represents the location and the radius of the spool that the front pneumatic actuator wraps around. The blue lines represent the pneumatic actuators, one on the front of the leg, and the other on the back of the leg. The actuators turn from blue (operating range) to pink (out of range) when the percent contraction of the actuators are out of the actuator specification range. Each actuator can stretch up to 3% of its length, and contract up to 25% of its length. Outside of these limits, the GUI provides a visual reference with the actuator turning from blue to pink. The small circles at the ends of each of the actuators represent the location of the upper and lower endpoints of the actuators. The coordinate system is in millimeters and (0, 0, 0) indicates the point of rotation, which is the knee joint in this case. The +x direction is anterior to the knee point of rotation, while the -x direction is posterior. The +y direction is superior to the knee point of rotation, while the -y direction is inferior. Although the z component of the S3 knee design is not shown in the graphic, the MATLAB GUI has the ability to enter the z locations as well. The +z

direction is lateral to the knee point of rotation, while the  $-z$  direction is medial to the knee point of rotation. Therefore, the upper attachment of the back actuator is located at (-110 mm, 200 mm, 0 mm) in Figure 4.2, which indicates an endpoint 110 mm (7.3 in) posterior to the knee, 200 mm (7.9 in) superior to the knee, and 0 mm lateral to the knee.

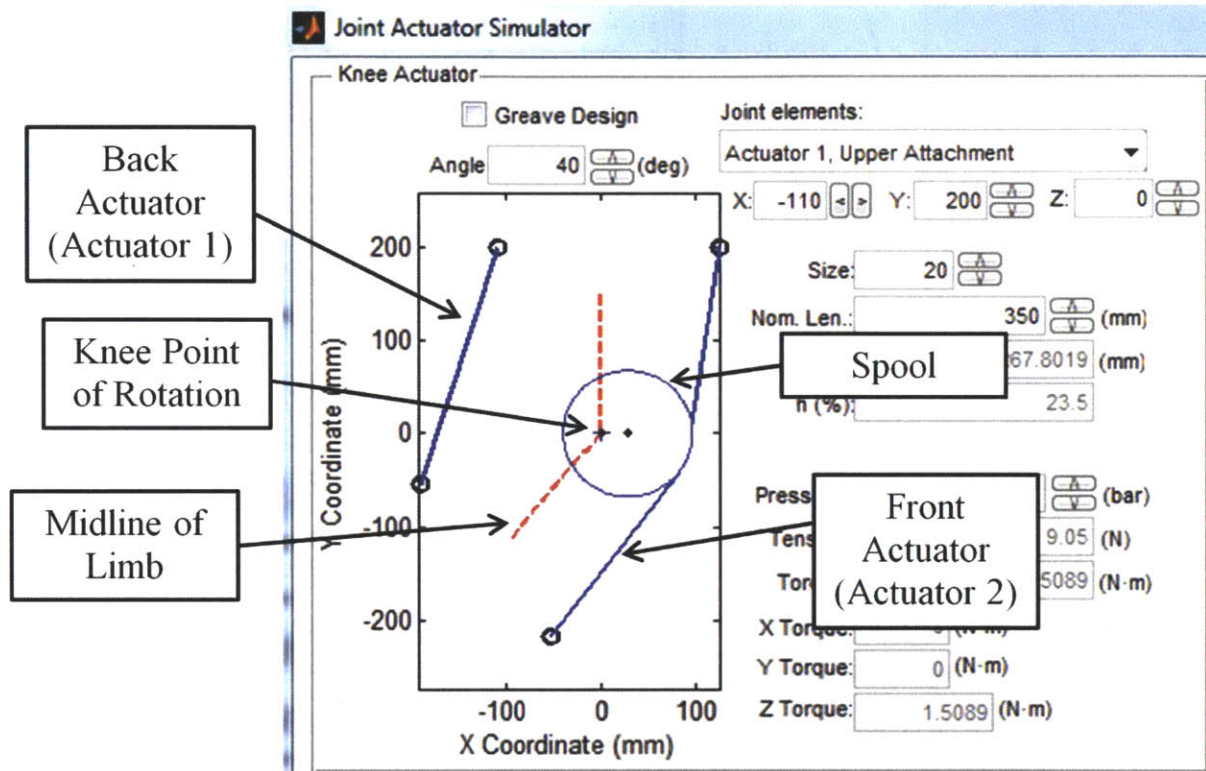
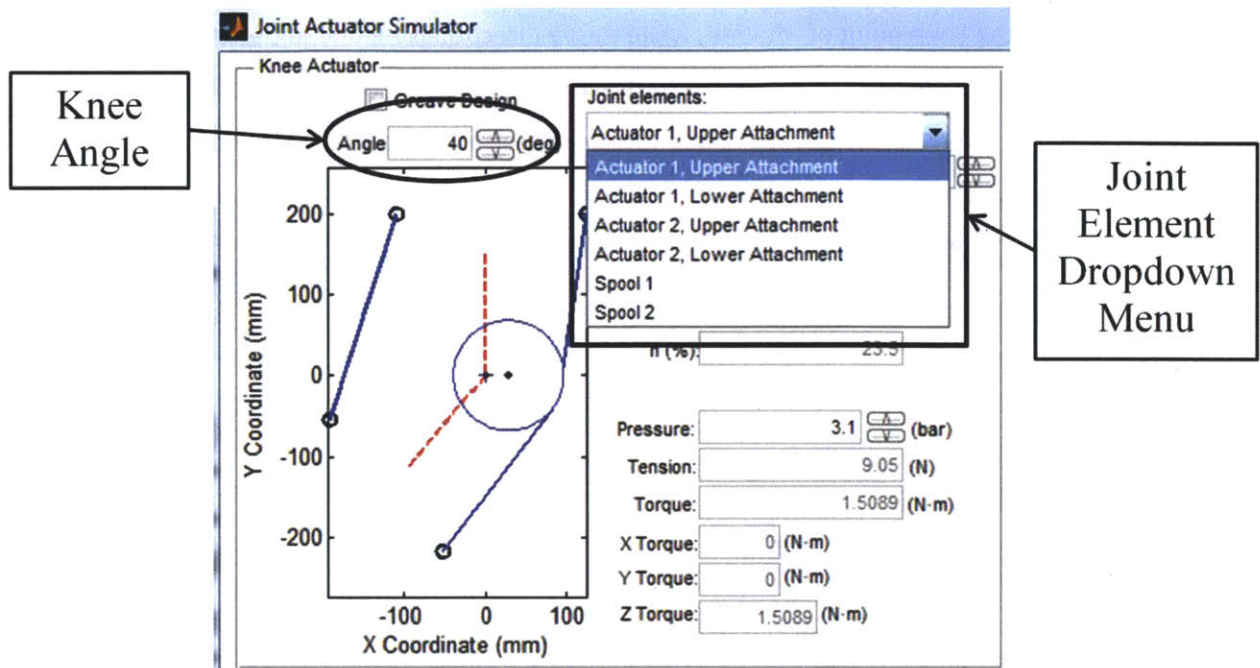


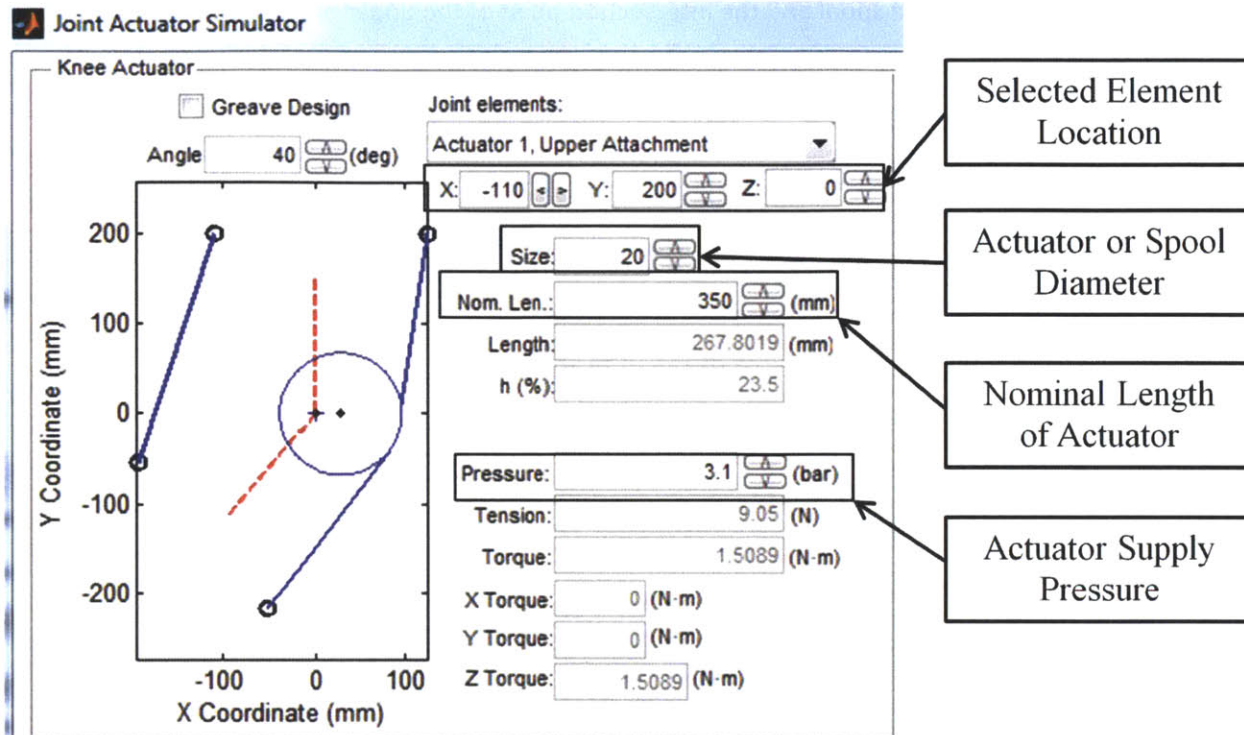
Figure 4.2 S3 computer simulator GUI

The user can change the angle the leg is moving through with the arrow pushbuttons above the graphical leg depiction. An angle of zero degrees indicates a straight leg, while an angle of 90 degrees indicates a perpendicular bent leg. The graphic in Figure 4.3 indicates a knee bent at a 40 degree angle. To change the location of the actuators and spools, the user can select which joint element to change by selecting the element from the joint element dropdown menu, as shown in Figure 4.3. The user can select the upper or lower attachment endpoints for either the back actuator (actuator 1) or the front actuator (actuator 2), along with either the back spool or the front spool. Actuator 1 and spool 1 are the elements on the back of the leg, while actuator 2 and spool 2 are the elements on the front of the leg. If the exoskeleton design being implemented does not include a spool on one side of the leg, as in the case of Figure 4.3, the spool can be modeled with a radius of 0 mm, and the actuator will not wrap around the spool.



**Figure 4.3 S3 computer simulator with the knee angle pushbuttons and the joint elements dropdown menu indicated**

After the joint element is selected, the user can change the x, y, and z location in millimeters of the selected element with the pushbuttons, as shown below in Figure 4.4. The pushbuttons that indicate size allow the user to input the diameter in millimeters of the actuators or the radius in millimeters of the spools, whichever is selected in the joint elements dropdown menu. The “nom. len.” pushbuttons indicate the nominal length of the selected actuator. The final input the user can select is the actuator supply pressure. The actuator specifications allow the actuators to be pressurized from a range of 0 kPa up to 500 kPa (0 bar up to 5.0 bar). All of the user inputs into the S3 computer simulator are indicated by white boxes, while the S3 computer simulator outputs are indicated by grayed out boxes.



**Figure 4.4 Additional user inputs for the S3 computer simulator**

The outputs of the S3 computer simulator GUI are shown in Figure 4.5. Length indicates the value of the current length of the actuator selected in the joint elements dropdown menu, given the current knee bend angle. The current lengths of the actuators change as the knee angle changes. As the knee flexion angle increases, the length of the actuator on the front of the leg increases, while the length of the actuator on the back of the leg decreases. The opposite occurs when the knee angle decreases during knee extension.

The MATLAB simulator calculates the current length by first determining whether the actuator is bent around a spool. When the actuator is straight, as is the back actuator in the case of Figure 4.5, the simulator calculates the actuator length as the straight line distance between the upper endpoint and the lower endpoint of the actuator. When the actuator is bent around a spool, as is the case of the front actuator in Figure 4.5, the simulator calculates the straight line distance between the upper attachment point of the actuator and the point where the actuator tangent line intersects the circle that represents the spool and sums that distance with the straight line distance between the lower attachment point of the actuator and the point where the actuator tangent line intersects the circle. Finally, the simulator adds the length of the arc along the spool circumference between the intersection point of the lower

portion of the actuator and the spool and the intersection point of the upper portion of the actuator and the spool.

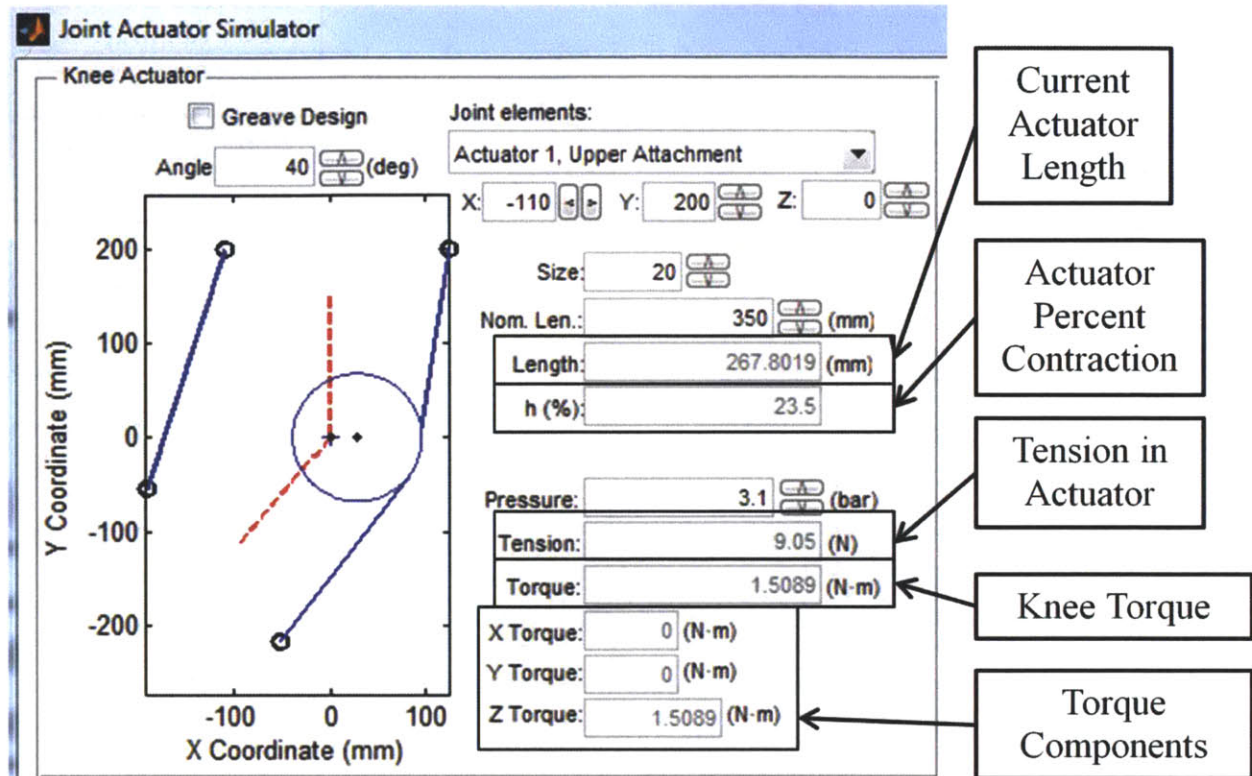


Figure 4.5 S3 computer simulator outputs

The actuator percent contraction is given by  $h$  (%) in the S3 computer simulator. The simulator calculates actuator percent contraction by the following equation:

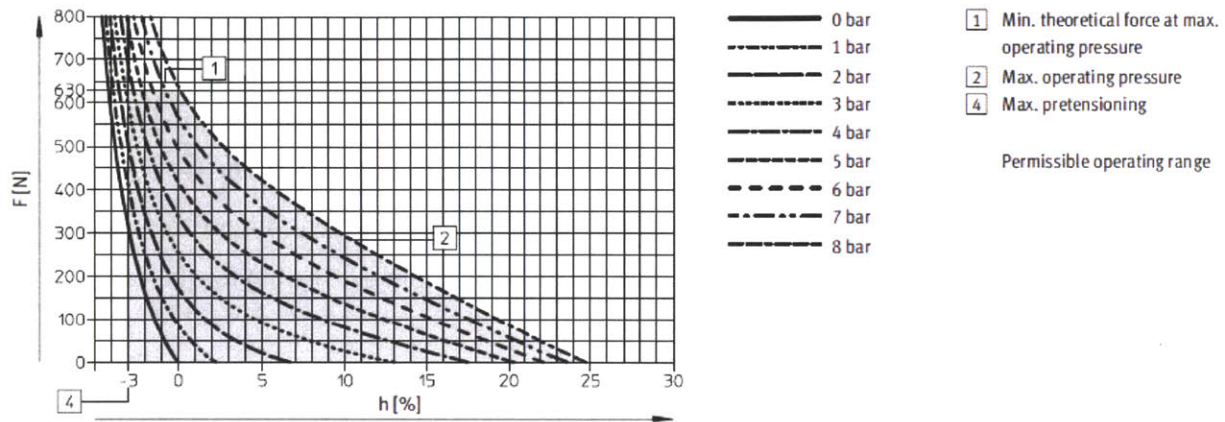
$$h (\%) = 1 - \frac{l}{l_0}$$

where  $h$  is the percent contraction of the actuator,  $l$  is the current length of the actuator, and  $l_0$  is the nominal length of the actuator.

The pneumatic actuator manufacturer, Festo (Brussels, Belgium), created graphs indicating the relationship between the tension force of the actuator, the supply pressure to the actuator, and the percent contraction of the actuator given the diameter of the actuator. An example graph is shown below in Figure 4.6. The operating range of the actuator falls within the gray area of the graph. The actuator can stretch up to 3% of its nominal length and can contract up to 25% of its nominal length. For a given percent contraction, greater supply pressures produce greater tensions. For a given supply pressure, greater percent contractions produce smaller tensions. The tension, percent contraction, and supply pressure relationships are programmed into the S3 MATLAB simulator. To find the tension in the



actuator, the nominal length of the actuator and the supply pressure to the actuator are input into the simulator by the user. The simulator then calculates the current length and percent contraction of the actuator based on the knee angle. Finally, the simulator uses the relationships depicted in Figure 4.6 to determine the tension in the actuator. Linear interpolation was used in the simulator to determine the tension in actuators with supply pressures between the integer values.



**Figure 4.6 Graph depicting relationship between tension force, percent contraction, and supply pressure for a 10 mm (0.4 in) diameter fluidic muscle actuator [www.festo.com]**

To calculate the knee torque in the S3 MATLAB simulator, the leg was modeled as a two link system, fixed at the hip point of rotation (Figure 4.7 (a)). The upper leg, or thigh, represents one link, fixed at the hip, while the lower leg, or shank, represents the other link. The actuator is the third body, which acts on both the upper and the lower leg. If the three components are separated, the forces and moments on each of the components can be calculated. Figure 4.7 (b) depicts the forces acting on the pneumatic actuator on the front of the leg. Assuming no acceleration of any of the components, the sum of forces acting on the pneumatic actuator can be set to zero. Therefore, because the tension in the actuator is known, the normal force the pneumatic actuator induces on the front of the leg can be calculated.

A diagram of the lower leg component is shown in Figure 4.7 (c). Once again, assuming no acceleration, the sum of the forces on the lower leg component is zero, and the sum of the moments about the knee point of rotation is also zero. Since the normal force the pneumatic actuator induces on the front of the leg has been calculated, and the tension force in the actuator is known, the forces imposed on the knee joint in the x and y direction can be calculated. The resulting knee torque is given by the following equations:

$$\sum M_{Knee} = \tau_{Knee} + (\mathbf{r}_1 \times \mathbf{T}) = 0$$

$$\tau_{Knee} = -(\mathbf{r}_1 \times \mathbf{T})$$

where  $M_{Knee}$  is the moment about the knee,  $\tau_{Knee}$  is the knee torque,  $\mathbf{r}_1$  is the distance from the knee point of rotation to the lower endpoint of the pneumatic actuator, and  $\mathbf{T}$  is the tension force in the actuator. Therefore, during knee flexion the knee torque is dependent on the distance to the lower endpoint of the front pneumatic actuator and the tension force in the pressurized actuator. Likewise, during knee extension the knee torque is dependent on the distance to the lower endpoint of the back pneumatic actuator and the tension force in the back of the leg actuator.

A diagram of the forces and moments imparted on the upper leg component is shown in Figure 4.7 (d). Assuming no acceleration, the forces acting on the upper leg component can be set equal to zero and the forces acting on the hip point of rotation can be calculated. The moments about the hip point of rotation can also be set equal to zero and the hip torque can be determined. The hip torque can be calculated by the following equation:

$$\sum M_{Hip} = \tau_{Knee} + \tau_{Hip} + (\mathbf{r}_2 \times \mathbf{T}) + (\mathbf{r}_3 \times \mathbf{N}) + (\mathbf{r}_3 \times \mathbf{F}_{k,x}) = 0$$

$$\tau_{Hip} = -\tau_{Knee} - (\mathbf{r}_2 \times \mathbf{T}) - (\mathbf{r}_3 \times \mathbf{N}) - (\mathbf{r}_3 \times \mathbf{F}_{k,x})$$

where  $M_{Hip}$  is the moment about the hip,  $\tau_{Knee}$  is the knee torque,  $\tau_{Hip}$  is the hip torque,  $\mathbf{r}_2$  is the distance from the hip point of rotation to the upper endpoint of the pneumatic actuator,  $\mathbf{T}$  is the tension force in the actuator,  $\mathbf{r}_3$  is the distance from the hip point of rotation to the knee point of rotation,  $\mathbf{N}$  is the normal force from the actuator acting on the knee point of rotation, and  $\mathbf{F}_{k,x}$  is the knee reaction force in the x direction. Therefore, the hip torque is dependent on the knee torque, the distance from the hip point of rotation to the upper endpoint of the actuator, the tension in the actuator, the distance from the hip point of rotation to the knee point of rotation, the normal force from the actuator acting on the knee, and the knee reaction force in the x direction. This torque equation will be used in future versions of the S3 MATLAB simulator, when the hip conceptual design is implemented.

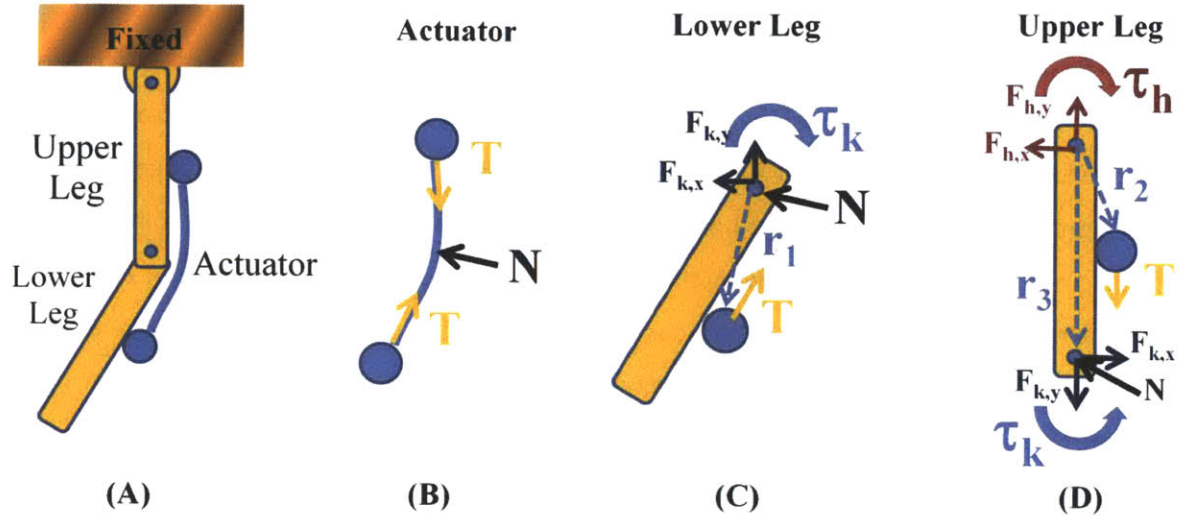


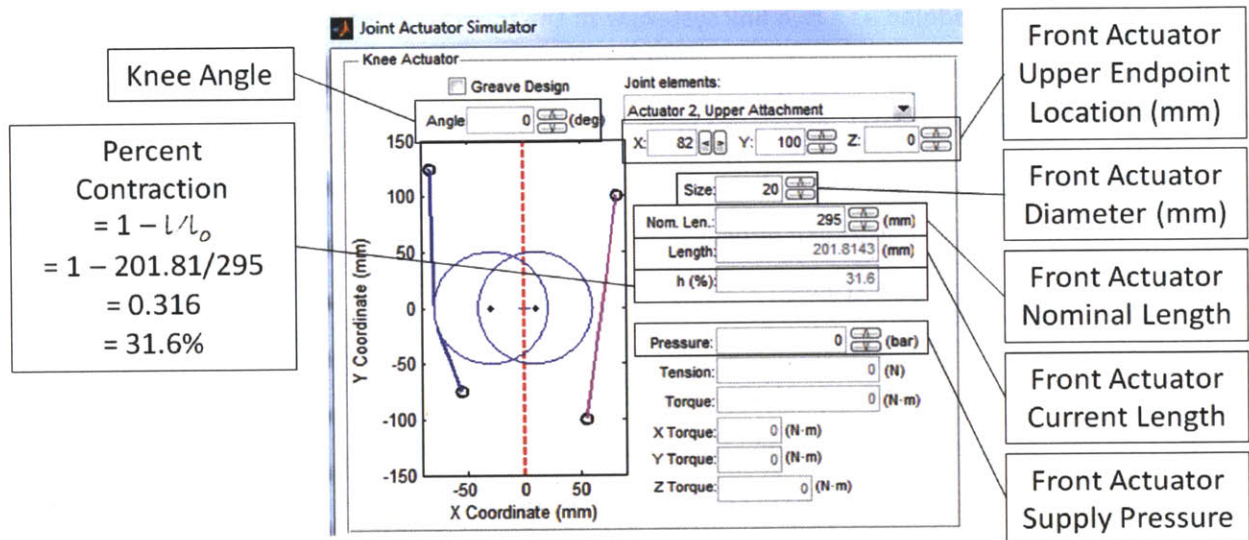
Figure 4.7 The leg modeled as a two link system with the forces and moments indicated on each component

## 4.2 Example Space Suit Simulation

As an example, a design for a person with 50% female anthropometry was input into the S3 computer simulator. The actuators lied directly in front of and behind the leg, in accordance with the midline of the leg, and wrapped around circular spools attached to the upper leg, one on the back of the leg and one on the front of the leg. The back actuator was 10 mm (0.4 in) in diameter and 200 mm (7.9 in) in length nominally, and the front actuator was 20 mm (0.8 in) in diameter and 295 mm (11.6 in) in length nominally. The spools had a 50 mm (2 in) radius. The thigh, knee, and calf circumferences of a 50% female are 51.6 cm (20.3 in), 34.6 cm (13.6 in), and 34.1 cm (13.4 in), respectively [NASA-STD-3000, 1994]. Assuming the thigh, knee, and calf are circular, the thigh, knee, and calf radii are 8.2 cm (3.2 in), 5.5 cm (2.2 in), and 5.5 cm (2.2 in), respectively. Therefore, the x locations of the upper and lower endpoints of the front actuator are 8.2 cm (3.2 in) and 5.5 cm (2.2 in), respectively. Likewise, the x locations of the upper and lower endpoints of the back actuator are -8.2 cm (-3.2 in) and -5.5 cm (-2.2 in) from the knee point of rotation. The complete design is included in Appendix B.

The x, y, and z locations of each of the endpoints of the actuators and the center points of the spools were input into the S3 computer simulator, along with the actuator diameters and nominal lengths. A view of the simulator at zero degrees of knee flexion with the actuator and spool geometries entered is depicted in Figure 4.8. As shown, the knee angle is 0 degrees, and the x, y, and z locations of the upper attachment endpoint of actuator 2, the front actuator, are 82 mm (3.2 in), 100 mm (3.9 in),

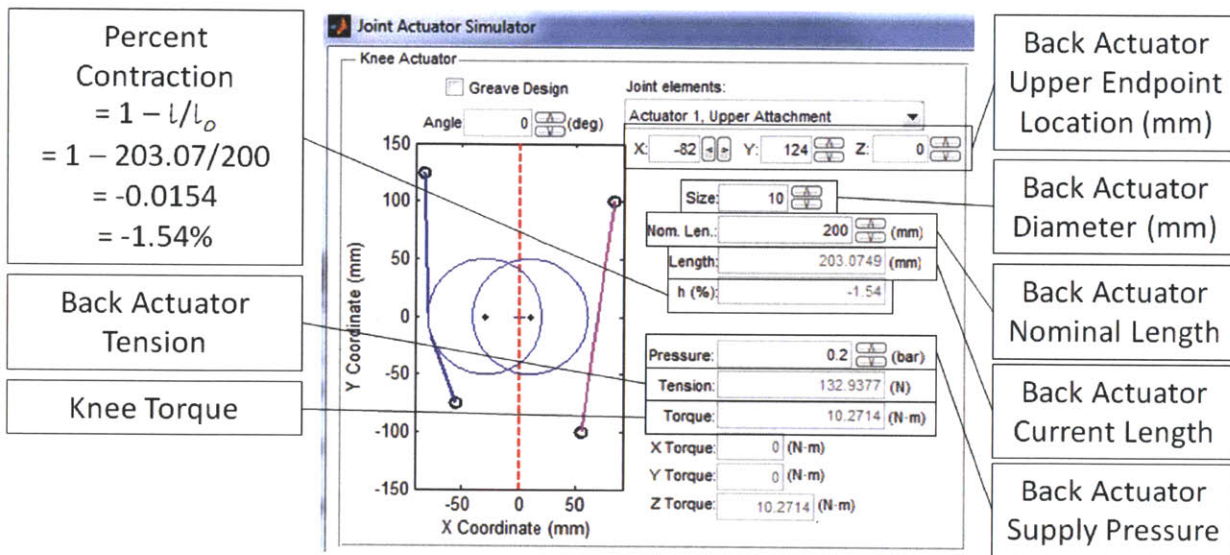
and 0 mm (0 in), respectively. The diameter of the front actuator is 20 mm (0.8 in), which is input as size, while the nominal length of the front actuator is 295 mm (11.6 in). The supply pressure to the front actuator is 0 kPa (0 bar) at 0 degrees of knee flexion and therefore contributes 0 Nm (0 ft-lb) to the knee torque. At the current view, the front actuator has changed from blue in color to pink. The front actuator is pink because it is currently at a percent contraction of 31.6%, which is out of range as the actuators can only contract to 25% of their nominal length. In this instance, the lower endpoint of the actuator would move along its slider, allowing the actuator to remain at its nominal length of 295 mm (11.6 in). While moving along its slider, the front actuator is not able to contribute to the torque at the knee. The sliders are not implemented in the S3 computer simulator, therefore when the percent contraction of the actuator is greater than 25%, it is assumed that the actuator would move along its slider, contributing no tension force to the knee torque calculation.



**Figure 4.8 Front actuator inputs to example design for 50% female anthropometry**

A view of the back actuator inputs into the S3 computer simulator for the example design for 50% female anthropometry is depicted in Figure 4.9. The x, y, and z locations of the upper endpoint of actuator 1, the back actuator, are -82 mm (-3.2 in), 124 mm (4.9 in), and 0 mm (0 in), as shown. The diameter of the back actuator is provided for size as 10 mm (0.4 in), and the nominal length of the back actuator is 200 mm (7.9 in). The knee torque of a pressurized EMU space suit at 0 degrees of knee flexion is -10 Nm (7.4 ft-lb) [Schmidt et al., 2001]. In the example design for 50% female anthropometry, a supply pressure of 20 kPa (0.2 bar) results in a 132.9 N (29.9 lb) tension force in the 10 mm (0.4 in) diameter back actuator stretched by 1.54%. This results in a knee torque in the z direction of magnitude

10.27 Nm (7.6 ft-lb), and therefore an overall knee torque of 10.27 Nm (7.6 ft-lb). Therefore, the error in the example design at 0 degrees of knee flexion is 0.27 Nm (0.2 ft-lb).

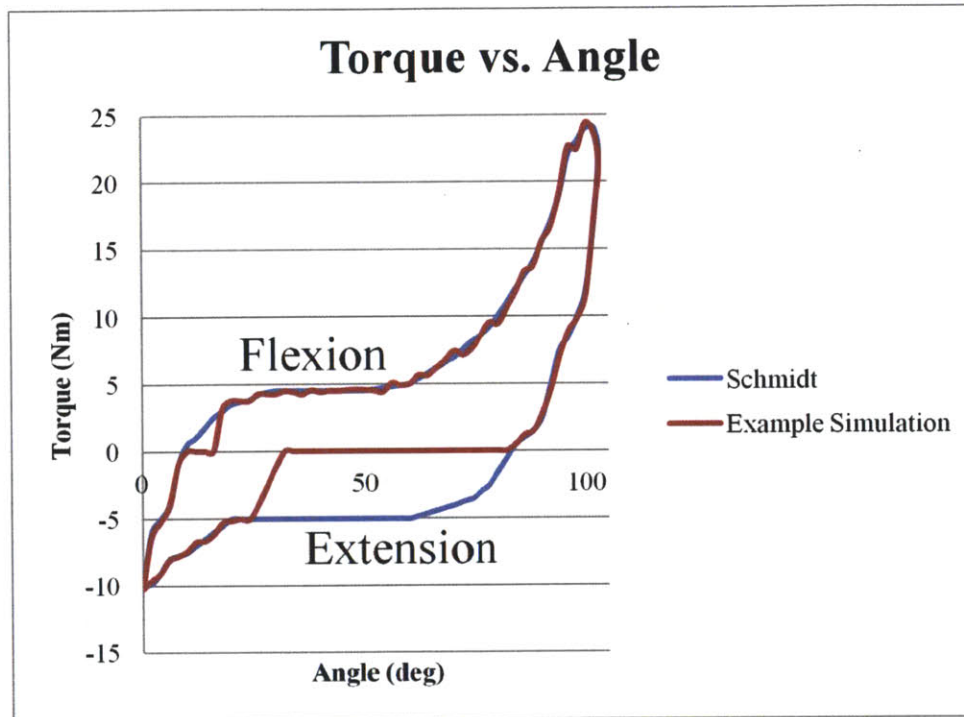


**Figure 4.9 Back actuator inputs to example design for 50% female anthropometry**

The torque versus angle output is depicted in Figure 4.10. When flexing the knee, the example design was able to simulate the knee torque of a pressurized EMU knee through all angles of flexion (0 deg – 103 deg), excluding 10 degrees to 16 degrees. During knee extension, the design was able to match EMU knee torques from 103 degrees to 84 degrees of knee extension, and also from 30 to 0 degrees. The back actuator did not reach its hard stop until 30 degrees, due to the short length of the actuator. Therefore, the back actuator did not induce a torque on the knee between 84 to 30 degrees of knee extension. The root-mean-square error (RMSE) was calculated for the example simulation. The RMSE was calculated by the following equation:

$$RMSE = \sqrt{\frac{\sum_{i=1}^n (x_{1,i} - x_{2,i})^2}{n}}$$

where  $n$  is the number of data points,  $x_{1,i}$  is the value of the torque for the example simulation at a given angle, and  $x_{2,i}$  is the value of the torque from Schmidt's data at a given angle. The RMSE of the example simulation is 2.31 Nm (1.7 ft-lb). Most of the error in the torque output is due to the inability of the back actuator to induce a torque on the knee through a large portion of the knee extension motion. However, the S3 example simulation design was able to mimic the joint torques of the EMU knee through the knee range of motion extremes, where it is most important to match the torques.



**Figure 4.10 Torque vs. angle curve of example simulation compared with Schmidt et al., 2001**

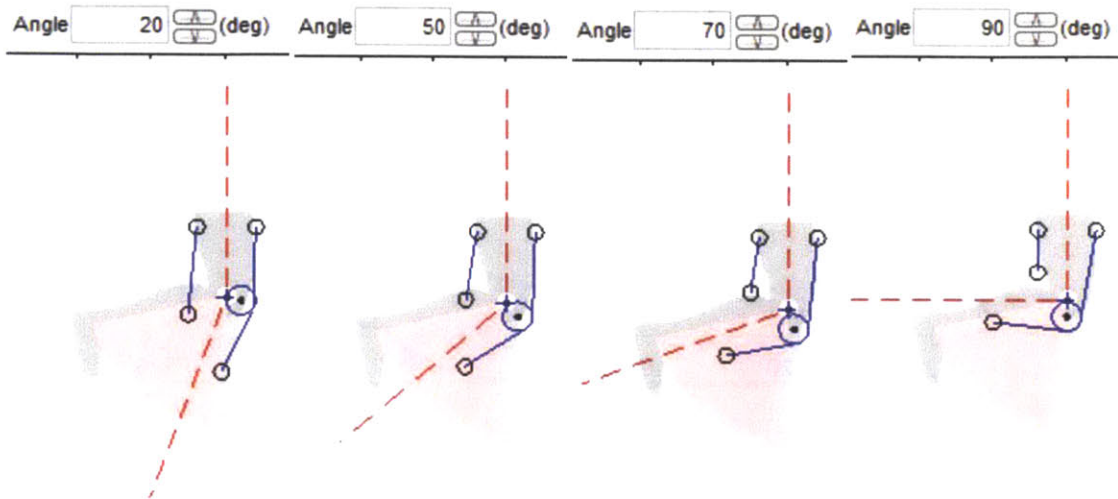
Several of the S3 design iterations can be input into the S3 computer simulator to determine feasible design solutions for subjects of varying anthropometries. Feasible design solutions include those that minimize the RMSE and closely mimic the joint torque at the range of motion extremes, while utilizing exoskeleton components that minimize bulk and weight. For the purposes of the S3 lower body exoskeleton, designs were compared that would accommodate a 95% male anthropometry and had the ability to mimic EMU knee joint torques, while still attempting to reduce weight and bulk.

### 4.3 Implementation of the S3 Knee Design

In order to incorporate the S3 knee design into the MATLAB simulator, the greave had to be simulated. In the original version of the computer simulator, the spools that the actuators wrapped around remained fixed to the upper leg component as the knee moved through its range of motion. Therefore, along with the lower leg the only components that moved during knee flexion and extension were the lower endpoints of each of the actuators, while the upper endpoints of the actuator and the spools remained fixed.

With a greave design attached to the exoskeleton, all components of the greave move with the lower leg. Therefore, the portions of the greave covering the shin and the knee remain fixed to the lower leg and move as the lower leg moves through its range of motion. To model the greave in the S3

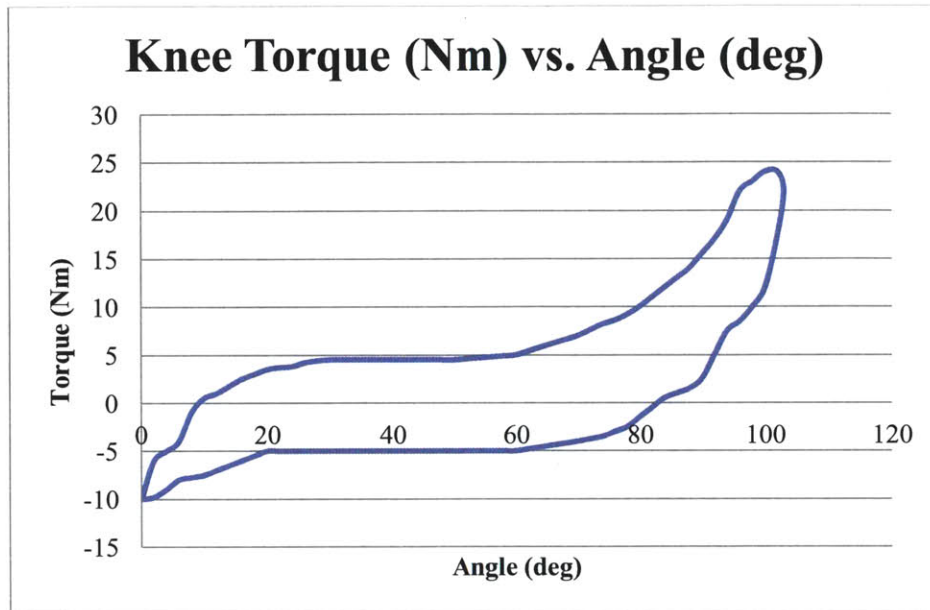
MATLAB simulator, the portion of the greave covering the knee can be modeled as a circle, similar to the spool in the original version of the simulation. Instead of keeping the circle fixed with respect to the upper leg, as the spools were in the original design, the circle representing the greave remains fixed to the lower leg and moves as the lower leg moves through its range of motion. Figure 4.11 demonstrates the circle representing the greave rotating with the lower leg. The user can activate the greave design in the simulator by checking a greave design checkbox.



**Figure 4.11 The circle representing the greave rotates with the lower leg as the knee flexion (kf) angle increases**

Once the greave design was incorporated, various exoskeleton designs were implemented in the simulator. The torque versus angle output of the simulator was compared to the torque versus angle curve gathered using a robot space suit testing method with the EMU space suit [Schmidt et al., 2001]. The EMU knee torque gathered during robot space suit testing is depicted in Figure 4.12. The curve indicates that the robot was in a straight leg position at zero degrees. The torque increased up to 24 Nm (17.7 ft-lb) when the knee was bent at 103 degrees. The torque then decreased during extension to a value of -10 Nm (-7.4 ft-lb) at complete extension. The positive or negative sign of the torque value at each given angle indicates direction of limb motion with respect to the neutral point of the limb. During knee flexion while wearing an EMU, the torque value first becomes positive around 10 degrees. The reason the torque becomes positive at 10 degrees of flexion is because the neutral point of the EMU leg during flexion is at a 10 degree angle. This means that if no external forces are acting on the pressurized EMU leg during flexion, the leg would like to return to the 10 degree neutral point, and to move the limb away from its neutral point requires a force in one direction or the other. Likewise, during knee extension the torque first becomes negative around an 80 degree knee bend. This indicates that the

neutral point of the EMU leg during extension is around 80 degrees. The neutral point of the limb is different during flexion and extension due to fabric material shifts between layers of the space suit. As the limb is flexing, the layers of the space suit move against one another. The normal force due to the pressure inside the space suit prevents the layers from immediately sliding back against one another during extension, thus changing the angle of the neutral point during extension.



**Figure 4.12 Knee torque versus angle curve of a pressurized EMU space suit [Schmidt et al., 2001]**

To incorporate the neutral points into the S3 knee design, the actuators will be activated at different angles as the leg moves through its range of motion. The back actuator will be pressurized when the torque values are negative. Therefore, if the subject wearing the S3 exoskeleton begins knee flexion starting at a zero degree straight leg, the actuator on the back of the leg will pressurize to aid the subject in the flexion motion. When the subject reaches the EMU flexion neutral point angle of 10 degrees, the front actuator will pressurize instead to resist flexion motion from 10 degrees of knee flexion to 103 degrees of knee flexion. When the subject begins to extend the knee, the front actuator will remain pressurized to aid in the extension motion from 103 degrees to about 80 degrees, at the EMU extension neutral point. At about 80 degrees, the back actuator will pressurize for the remainder of the knee extension motion to resist motion to extension.

Because the S3 knee design will be tested on MIT's robot space suit tester, which has the anthropometry of a 95% male, the thigh and shank attachment points of the actuators will be offset anterior and posterior to the knee point of rotation according to 95% male leg dimensions. The thigh circumference of a 95% male is 67.4 cm (26.5 in) and the calf circumference is 41.4 cm (16.3 in) [NASA-72



STD-3000, 1994]. Thus, assuming the thigh and calf circumferences are circles, the thigh diameter and calf diameter of a 95% male are 21.5 cm (8.4 in) and 13.2 cm (5.2 in), respectively. Assuming the midline of the leg is located at the center of the circles representing the thigh and calf, the upper attachment points of the actuators should be located 10.8 cm (4.2 in) anterior and posterior to the midline of the upper leg, and the lower attachment points of the actuators should be located 6.6 cm (2.6 in) anterior and posterior to the midline of the lower leg. Therefore, the dimensions of a 95% male set the guidelines for the x locations of the pneumatic actuator endpoints.

The y locations of the actuator endpoints were selected based on the desired length of the actuators and whether the actuator endpoints were going to be symmetric about the knee or shifted superior or inferior. The actuators are sold in three diameter sizes: 10 mm (0.4 in), 20 mm (0.8 in), or 40 mm (1.6 in). Due to the desire to minimize weight and bulk, the 40 mm (1.6 in) diameter actuators were not implemented in the S3 computer simulator. The size of the circle representing the greave was selected based on 95% male anthropometry. The knee circumference of a 95% male is 42.9 cm (16.9 in) [NASA-STD-3000, 1994]. Assuming the knee is a circle, the radius of the knee is thus 6.9 cm (2.7 in).

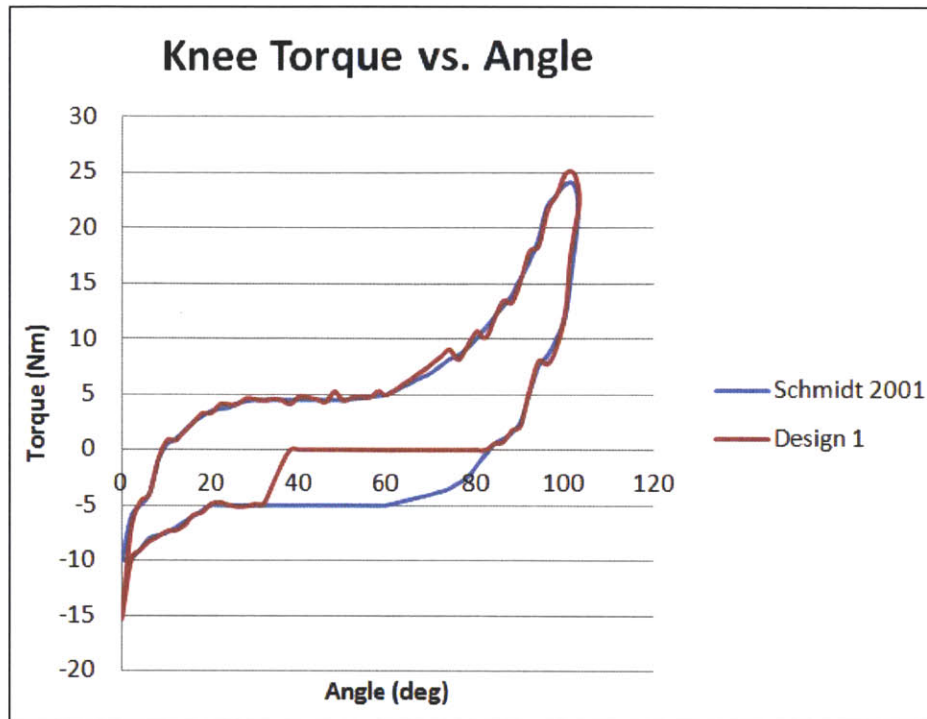
#### **4.4 S3 Knee Joint Design Results**

A design was selected to be implemented in the S3 computer simulator to serve as a baseline for alternative designs. The baseline design is presented below in Table 4.1. The knee point of rotation is located at  $(x, y, z) = (0, 0, 0)$ . The x, y, and z of the design are the locations of the upper and lower endpoints of the actuators when the leg is straight at zero degrees of knee flexion. In the baseline design, the x locations of the upper and lower endpoints of the actuators were selected based on 95% male anthropometry. The radius of the greave was also selected based on anthropometry. For the back actuator, the y locations were selected so that the actuator would be shifted superior on the leg and not symmetric about the knee. For the front actuator, the y locations were selected so that the actuator would be symmetric about the knee point of rotation. The back actuator was selected to be 280 mm (11 in) in length and 10 mm (0.4 in) in diameter while the front actuator was selected to be 513 mm (20.2 in) in length and 20 mm (0.8 in) in diameter.

**Table 4.1 Baseline design implemented in the S3 computer simulator**

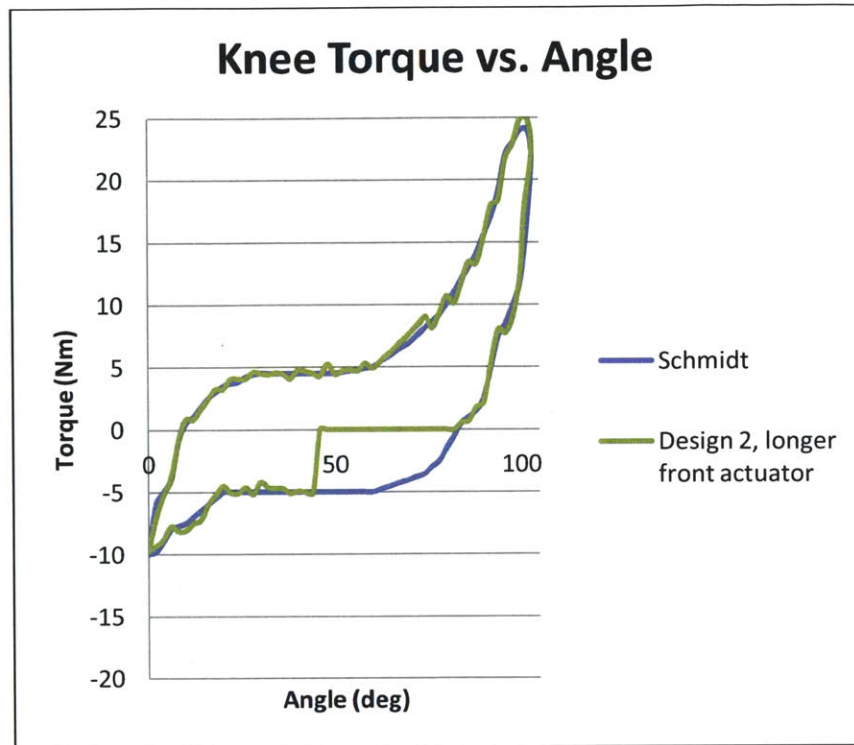
Design 1						
		X (mm)	Y (mm)	Z (mm)	Actuator Geometry	
Back Actuator	Upper	-108	183	0	280 mm nominal length	10 mm diameter
	Lower	-65	-100	0		
Front Actuator	Upper	108	183	0	513 mm nominal length	20 mm diameter
	Lower	65	-184	0		
Greave		22	0	0	68 mm radius	

The torque versus angle output of design 1 is shown in Figure 4.13 compared against data gathered from Schmidt [Schmidt et al., 2001]. The RMSE of design 1 is 2.25 Nm (1.7 ft-lb). The torque data in the torque versus angle curves is not smooth due to small changes in supply pressure (10 kPa or 0.1 bar), which cause large changes in the actuator tension, resulting in large changes in the torque. The flat portion of the curve at 0 Nm (0 ft-lb) during knee extension is due to the location of the hard stop of the back actuator. The actuator does not produce a torque until it reaches the hard stop. By changing the length of the actuator and the location of the hard stop, the torque can be more closely matched. The pressure to be supplied to the actuators was selected at each angle in order to minimize the torque error. While supply pressure could have been selected to reduce the number of jumps between positive torque error and negative torque error, this would have resulted in a larger RMSE. Therefore, the supply pressure that minimized the error at each angle was selected.



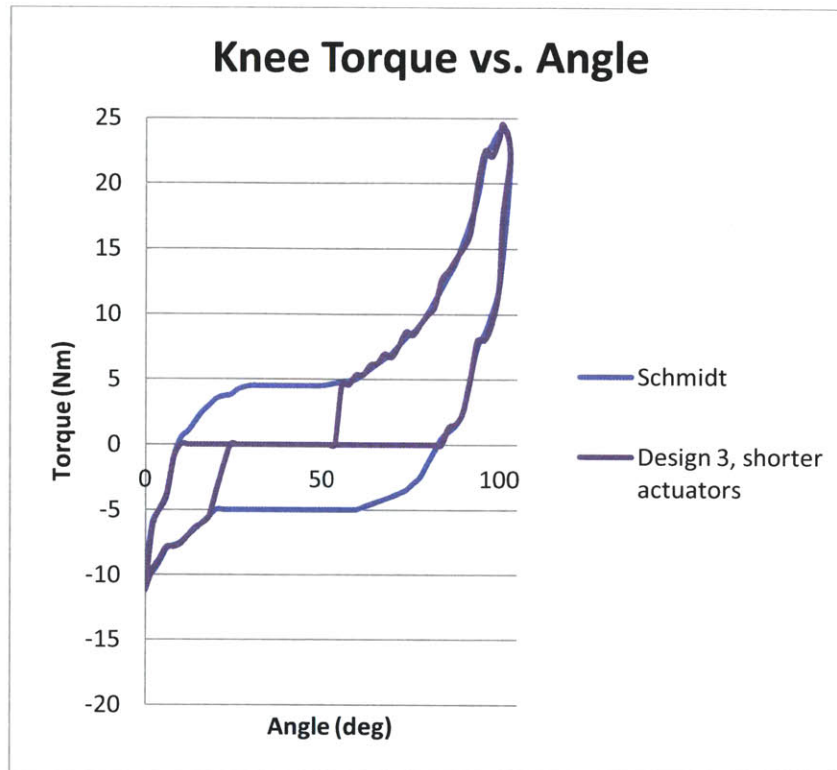
**Figure 4.13 Knee torque versus angle curve of baseline design compared against Schmidt 2001 data**

To study how the actuator lengths and diameters affect RMSE, design 2 included a longer back actuator of 350 mm (13.8 in) in length and a larger back actuator diameter of 20 mm (0.8 in). Design 2 was able to mimic the joint torque properties of the EMU knee during all angles of flexion, as indicated by the upper portion of the hysteresis curve (Figure 4.14). During extension, design 2 was able to mimic the joint torques of the EMU knee through 103 deg to 84 deg, and again through 44 deg to 0 deg, as shown by the lower portion of the hysteresis curve. The RMSE of design 2 was 1.85 Nm (1.9 ft-lb), which is less than the RMSE of design 1. Design 2 was therefore able to mimic the joint torque properties of the EMU knee through a greater range of motion than design 1, and was also able to reduce the RMSE.



**Figure 4.14 Knee torque versus angle curve of design 2 compared against Schmidt 2001 data**

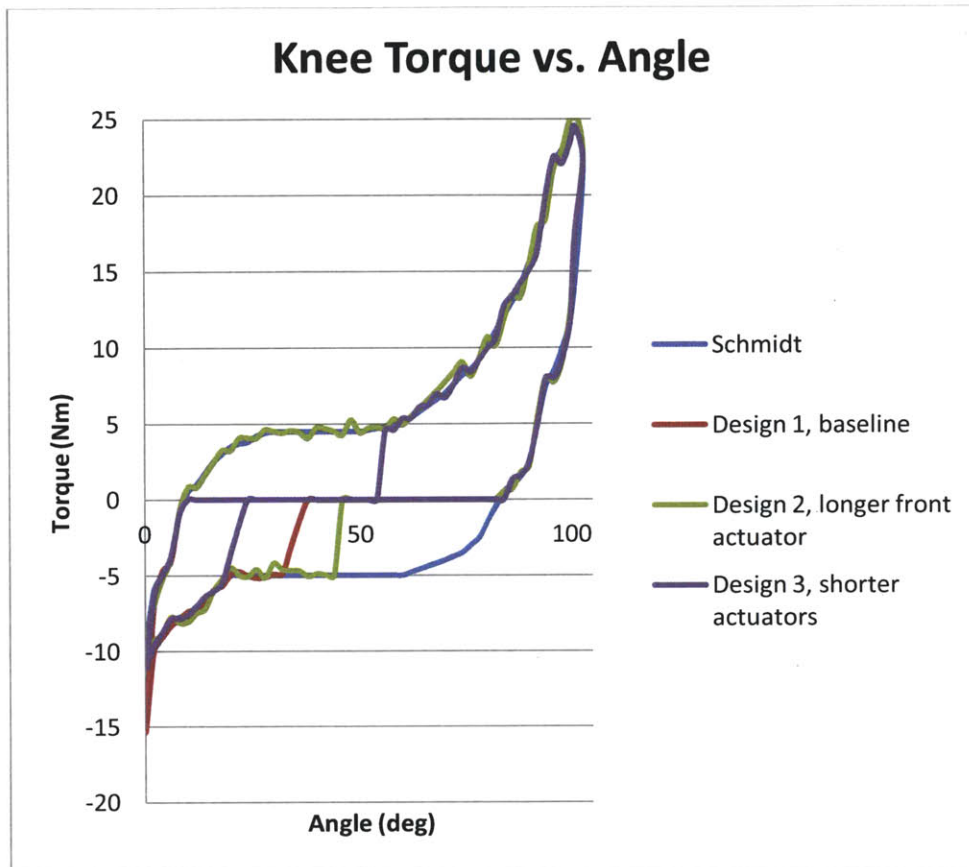
Design 3 included shorter back and front actuator lengths of 150 mm (5.9 in) and 250 mm (9.8 in), respectively. The details of all of the designs implemented in the S3 computer simulator are included in Appendix B. The torque versus angle curve of design 3 compared against Schmidt's EMU data is included in Figure 4.15. As shown by the upper portion of the curve, design 3 was able to mimic the joint torque properties of the EMU knee from 0 deg to 10 deg and again from 56 deg to 103 deg during knee flexion. During knee extension, design 3 was able to mimic the joint torques from 103 deg to 84 deg and again from 22 deg to 0 deg, as shown by the lower portion of the hysteresis curve. The RMSE of design 3 is 3.10 Nm (2.3 ft-lb). Therefore, design 3 did not improve upon the baseline design in terms of mimicking the joint torques of the EMU knee through the greatest range of motion, nor in terms of minimizing the RMSE.



**Figure 4.15 Knee torque versus angle curve of design 3 compared against Schmidt 2001 data**

The torque versus angle curves for designs 2 and 3 are compared against design 1 and Schmidt's 2001 data, as shown in Figure 4.16. The RMSE of design 2 is 1.85 Nm (1.9 ft-lb) and the RMSE of design 3 is 3.10 Nm (2.3 ft-lb). As shown in the torque versus angle curves, design 2 improves upon design 1 by reaching its hard stop during knee extension at 44 degrees, while design 1 did not reach the hard stop until 36 degrees. Therefore, design 2 could more closely match the torque curve collected by Schmidt. Because the actuators were short in length, the back actuator of design 3 did not reach the hard stop until 22 degrees of knee extension. Design 3 also did not reach the hard stop during knee flexion until 56 degrees, while designs 1 and 2 were able to achieve torques throughout all angles of knee flexion. Therefore, longer and thicker actuators are able to achieve the desired torques through a greater range of motion than shorter and thinner actuators, thus decreasing the RMSE. Longer actuators are able to achieve torques through a greater range of motion because the actuators can contract up to 25% of their nominal lengths; therefore, the stroke length of longer actuators is greater than the stroke length of short actuators, allowing the long actuators to be actively resisting knee motion for a greater range of angles. Actuators with a larger diameter are able to achieve greater tensions at the endpoints than actuators with smaller diameters; therefore, actuators with larger diameters are able to achieve the desired torques without as much actuator contraction, allowing for active control through a greater

range of motion. Although long and thick actuators accommodate a greater range of motion, they also add weight and bulk to the S3 design, therefore the costs of adding weight and bulk need to be traded with the benefits of a lower RMSE.



**Figure 4.16 Designs 2 and 3 compared with baseline design 1 and Schmidt data**

To allow for a S3 design that is low weight and low bulk, short length actuators are desired, with small diameters. To compare how diameter affects RMSE, two back actuator designs were studied, one with a 10 mm (0.4 in) diameter and one with a 20 mm (0.8 in) diameter, while the nominal length remained fixed at a short 200 mm (7.9 in) length. To compare how length affects RMSE, two front actuator designs were studied, one with a 300 mm (11.8 in) nominal length and one with a 487 mm (19.2 in) nominal length, while the diameter remained fixed at 20 mm (0.8 in). Therefore, four designs were implemented in the S3 computer simulation (designs 4-7), utilizing all combinations of the two back actuator and two front actuator designs. The detailed designs are included in Appendix B. The actuator lengths and diameters for each design are described by Table 4.2. Designs 4 and 5 have a short front actuator of 300 mm (11.8 in) in length, while designs 6 and 7 have a long front actuator of 487 mm

(19.2 in) in length. Designs 4 and 6 have a 10 mm (0.4 in) small diameter back actuator, while designs 5 and 7 have a 20 mm larger (0.8 in) diameter back actuator.

**Table 4.2 Nominal lengths and diameters of front and back actuators for designs 4-7**

			Front Actuator, Diameter 20 mm	
			Front Actuator Nominal Length (mm)	
			300	487
Back Actuator, Nominal Length 200 mm	Back Actuator Diameter (mm)	10	Design 4	Design 6
		20	Design 5	Design 7

Comparison plots of designs 4-7 are shown in Figure 4.17. The RMSE values of the four designs are as follows:

- Design 4: RMSE = 2.88 Nm (2.12 ft-lb)
- Design 5: RMSE = 2.72 Nm (2.01 ft-lb)
- Design 6: RMSE = 2.30 Nm (1.70 ft-lb)
- Design 7: RMSE = 2.10 Nm (1.55 ft-lb)

Figure 4.17 (a) depicts a comparison of designs 4 and 5, which both have a front actuator of 300 mm (11.8 in) nominal length and 20 mm (0.8 in) diameter; however, design 4 has a back actuator of 200 mm (7.9 in) nominal length and 10 mm (0.4 in) diameter, while design 5 has a back actuator of 200 mm (7.9 in) nominal length and 20 mm (0.8 in) diameter. Therefore, Figure 4.17 (a) is a comparison between back actuator diameters given front actuator nominal lengths of 300 mm (11.8 in).

Neither designs 4 nor 5 were able to mimic the EMU knee torques through the full range of flexion and extension. Design 5 has a slight advantage over design 4 in that the back actuator of design 5 reaches its hard stop during extension at 36 degrees, while the back actuator in design 4 does not reach the hard stop until 30 degrees. Therefore, design 5 can cause a knee torque 6 degrees sooner. Design 5 also has a RMSE advantage of 0.16 Nm (0.12 ft-lb). Therefore, a larger back actuator diameter is advantageous when comparing designs 4 and 5.

Figure 4.17 (b) depicts a comparison of designs 6 and 7, which both have a front actuator of 487 mm (19.2 in) nominal length and 20 mm (0.8 in) diameter; however, design 6 has a back actuator of 200 mm (7.9 in) nominal length and 10 mm (0.4 in) diameter, while design 7 has a back actuator of 200 mm (7.9 in) nominal length and 20 mm (0.8 in) diameter. Therefore, Figure 4.17 (b) is a comparison between back actuator diameters given front actuator nominal lengths of 487 mm (19.2 in).

Both design 6 and 7 were able to mimic the EMU knee torque through the full range of knee flexion, however neither design was able to mimic knee torques through the full range of knee extension. The back actuator of design 7, however, reached its hard stop at 36 degrees while design 6 reached its hard stop at 30 degrees. Therefore, design 7 was able to more closely mimic the torque for 6 additional degrees of extension. Additionally, design 7 had a RMSE advantage of 0.20 Nm (0.15 ft-lb). For designs 6 and 7, the larger back actuator diameter was able to mimic knee torque for a greater angle range and was able to reduce RMSE.

Figure 4.17 (c) depicts a comparison of designs 4 and 6, which both have a back actuator of 200 mm (7.9 in) nominal length and 10 mm (0.4 in) diameter; however, design 4 has a front actuator of 300 mm (11.8 in) nominal length and 20 mm (0.8 in) diameter, while design 6 has a front actuator of 487 mm (19.2 in) nominal length and 20 mm (0.8 in) diameter. Therefore, Figure 4.17 (c) is a comparison between front actuator nominal lengths given back actuator diameters of 10 mm (0.4 in).

Neither design 4 nor 6 were able to mimic EMU knee extension torques until the back actuators reached their hard stops at 30 degrees. However, design 6 was able to mimic knee torques through the full range of knee flexion angles, while design 4 was only able to achieve knee torques from 0 to 10 degrees and 52 to 103 degrees. For this reason, design 6 had a lower RMSE of 2.30 Nm (1.70 ft-lb), while design 4 had a RMSE of 2.88 Nm (2.12 ft-lb). Therefore, design 6 had the ability to mimic knee flexion torques for an additional 42 degrees, and had a RMSE advantage of 0.58 Nm (0.43 ft-lb) over design 4. Therefore, a front actuator with a longer nominal length has better performance when comparing designs 4 and 6.

Figure 4.17 (d) depicts a comparison of designs 5 and 7, which both have a back actuator of 200 mm (7.9 in) nominal length and 20 mm (0.8 in) diameter; however, design 5 has a front actuator of 300 mm (11.8 in) nominal length and 20 mm (0.8 in) diameter, while design 7 has a front actuator of 487 mm (19.2 in) nominal length and 20 mm (0.8 in) diameter. Therefore, Figure 4.17 (d) is a comparison between front actuator nominal lengths given back actuator diameters of 20 mm (0.8 in).



The back actuators of designs 5 and 7 did not reach their hard stop until 36 degrees of knee extension. Design 7, however, was able to mimic knee torques through the full range of knee flexion angles, while design 5 was only able to achieve knee torques from 0 to 10 degrees and from 52 to 103 degrees. The RMSE of design 5 was 2.72 Nm (2.01 ft-lb) while the RMSE of design 7 was 2.10 Nm (1.55 ft-lb). Therefore, design 7 was able to mimic knee flexion torques through 42 additional flexion angles, while offering a RMSE advantage of 0.62 Nm (0.46 ft-lb). For designs 5 and 7, the front actuator with the longer nominal length obtained better performance.

Figure 4.17 (a) and (b) provided comparisons between back actuator diameters, given designs with the same front actuator geometries. In both cases, the design with the larger back actuator diameter was able to mimic EMU knee torques for a greater angle range of motion and was able to lower the RMSE below the RMSE of the smaller back actuator diameter designs. This suggests that for designs 4-7, a 20 mm (0.8 in) diameter back actuator results in improved performance as far as mimicking the joint torque properties of the EMU space suit.

Figure 4.17 (c) and (d) show comparisons between the nominal lengths of front actuators given back actuators of the same diameter. In both cases, the designs with a longer front actuator nominal length were able to mimic joint torques for a greater angle range of motion and were able to lower the RMSE below the RMSE of the designs with shorter front actuator nominal lengths. This suggests that for designs 4-7, a 487 mm (19.2 in) nominal length front actuator results in improved performance as far as mimicking the joint torque properties of the EMU space suit.

The comparison of designs 1-3 demonstrated that design 2 was able to mimic EMU knee torque through the greatest angle range of motion and was able to produce the smallest RMSE of the three designs. This result suggests that designs with long front and back actuators and large diameter actuators produce the best performance in terms of RMSE and torque capabilities through the greatest range of motion.

The comparison of designs 4-7 demonstrated that design 7 was able to mimic EMU knee torque through the greatest angle range of motion and was able to produce the smallest RMSE of the four designs. This result also suggests that designs with longer front actuator nominal lengths and larger back actuator diameters produce the best performance in terms of RMSE and torque capabilities through the greatest range of motion.

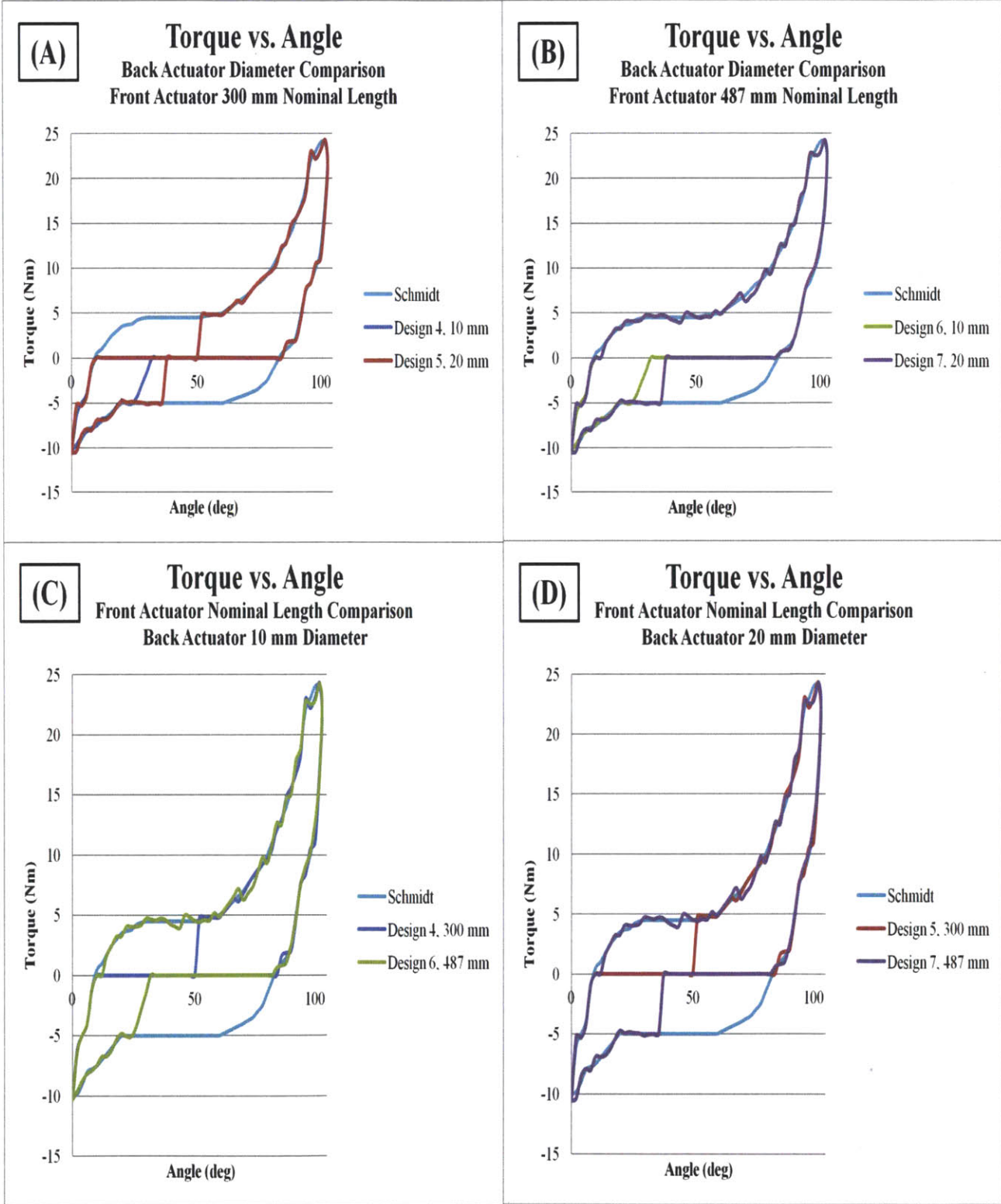


Figure 4.17 S3 Knee Design Comparisons

Five actuators were available for robot testing of the S3 knee. Two actuator lengths are available for the back actuator in the S3 knee design: 200 mm (7.9 in), and 495 mm (19.2 in). Both back actuators have a diameter of 10 mm (0.4 in). There are three actuator lengths available for the front actuator in the S3 knee design: 300 mm (11.8 in), 350 mm (13.8 in), and 495 mm (19.5 in). All three front actuators have a diameter of 20 mm (0.8 in). Six combinations of front and back actuators were created and tested in the S3 knee computer simulator to determine the torque versus angle curve of each design and the RMSE of each design. The design combinations are described by Table 4.3.

**Table 4.3 Front and back actuator combinations**

		Front Actuator, 20 mm Diameter			
		Nominal Length (mm)			495
		300	350	495	
Back Actuator, 10 mm Diameter	Nominal Length (mm)	200	Combo 1	Combo 2	Combo 3
		495	Combo 4	Combo 5	Combo 6

The RMSE of each combination are as follows:

- Combo 1 RMSE = 2.88 Nm (2.12 ft-lb)
- Combo 2 RMSE = 2.68 Nm (1.98 ft-lb)
- Combo 3 RMSE = 2.29 Nm (1.69 ft-lb)
- Combo 4 RMSE = 2.55 Nm (1.88 ft-lb)
- Combo 5 RMSE = 2.32 Nm (1.71 ft-lb)
- Combo 6 RMSE = 1.86 Nm (1.37 ft-lb)

Comparisons of each of the designs are shown in Figures 4.18-4.21 below. Figure 4.18 depicts comparisons between varying front actuator lengths given constant back actuator lengths. Figures 4.19 through 4.21 depict comparisons between varying back actuator lengths given constant front actuator lengths. A description of each comparison follows.

Figure 4.18 (a) compares the torque versus angle curves of three front actuator lengths (300 mm, 350 mm, 495 mm) given a short back actuator (200 mm in length). Following the combo 3 hysteresis curve clockwise from its lowest torque point, the torques are simulated from angles 0 to 103 degrees, the full range of flexion. Following the lower trace of the curve as the knee extends, combo 3 is able to mimic the torque from 103 to 84 degrees and again from 30 to 0 degrees. Following the combo 1

hysteresis curve clockwise from its lowest torque point, the torques are simulated from angles 0 to 10 degrees and again from 52 to 103 degrees, the maximum angle of flexion. Following combo 2 clockwise from its lowest torque point, is it active through angles 0 to 10 degrees and again from 40 to 103 degrees. Following the lower trace of the curve as the knee extends, combos 1 and 2 are able to mimic the torque from 103 to 84 degrees and again from 30 to 0 degrees, which is the same range of extension motion that combo 3 was active through. In terms of mimicking torque through the greatest range of motion, combo 3 has the best performance. In terms of reducing RMSE, combo 3 also has the best performance. Therefore, the actuator with the longest front actuator length had the best performance, given equal short back actuator lengths.

Figure 4.18 (b) compares the torque versus angle curves of three front actuator lengths (300 mm, 350 mm, 495 mm) given a long back actuator (495 mm in length). As shown in Figure 4.18 (b), combo 6 is able to mimic the joint torque behavior throughout the entire flexion range of motion, shown on the upper portion of the hysteresis curve. Combo 4 is active during flexion from angles 0 to 10 degrees and again from 52 to 103 degrees, and combo 5 is active during flexion from angles 0 to 10 degrees and again from 40 to 103 degrees. Combos 4, 5, and 6 all mimic extension range of motion, as shown on the lower portion of the hysteresis curve, from 103 to 84 degrees, and again from 44 to 0 degrees. Therefore, in terms of mimicking torque through the greatest range of motion, combo 6 has the best performance. In terms of reducing RMSE, combo 6 also has the best performance. Therefore, the actuator with the longest front actuator length had the best performance, given equal long back actuator lengths.

Therefore, after viewing Figure 4.18, it can be determined that the front actuator with the longest length (495 mm) has the best performance in terms of mimicking joint torque through the greatest range of motion, and in terms of reducing RMSE, regardless of length of back actuator.

Figure 4.19 compares the torque versus angle curves of two back actuator lengths (200 mm, 495 mm) given a short front actuator (300 mm in length). As shown in Figure 4.19, combo 4 is able to mimic the joint torque behavior during extension, as shown in the lower portion of the hysteresis curve, throughout angles 103 to 84 degrees and again from 44 to 0 degrees, while combo 1 is active during extension from angles 103 to 84 degrees and again from 30 to 0 degrees. Combos 1 and 4 both mimic flexion range of motion, as shown by the upper portion of the hysteresis curve, from 0 to 10 degrees and again from 52 to 103 degrees. Therefore, in terms of mimicking torque through the greatest range of motion, combo 4 has the best performance. In terms of reducing RMSE, combo 4 also has the best

performance. Therefore, the actuator with the longest back actuator length had the best performance, given equal short front actuator lengths.

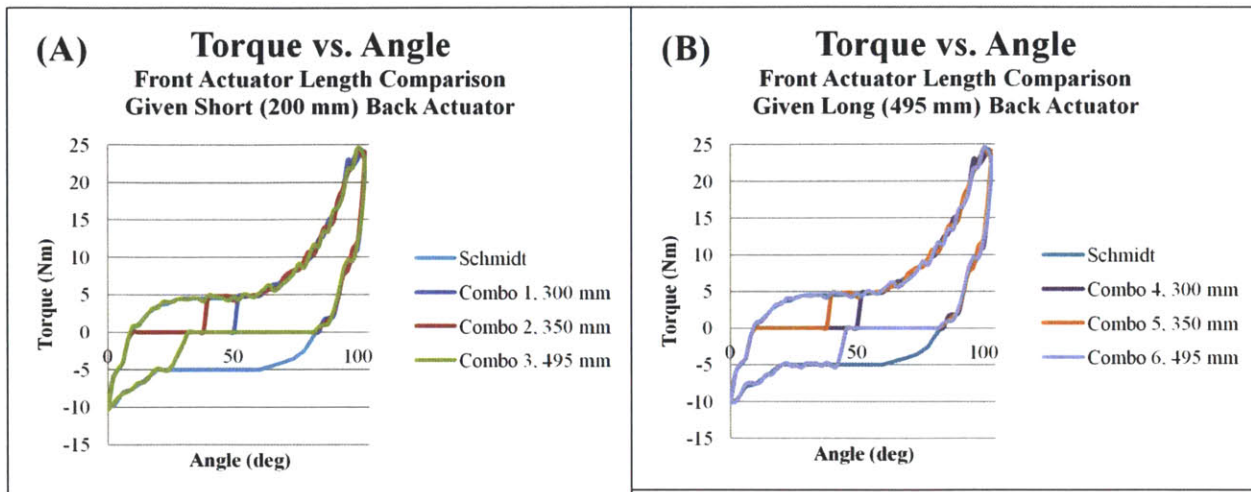


Figure 4.18 (a) Front actuator length comparison given short (200 mm or 7.9 in) back actuator, (b) Front actuator length comparison given long (495 mm or 19.5 in) back actuators

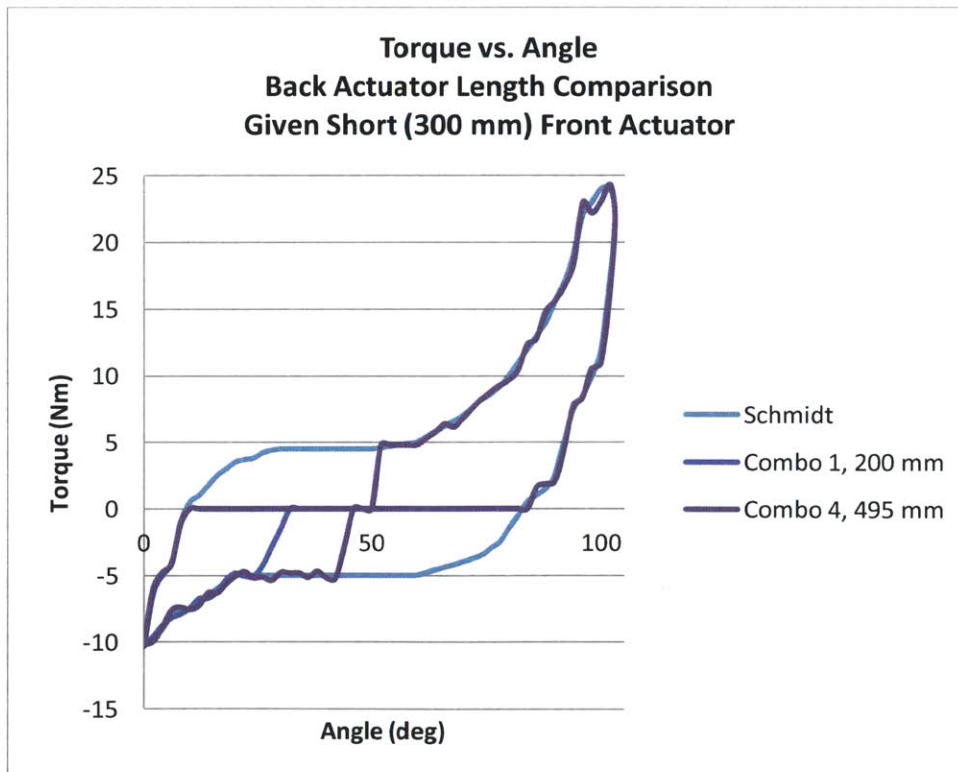
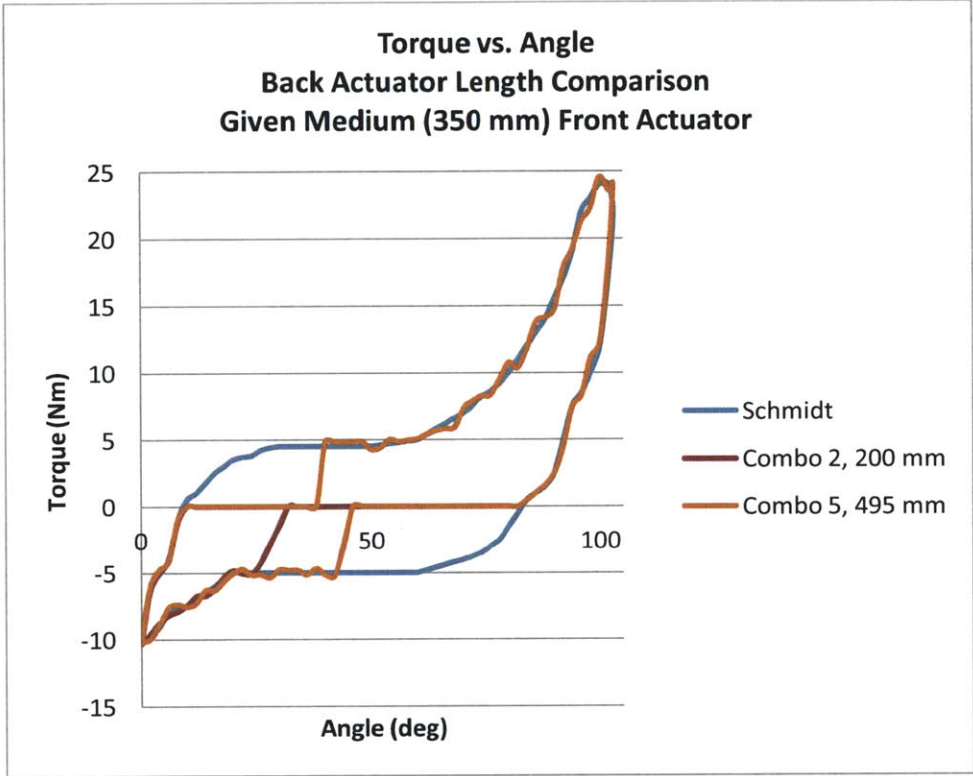


Figure 4.19 Back actuator length comparison given short (300 mm or 11.8 in) front actuator length

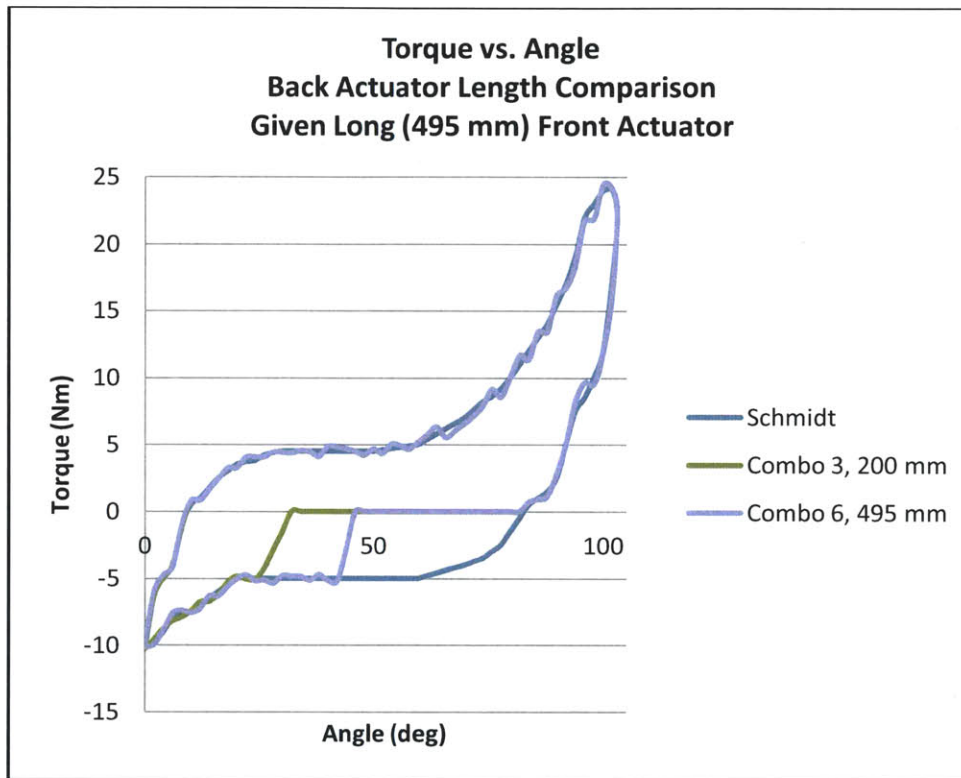
Figure 4.20 compares the torque versus angle curves of two back actuator lengths (200 mm, 495 mm) given a medium front actuator (350 mm in length). As shown in Figure 4.20, combo 5 is able to mimic the knee extension joint torque behavior, as shown by the lower portion of the hysteresis curve, throughout angles 103 to 84 degrees and again from 44 to 0 degrees, while combo 2 is active through angles 103 to 84 degrees and again from 30 to 0 degrees. Combos 2 and 5 both mimic flexion range of motion, as shown by the upper portion of the hysteresis curve, from 0 to 10 degrees and again from 40 to 103 degrees. Therefore, in terms of mimicking torque through the greatest range of motion, combo 5 has the best performance. In terms of reducing RMSE, combo 5 also has the best performance. Therefore, the actuator with the longest back actuator length had the best performance, given equal medium front actuator lengths.



**Figure 4.20 Back actuator length comparison given medium (350 mm or 13.8 in) front actuator length**

Figure 4.21 compares the torque versus angle curves of two back actuator lengths (200 mm, 495 mm) given a long front actuator (495 mm in length). As shown in Figure 4.21, combo 6 is able to mimic the joint torque behavior during knee extension, as shown by the lower portion of the hysteresis curve, throughout angles 103 to 84 degrees and again from 44 to 0 degrees, while combo 3 is active through angles 103 to 84 degrees and again from 30 to 0 degrees. Combos 3 and 6 both mimic torque

through the full range of flexion motion, as shown by the upper portion of the hysteresis curve. Therefore, in terms of mimicking torque through the greatest range of motion, combo 6 has the best performance. In terms of reducing RMSE, combo 6 also has the best performance. Therefore, the actuator with the longest back actuator length had the best performance, given equal long front actuator lengths.



**Figure 4.21 Back actuator length comparison given long (495 mm or 19.5 in) front actuator**

Therefore, in Figures 4.19-4.21, the back actuator with the longest length obtained the best performance in terms of mimicking torque through the greatest range of motion and also in terms of reducing the RMSE, regardless of the front actuator length. Overall, the front actuator with the longest length performed best regardless of back actuator length, and the back actuator with the longest length performed best regardless of front actuator length.

Table 4.4 includes a comparison of the designs implemented in the S3 knee simulation. The designs are ordered from the highest performing designs on the left to the lowest performing designs on the right. The best performance was with the design that had the lowest RMSE and the greatest percentage of angle range of motion the actuators were active through.

According to the table, the actuators with longest length perform best given the same actuator diameters. The larger diameter actuators perform better than the actuators with smaller diameters, given the same actuator length. When comparing between actuators of different lengths and diameters, the best performance tends to be with the actuator with the larger diameter. For example, design 2 had the lowest RMSE, but it was closely following by combo 6, where there was a difference in RMSE of 0.01 Nm (0.007 ft-lb). Even though the back actuator of combo 6 was 145 mm (5.7 in) longer than design 2, design 2 had slightly better performance; the larger RMSE in combo 6 is due to the fact that the back actuator has a smaller diameter. Therefore, the best performance lies with long actuators with large diameters, but if length and diameter are traded, it is better to select the actuator with the larger diameter than the longer actuator.

Designs 1 and 7 actively mimicked joint torque through the same percentage of the full range of motion, however design 7 performed better than design 1 in terms of reducing the RMSE. It is interesting that design 7 had shorter front and back actuator lengths than design 1 but still performed better than design 1. The difference between designs 1 and 7 is that the back actuator diameter is larger for design 7, supporting the claim that actuators with larger diameters will improve performance more than actuators with longer nominal lengths. Therefore, while actuators with longer lengths and diameters tend to perform better than shorter and thinner actuators, there is a greater performance increase when larger diameter actuators are used.

According to Table 4.4, RMSE does not seem to be greatly affected by the back actuator length, while the front actuators that are 350 mm (13.78 in) in length or shorter all perform in the bottom half in terms of reducing the RMSE and increasing the percentage of the angles through which the actuators were active. This suggests that perhaps a front actuator with a long length will help reduce RMSE more than a back actuator with a long length.

Overall, it seems as though the most successful designs have front actuators greater than 350 mm (13.78 in) in length. Additionally, designs which utilize 20 mm (0.8 in) diameter back actuators should be selected because as in the case of the comparison between design 2 and combo 6, the actuator with the larger diameter performed better in terms of RMSE even though combo 6 had a back actuator that was 145 mm (5.7 in) greater in length. Therefore, to save bulk, a shorter back actuator with a larger diameter is preferred over a longer back actuator with a smaller diameter.



**Table 4.4 Comparison of the designs implemented in the S3 knee simulator**

		Design 2	Combo 6	Design 7	Design 1	Combo 3	Design 6	Combo 5	Combo 4	Combo 2	Design 5	Design 4 (Combo 1)	Design 3
<b>Back Actuator</b>	<b>Nominal Length (mm)</b>	350	495	200	280	200	200	495	495	200	200	200	150
	<b>Diameter (mm)</b>	20	10	20	10	10	10	10	10	10	20	10	10
<b>Front Actuator</b>	<b>Nominal Length (mm)</b>	513	495	487	513	495	487	350	300	350	300	300	250
	<b>Diameter (mm)</b>	20	20	20	20	20	20	20	20	20	20	20	20
<b>RMSE (Nm)</b>		1.85	1.86	2.1	2.25	2.29	2.3	2.32	2.55	2.68	2.72	2.88	3.1
<b>Active ROM Percentage (%)</b>		80.6	80.6	76.7	76.7	73.8	73.8	65	59.2	58.3	55.3	52.4	46.6

Although actuators with larger diameters and longer nominal lengths have resulted in the best RMSE performance, they also result in larger bulk and greater weight characteristics. The S3 computer simulator is a useful tool for space suit researchers to use because it allows researchers to perform trades of the costs of designs with added weight and bulk and the benefits of designs with low RMSE. Researchers can decide whether the design with the best performance is the most important objective of their specific project goals, or whether a design with the least weight and bulk is most important.

Because the main objective of the S3 project is to design a space suit simulator exoskeleton that minimizes weight and bulk characteristics while mimicking the joint torque properties of a pressurized space suit, a design that minimizes weight and bulk may be preferred over a design that produces the best RMSE, as long as the joint torque can still be matched at the range of motion extremes, where the torques are greatest. While actuators that are short in length are not able to mimic torques through the full angle range of motion, the actuators can be placed so they reach their hard stop before the angle range of motion extremes, allowing the designs to follow joint torques when the torque values are the largest. At the intermediate flexion and extension angles, the magnitude of the EMU knee torques is around 5 Nm (3.69 ft-lb). Therefore, if the actuator is short and not able to achieve torques through the intermediate angles, the disadvantage in RMSE will not be as large as if the actuators were not able to achieve the torques at the range of motion extremes. Therefore, a design that is able to mimic the joint torque properties of the EMU space suit knee at the range of motion extremes while minimizing weight and bulk characteristics is preferred for the S3.

## 4.5 Summary

A S3 computer simulator was created that allows the user to input the location of the endpoints of the pneumatic actuators along with their geometries, the radius and location of spools for the actuators to wrap around, the supply pressure to each of the actuators, and the knee joint angle. The simulator calculates the percent contraction of each of the actuators, the tension at the endpoints of the actuators, and the knee torque. The S3 computer simulator can be used to determine feasible lower body exoskeleton designs that are able to mimic the joint torque of a pressurized space suit through the joint range of motion, particularly at the range of motion extremes, while minimizing the RMSE. The supply pressures needed to achieve the desired joint torques at each angle will also be useful in the design of the S3 controller.

An example design for 50% female anthropometry was input in the S3 computer simulator. The example simulation included a front actuator of 20 mm (0.8 in) diameter and 295 mm (11.6 in) nominal length wrapped around a spool attached to the front of the upper leg. The back actuator was 10 mm (0.4 in) in diameter and 200 mm (7.9 in) in length and also wrapped around a spool, attached to the back of the upper leg. Both spools and actuators were aligned with the midline of the leg. The 50% female anthropometry design was able to mimic the knee torque of a pressurized EMU leg through all angles of knee flexion except between 10 and 16 degrees, and through all angles of knee extension except between 84 and 30 degrees. The RMSE was 2.31 Nm (1.70 ft-lb), where most of the error occurred at the intermediate angles, when the back actuator was not yet at its hard stop. This example demonstrates how the user goes through the process of selecting the location of the actuators and spools depending on subject anthropometry, and how to use the S3 computer simulator to gather information about the knee torque through the knee range of motion.

The greave design of the S3 knee concept was implemented into the S3 computer simulator by modeling the portion of the greave covering the knee as a circle that rotates with the lower leg. Therefore, the lower endpoints of each of the actuators along with the circle representing the greave move with the lower leg because each of these components is attached to the greave, which is strapped around the subject's lower leg.

Several designs were input into the S3 computer simulator based on 95% male anthropometry. The torque versus angle output curves of each of the designs were compared with the EMU data gathered by Schmidt using a pressurized EMU on MIT's robot space suit tester [Schmidt et al., 2001]. A baseline design was input and subsequent designs were selected to measure if varying actuator

dimensions affected RMSE. Design 2, which had a front actuator with a longer nominal length than the baseline design 1, was able to mimic the joint torque of the EMU knee throughout a larger range of motion and was able to reduce the RMSE. Design 3, which had front and back actuators with shorter nominal lengths, did not improve upon the baseline design in RMSE or the range of motion the actuator was active through.

Designs 4, 5, 6, and 7 were studied to measure how changes in actuator length and diameter affected RMSE and the range of motion the actuators were active through. Design 7, which had the longest actuators and largest diameters, was able to achieve the lowest RMSE and mimic the joint torque through the greatest range of motion. Although design 7 had the best performance of the four designs, it also had the greatest weight and bulk due to the larger length and diameter actuators. The tradeoffs between improved performance and added weight and bulk were discussed.



## 5.1 Overview

Although pressurized space suit mobility has improved since the first spacewalks in the 1960s, pressurized space suits still impose high joint torques on the astronauts and result in reduced mobility [Holschuh, 2009; Bethke, 2005; Schmidt, 2001; Kosmo & Ross, 1998]. In order to reduce the high joint torques and improve astronaut mobility, space suit research is needed. Using NASA space suits for all space suit research, however, is impractical. The NASA suits are expensive and bulky, making them difficult to transport, and in limited supply, making them difficult to get access to [ILC Dover, 1994].

A space suit simulator exoskeleton with the ability to mimic the angle range of motion and joint torque properties of pressurized space suits is a useful tool for space suit designers and researchers. Space suit designers can compare the joint torque properties of new space suit concepts and prototypes against the joint torques of the current NASA space suits. Space suit researchers can study the energy expenditure of working in space suits that impose high joint torques on the subjects and limit their range of motion. In addition, a space suit simulator exoskeleton can adhere to usual orientations and confined spaces typical of NASA partial weight-bearing reduced gravity simulators. This tool can allow for space suit torque and range of motion experimentation, without the added difficulty of accessing a NASA pressurized suit. In order to develop a space suit simulator exoskeleton, the joint torque and angle range of motion properties of the current NASA pressurized space suits were compiled into a joint torque database. Next, actuators that have been used in exoskeletons for the biomedical and military industries were studied. Actuators that actively control the joint torque behaviors of exoskeletons allow for precise control of resistance to motion, a desired property of the S3 exoskeleton. Actuators used for active control of the joint torque properties of exoskeletons were qualitatively compared according to weight and bulk characteristics in order to select low weight, low bulk actuators for the S3 exoskeleton. Upon selection of actuators, the knee joint exoskeleton design was completed. Conceptual designs of the S3 hip joint were also proposed. Finally, the S3 computer simulator was improved to incorporate the design characteristics of the S3 knee joint. The computer simulator was developed to input various actuator and spool dimensions and locations and determine the torque output as the knee moves through its range of motion.

This chapter discusses the results from the S3 project, including the space suit joint database, the actuator comparisons, the conceptual design of the S3 joints, and the S3 computer simulator. Key

challenges for the continuing development of the S3 project are discussed, along with recommendations for improvement. Next steps for the S3 project are then outlined. The chapter concludes with final comments regarding the S3 project.

## 5.2 Space Suit Joint Database

The space suit joint database was created to help set the requirements for the S3 exoskeleton angle and torque bounds for the body degrees of freedom for multiple pressurized space suits. Six pressurized space suits are included in the joint database, along with torque and range of motion information for 15 degrees of freedom. Additionally, torque versus angle curves are included for some of the space suits, in order to match joint torque to angle for precise mimicking of the space suit joint torques with the S3. The space suit joint database was created by reviewing the space suit literature. Three space suit joint torque testing methods are prevalent in the literature: empty pressurized suit testing, human-in-the-suit testing, and robot space suit testing. Joint torque data gathered using all three methods was input into the simulator and aided in setting the S3 range of motion and torque requirements for each degree of freedom. The full space suit joint database is included in Appendix A.

The angle range of motion data was gathered primarily from biomechanics references, which included shirt-sleeve mobility for males and females of varying anthropometry. Unsuiting range of motion information was included in the joint database so that the S3 requirements would include angle ranges that can accommodate future space suit mobility. Therefore, future space suit joint torques can be simulated by the S3 exoskeleton by modifying the controller software code. The joint torques in the joint database include current pressurized space suit torques gathered with the various joint torque testing methods.

## 5.3 Actuator Comparison

Four actuator types that have been used for active control in exoskeleton design were compared qualitatively by their weight and bulk characteristics: hydraulic actuators, pneumatic actuators, MR fluid actuators, and electric actuators. Gross estimates of the weight of the actuators used in previous exoskeleton designs were determined. Pneumatic actuators, also known as fluidic muscles, developed by Festo (Brussels, Belgium) weigh only 0.14 kg (0.3 lbs) for a 1 m (3.28 ft) long actuator with a 10 mm (0.40 in) diameter ([www.festo.com](http://www.festo.com)). The pneumatic muscles weigh less than the hydraulic, MR fluid, and electric actuators according to gross weight estimates. For the actuators whose weights were not specifically mentioned in the literature, gross weight estimates were made based on

the exoskeleton weight, the number of actuators and active degrees of freedom, and the exoskeleton material.

Qualitative comparisons of the bulk characteristics of actuators were conducted visually by studying the approximate volume taken up surrounding the subject's lower body and the number of actuators needed for each degree of freedom. The hydraulic actuators used in the HULC lower body exoskeleton are less bulky than the exoskeleton designs that use pneumatic, MR fluid, and electric actuators. However, the structure needed to support the pneumatic actuators is not as bulky as the exoskeleton structures of the electric and MR fluid actuation devices because of the low weight of the pneumatic actuators.

Due to the desired low weight and bulk characteristics of the S3 exoskeleton, the pneumatic actuators were selected. The pneumatic actuators have the lowest weight characteristics after qualitative comparisons between the actuation devices. Although the pneumatic actuators are not the least bulky of the actively controlled actuators, they have an additional advantages, namely, they are flexible and mimic the spring-like properties of a pressurized space suit well. The pneumatic actuators selected are hollow elastomer cylinders embedded with aramid fibers that create force output at the endpoints of the actuator as they fill with air, thereby increasing the actuator diameter and decreasing the actuator length.

## **5.4 Conceptual Design**

The pneumatic actuators were used in the design of the S3 knee joint. Because the pneumatic actuators are unidirectional, two actuators are required for one degree of freedom. Therefore, an actuator is used on the front of the leg to actively resist knee flexion motion, while another actuator is used on the back of the leg to actively resist knee extension motion. The final S3 knee conceptual design has one actuator directly in front of the midline of the leg, wrapping around the knee joint, and the other actuator directly behind the midline of the leg, behind the knee. The actuators are placed along the midline of the leg in order to avoid the out of plane torques that would have been present with a design laterally offset with actuators along the side of the leg. In order to protect the kneecap from the forces produced by the pressurized actuator, a greave is incorporated into the S3 knee joint design. A greave is a shin guard-like device that covers the shank and the kneecap of the leg. Sliding rails are also included in the S3 knee design at the endpoints of the actuators to take up the slack in the actuators when they are not pressurized; this will prevent the actuators from buckling.

Two conceptual designs for the hip joint were also developed. One of the hip design concepts does not include a rigid exoskeleton structure, while the other design concept includes rigid exoskeleton components. The first design once again includes two pneumatic actuators per degree of freedom. Because the S3 hip joint will actively control hip flexion/extension and also hip abduction/adduction, four pneumatic actuators are required per leg, two to resist flexion/extension motion, and two to resist abduction/adduction motion. The two actuators on the back of the leg pressurize to resist hip flexion, while the two actuators on the front of the leg pressurize to resist hip extension. The two actuators closest to the midline of the body pressurize to resist hip abduction, while the two actuators closest to the outside of the body pressurize to resist hip adduction. While this design concept is lightweight and actively resists motion for two degrees of freedom of the hip, the absence of rigid structural components would make it difficult to quantify joint torques about the hip point of rotation. Additionally, while the forces produced by the pneumatic actuators can be partially transferred through the rigid structural components of an exoskeleton, the forces will be applied directly to the subject's body without hard structural components.

The alternative conceptual design of the hip joint includes an exoskeleton hard structure based off of the BLEEX exoskeleton design [Chu et al., 2005]. In this concept, the pneumatic actuators wrap around the hard exoskeleton components to resist motion for the two hip degrees of freedom. The exoskeleton hip design allows for quantifiable hip torque calculations and a hard surface for the actuator forces to be transferred to, but has the disadvantage of increased complexity.

## **5.5 S3 Computer Simulation**

The S3 computer simulation was developed to determine the locations of components of the S3 knee design that are able to mimic knee torques through large ranges of motion and produce small RMSE. The S3 computer simulator allows the user to input the knee angle, actuator supply pressures, and geometries and locations of the spools and actuators. The simulator then calculates the percent contraction of each of the actuators, the tension at the endpoints of the actuators, and the knee torque at each knee flexion angle. The percent contraction of the actuators is calculated by comparing the actuator lengths at the current knee flexion angle to the nominal lengths of the actuators. The tension at the endpoints of the actuators is determined through lookup tables that describe the relationship between the percent contraction of the actuator, the supply pressure to the actuator, and the tension at the endpoints of the actuators. The knee joint torque calculation is a function of the location of the lower endpoints of the actuators and the tensions in the actuators.



To determine potential actuator lengths and geometries for the S3 knee design, a variety of actuators were input into the S3 computer simulation. In general, actuators with larger diameters and longer lengths are able to mimic the EMU knee joint torques through a greater range of motion and are also able to minimize RMSE. However, actuators with larger diameters and longer lengths also add weight and bulk to the exoskeleton. Therefore, the benefits of improved performance need to be traded against the costs of adding weight and bulk. While the longer and thicker actuators obtain the best performance among the designs compared, the shorter and thinner actuators are also able to mimic EMU knee joint torque properties at the knee range of motion extremes, where it is most important to mimic the joint torques because they are the greatest at the extreme angles. Therefore, smaller actuators may be preferred over longer actuators if the difference in performance is due to loss of the ability to mimic the joint torques at the intermediate angles.

## **5.6 Moving Forward**

### ***5.6.1 Key Challenges***

There are several key challenges moving forward with the S3 project. The S3 will include three actively controlled joints, and several additional passive degrees of freedom. The knee and the hip joints will be actively controlled in the final version of the S3. The third joint to be actively controlled is still to be determined. One joint that would be useful to space suit researchers is the shoulder. The shoulder provides motion for four degrees of freedom: flexion/extension, abduction/adduction, interior/exterior transverse rotation, and humeral rotation. The energy expended through shoulder motion is also significant for astronauts working on EVA. Astronauts on EVA at the ISS are typically attached to the station via a robotic arm, allowing for minimal lower body movements, while most motion and repair work is done using the upper limbs. On future human planetary exploration missions, full body mobility will be critical to assemble planetary infrastructure and collect science samples. A challenge with the S3 shoulder design is that the shoulder joints of the current pressurized space suits vary greatly. Soft shoulder designs do not create large pressure points on the top of the shoulder while shoulder designs that include scye bearings do. While the joint torques and angle range of motion of various shoulder designs can be simulated with actively controlled actuators, the feel of the pressurized suits, such as the feel of scye bears on the shoulder, cannot be simulated with actuators alone. A key challenge is to decide if and how to simulate the feel of key components of current pressurized space suits, such as the feel of working in a pressurized space suit that includes a shoulder scye bearing.

A second challenge is to determine how to simulate the joint torques for complex motions of joints with multiple degrees of freedom. Thus far, most space suit torque data has been gathered for simple motions in a single degree of freedom plane [Matty, 2010; Holschuh et al., 2009; Stirling, 2008; Morgan et al., 1996], and the joint torques during complex motions have only been determined for select EMU motions [Schmidt, 2001; Frazer, 2003]. For example, the hip can move in multiple degrees of freedom. The torque versus angle curves have been measured during space suit hip flexion/extension motion and also during hip abduction/adduction motion, however the torque is not known if the subject were to move their leg forward and to the side, in a swinging motion, for example. The challenge is to determine how to extrapolate joint torque data for single degree of freedom motion to complicated motions.

### ***5.6.2 Recommendations for Improvement***

The current S3 knee design includes greave and exoskeleton structure dimensions that accommodate the anthropometry of a 95% male because the knee joint will be tested on MIT's RSST which has 95% male dimensions. The design has not yet been scaled down to fit a 5% female or any of the anthropometries in between. Because the exoskeleton structure may not be as extensive for a 5% female, the actuator lengths and dimensions may not need to be as large to achieve the desired knee joint torques seen in a pressurized EMU knee. If greave and actuator endpoint locations that accommodate a 5% female were implemented in the S3 computer simulation, it can be determined if alternative actuators should be selected for 5% female. Researchers could also determine if the same actuators used on a subject with 95% male anthropometry would hurt performance if used on a subject with 5% female anthropometry. Although a design that will accommodate 95% male anthropometry is sufficient for robot testing of the S3 knee, the scaling of components is important for future designs that will accommodate a wider range of subject anthropometries.

As additional actively controlled joints are developed for the S3, the exoskeleton component integration between joints should be carefully laid out. While the S3 knee joint component does not interfere with the S3 hip joint component on a 95% male, there may be interference between joint components on a 5% female, especially if the same actuator lengths and diameters are used on all subjects. Therefore, the integration of the S3 components and the interfaces between actively controlled joints and degrees of freedom should be decided upon before robot testing of the hip component.

Several enhancements to the S3 computer simulation should be made. The current simulation includes the conceptual design of the S3 knee joint. A future version of the simulator should include the conceptual design of the hip degrees of freedom. The simulation should also be updated to include the third actively controlled joint that is yet to be determined.

The current S3 computer simulation assumes constant velocity or no angular acceleration of the leg during knee flexion and extension. This affects the knee torque calculation, which does not include acceleration or leg moment of inertia affects. Because there is angular acceleration of the leg during normal motion, a future version of the S3 computer simulator should incorporate the acceleration and moment of inertia components of the knee torque calculation. The moment of inertia of the leg has already been characterized in the literature; however, the moment of inertia of the S3 exoskeleton components should be characterized and included in the simulation to improve the joint torque calculations.

Finally, the S3 computer simulation should be automated so that after the user inputs the spool and actuator dimensions and locations, the simulation could automatically determine the torque values output as the joint moves through its range of motion. Instead of the user manually determining the supply pressure that reduces the RMSE at each angle, the simulation should automatically minimize torque error at each angle and move forward to the next joint angle. The simulation could then output the torque versus angle curve of the input design as well as the supply pressures that produced the joint torques with the smallest error at each given angle. A more automated procedure would allow for more designs to be analyzed in a shorter amount of time.

### ***5.6.3 Directions for Future Research***

There is much work still to be done with the S3 project. The final design of the hip joint must be selected, that is able to mimic the joint torques of the flexion degree of freedom and also the abduction degree of freedom. Once the conceptual design of the S3 hip joint is decided upon, the S3 computer simulation must be updated to incorporate the hip design. Several actuator geometries can be input into the S3 computer simulation to determine actuator diameters and lengths that reduce torque RMSE of the hip degrees of freedom and mimic the joint torques through a large range of hip motion.

The third joint that will be actively controlled must be selected, designed, and also incorporated into the S3 computer simulation. The knee joint design must be manufactured and various actuator lengths and diameters can be tested with the knee design on MIT's robotic space suit tester. The torque versus angle curves output from the robot joint torque testing can be compared to the curves produced

with the same designs input into the S3 computer simulation. Any differences in the S3 computer simulation torque versus angle curves can be updated as needed. The final two actively controlled joints must also be tested on the robot space suit tester. Final design modifications can be made to the joints as needed. In the future, a full body space suit simulator exoskeleton can be developed to mimic the joint torques of pressurized space suits for multiple degrees of freedom.

## 5.7 Final Conclusions

The first step in the development of the S3 exoskeleton was to develop a space suit joint database which is a compilation of joint torque and angle range of motion characteristics of six pressurized space suits and 15 degrees of freedom. The space suit joint database was used to set requirements for the S3 exoskeleton angle and torque bounds. Next, weight and bulk characteristics of actuators that have been used to actively control joint torques in previous exoskeleton designs were qualitatively compared, and pneumatic actuators were selected. The actuators were selected based on low weight characteristics and their ability to mimic the spring-like properties of a pressurized space suit. The final S3 knee design includes one pneumatic actuator to actively resist knee flexion and one pneumatic actuator to actively resist knee extension. The leg is protected with a greave shin guard-like device. Two conceptual designs for the hip joint were also developed: one which includes a rigid exoskeleton structure, and another that does not include rigid exoskeleton components. Finally, the S3 computer simulation was developed in MATLAB as a tool to determine feasible actuator and spool dimensions and locations that are able to mimic space suit joint torques through large ranges of motion and produce small torque root mean square errors.

The S3 exoskeleton can mimic the joint torque and angle ROM properties of a pressurized space suit. This tool allows for space suit experimentation without the added hassles of high cost, limited accessibility, and transportation difficulty associated with using a NASA suit for research. The S3 exoskeleton improves the current state of the art in joint torque simulators because it is the first space suit simulator with the ability to actively control resistance to motion. In addition, the S3 exoskeleton is also the first simulator with the ability to mimic several pressurized space suits with one exoskeleton design. By using actuators that allow for active control of joint torque, the resistance to motion is modified for each suit with alterations in the software code without having to exchange any hard components of the exoskeleton. The S3 project uses hysteresis curves gathered with a robot space suit testing method to accurately match joint torques for each degree of freedom angle; the torques gathered with this method incorporate the volume and pressure effects of having a person in the suit,

which provides a more accurate joint torque measurement. Finally, the S3 exoskeleton utilizes pneumatic actuators, which have been used in previous exoskeleton designs, to provide a low weight, flexible design, with the ability to mimic the spring-like properties of the space suit.



## Bibliography

- Ahlstrom, V., & Longo, K. (2003). *Human Factors Design Standard (HF-STD-001)*. Atlantic City International Airport, NJ: Federal Aviation Administration William J. Hughes Technical Center.
- Bethke, K. (2005). *The Second Skin Approach: Skin Strain Field Analysis and Mechanical Counter Pressure Prototyping for Advanced Spacesuit Design*. Aeronautics & Astronautics. Cambridge, MA, Massachusetts Institute of Technology. **Master of Science**.
- Blaya, J. A. (2003). *Force-Controllable Ankle Foot Orthosis (AFO) to Assist Drop Foot Gait*. Department of Mechanical Engineering. Cambridge, MA, Massachusetts Institute of Technology. **Master of Science**.
- Braden, J. R., & D.L. Akin (2004). *Design of a Modular Testbed for Advanced Space Suit Development Testing*. Space 2004 Conference and Exhibit. San Diego, CA.
- Carr, C. E., & D.J. Newman (2008). "Characterization of a lower-body exoskeleton for simulation of space-suited locomotion." Acta Astronautica **62**: 308-323.
- Carr, C. E., & D.J. Newman (2005). *When is Running More Efficient Than Walking in a Space Suit?* 35th International Conference on Environmental Systems. Rome, Italy.
- Chen, J. Z., & W.H. Liao (2010). "Design, testing and control of a magnetorheological actuator for assistive knee braces." Smart Materials and Structures **19**.
- Chu, A., Kazerooni, H., & A. Zoss (2005). *On the Biomimetic Design of the Berkeley Lower Extremity Exoskeleton (BLEEX)*. International Conference on Robotics and Automation. Barcelona, Spain.
- Department of Defense Handbook: *Human Engineering Design Guidelines (MIL-HDBK-759C)* (1995).
- De Witt, J.K., Perusek, G.P., Lewandowski, B.E., Gilkey, K.M., Savina, M.C., Samorezov, S., & W.B. Edwards. *Locomotion in simulated and real microgravity: horizontal suspension vs. parabolic flight*. Aviat Space Environ Med **81**(12): 1092-9 (2010).
- Dionne, S. (1991). *AX-5, Mk III, and Shuttle Space Suit Comparison Test Summary*. SAE. Moffett Field, CA.
- Duda, J. *Space Suit Simulator (EVA S3) for Partial Gravity EVA Experimentation and Training*. NASA SBIR Phase 2 Proposal, Aurora Flight Sciences (2010).
- Ferris, D. P., Czerniecki, J.M., & B. Hannaford (2005). "An Ankle-Foot Orthosis Powered by Artificial Pneumatic Muscles." J Appl Biomech **21**(2): 189-197.
- Frazer, A. L., Pitts, B.M., Schmidt, P.B., Hoffman, J.A., & D.J. Newman (2002). *Astronaut Performance: Implications for Future Spacesuit Design*. International Astronautical Conference. Houston, TX.
- Genc, K.O., Mandes, V.E., & P. Cavanagh (2006). *Gravity Replacement During Running in Simulated Microgravity*. Aviation, Space, and Environmental Medicine, **77**(11): 1117-1124.

Graziosi, D., & R. Lee (2003). I-Suit Advanced Spacesuit Design Improvements and Performance Testing. SAE International.

Holschuh, B., Waldie, J., Hoffman, J., & D. Newman (2009). Characterization of Structural, Volume and Pressure Components to Space Suit Joint Rigidity. SAE International 2009.

Ikeuchi, Y., Ashihara, J., Hiki, Y., Kudoh, H., & T. Noda (2009). Walking Assist Device with Bodyweight Support System. IEEE/RSJ International Conference on Intelligent Robots and Systems. St. Louis, MO.

ILC Dover, Inc. Space Suit Evolution: From Custom Tailored to Off-The-Rack, 1994.

Joint Motion: Clinical Measurement and Evaluations, Roger Soames, Elsevier, 2003.

Kosmo, J. J., & A. Ross (1998). Space Suit Mobility Evaluations in Lunar/Mars Gravity Environments. 28th International Conference on Environmental Systems. Danvers, MA.

Kozloski, L. D. (1994). U.S. Space Gear: Outfitting the Astronaut. Washington, Smithsonian Institution Press.

Lockheed Martin Corporation (2008). HULC: Exoskeletons Augment Strength and Endurance. P. Card.

Matty, J. E., Aitchison, L. (2009). A Method for and Issues Associated with the Determination of Space Suit Joint Requirements. SAE International

Matty, J. (2010). Results and Analysis from Space Suit Joint Torque Testing. 40th International Conference on Environmental Systems.

Meyen, F. E., Holschuh, B., Kobrick, R.L., Jacobs, S., & D.J. Newman (2011). Robotic Joint Torque Testing: A Critical Tool in the Development of Pressure Suit Mobility Elements. 41 International Conference on Environmental Systems. Portland, OR.

Morgan, D. A., Wilmington, R.P., Pandya, A.K., Maida, J.C., & K.J. Demel (1996). Comparison of Extravehicular Mobility Unit (EMU) Suited and Unsuited Isolated Joint Strength Measurements. Houston, TX, NASA Johnson Space Center.

NASA-STD-3000 Handbook. Man-Systems Integration Standards. Volume III. National Aeronautics and Space Administration, August 1994.

Newman, D., Marquez, J., Ferreira, I., Tan, J., & J. Edmonds (2007). MIT Robotic Testing of Right Knee Joint for the Space Suit Simulator. Cambridge, MA, MIT Man-Vehicle Lab.

Openshaw, S., & E. Taylor. Ergonomics and Design: A Reference Guide. Allsteel Inc. (2006).

Perusek, G., Lewandowski, B., Gilkey, K., Nall, M., Just, M., Cavanagh, P., Kuklis, M., Novotny, S., & J. DeWitt (2007). Exercise Countermeasures and a New Ground-Based Partial-g Analog for Exploration. 45<sup>th</sup> AIAA Aerospace Sciences Meeting. Reno, Nevada.



- Portree, David S. F.; Robert C. Treviño (October 1997). "Walking to Olympus: An EVA Chronology". *Monographs in Aerospace History Series #7*. NASA History Office. pp. 15–16. <<http://history.nasa.gov/monograph7.pdf>>.
- Pratt, J., Krupp, B., & C. Morse (2002). "Series elastic actuators for high fidelity force control." Industrial Robot: An International Journal **29**(3): 234-241.
- Pratt, J. E., Krupp, B.T., Morse, C.J., & S.H. Collins (2004). The RoboKnee: An Exoskeleton for Enhancing Strength and Endurance During Walking. IEEE International Conference on Robotics & Automation. New Orleans, LA.
- Ripps, T. B., Garcia, J.M., Macleod, S.R. & S. Jacobs (2011). The Demonstrator Suit: Evaluating a Full Pressure Suit through Manned and Unmanned Testing. 41st International Conference on Environmental Systems. Portland, OR.
- Schmidt, P.B (2001). "An Investigation of Space Suit Mobility with Applications to EVA Operations." PhD Thesis, MIT.
- Schmidt, P. B., Newman, D.J., & E. Hodgson (2001). Modeling Space Suit Mobility: Applications to Design and Operations. International Conference on Environmental Systems. Orlando, FL.
- Stirling, L.A. "Development of Astronaut Reorientation Methods: A Computational and Experimental Study." PhD Thesis, MIT 2008.
- Suzuki, K., Mito, G., Kawamoto, H., Hasegawa, Y., & Y. Sankai (2007). "Intention-based walking support for paraplegia patients with Robot Suit HAL." Advanced Robotics **21**(12): 1441-1469.
- Thakkar, S. (2002). Energy Economy Gait Analysis of an Autoadaptive Prosthetic Knee. Electrical Engineering and Computer Science. Cambridge, MA, Massachusetts Institute of Technology. **Master of Science**.
- Thomas, K.S., McMann, H. J. (2006). US Spacesuits. Chichester, UK, Praxis Publishing Ltd.
- Winter, D. A. (1990). Biomechanics and Motor Control of Human Movement. New York City, USA, Wiley-Interscience Publication.
- Zoss, A. B., Kazerooni, H., & A. Chu (2006). Biomechanical Design of the Berkeley Lower Extremity Exoskeleton (BLEEX). IEEE/ASME Transactions on Mechatronics. **11**.


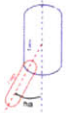



## Appendix A: Space Suit Joint Database


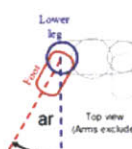
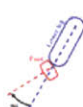
The tables in section A.1 indicate the minimum and maximum angles that describe the degree of freedom range of motion from several references. The tables in section A.2 indicate the minimum and maximum torque that describes the degree of freedom joint torque from several references. The tables in section A.2 also depict torque versus angle curves collected for pressurized space suits. For both tables, the blue body in the visual depiction indicates the reference body, the red body indicates the action body, and the arrow indicates the positive sense of rotation. The body is viewed from either the right side, the front of the person, or the top of the person. The abbreviation for the degree of freedom is indicated. The minimum and maximum values (for angle or torque) are indicated for each space suit and space suit pressurization level. The brackets indicate the reference source, which are listed after the tables. Finally, the S3 specifications for the angle and torque bounds of each degree of freedom are listed in the tables.

### A.1 Range of Motion

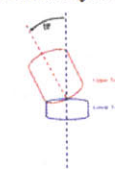
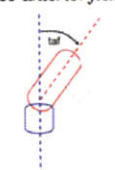
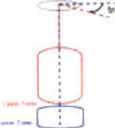
#### A.1.1 Hip

Visual Depiction*	Abbreviation	Unsuited Human Data [3]		Unsuited Human Data [5]		Unsuited Human Data [6]		S3 Specifications	
		Minimum (deg)	Maximum (deg)	Minimum (deg)	Maximum (deg)	Minimum (deg)	Maximum (deg)	Min	Max
 <i>Hip flexion</i>	hf	0	148	0	126	-20	120	-20	148
 <i>Hip abduction</i>	ha					-30	45	-30	45
 <i>Thigh rotation</i>	tr			-49	44	-45	45	-49	45

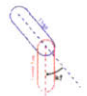

### A.1.2 Ankle

	Visual Depiction*	Abbreviation	Unsuited Human Data [3]		Unsuited Human Data [5]		S3 Specifications	
			Minimum (deg)	Maximum (deg)	Minimum (deg)	Maximum (deg)	Min	Max
ANKLE	<p><i>Ankle flexion</i></p> 	af	-91.1	17.4	-50	42	-91.1	42
	<p><i>Ankle rotation</i></p> 	ar			-47	55	-47	55
	<p><i>Ankle inversion</i></p> 	ai			-33	30	-33	30

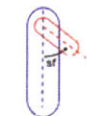
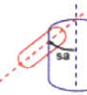
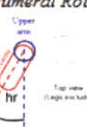

### A.1.3 Torso

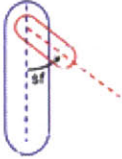
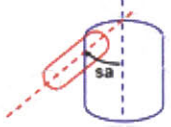
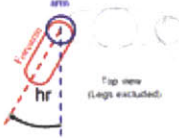
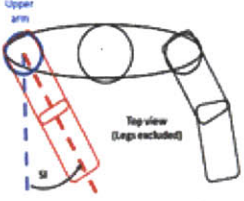
	Visual Depiction*	Abbreviation	Unsuited Human Data [4]		Unsuited Human Data [6]		S3 Specifications	
			Minimum (deg)	Maximum (deg)	Minimum (deg)	Maximum (deg)	Min	Max
TORSO	<p><i>Torso lateral flexion</i></p> 	tlf	-21	21	-30	30	-30	30
	<p><i>Torso anterior flexion</i></p> 	taf	-21	46	-30	55	-30	55
	<p><i>Torso rotation</i></p> 	tro	-46	46	-40	40	-46	46

### A.1.4 Knee & Elbow

	Visual Depiction*	Abbreviation	Demonstrator 4.8psi [7]		Unsuited Human Data [3]		Unsuited Human Data [5]		S3 Specifications	
			Minimum (deg)	Maximum (deg)	Minimum (deg)	Maximum (deg)	Minimum (deg)	Maximum (deg)	Min	Max
KNEE		kf	0	95	0	145.6	0	126	0	145.6
ELBOW		ef	0	120	0	165.9	0	152	0	165.9

### A.1.5 Shoulder

	Visual Depiction*	Abbreviation	Demonstrator 4.8psi [7]		Unsuited Human Data [3]		Unsuited Human Data [4]	
			Minimum (deg)	Maximum (deg)	Minimum (deg)	Maximum (deg)	Minimum (deg)	Maximum (deg)
Shoulder		sf	-10	115	-87.9	217	-32	95
		sa	0	110			-25	68
		hr	-90	55	-130.9	96.7		
		si	-120	20	192.9 ROM			

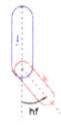
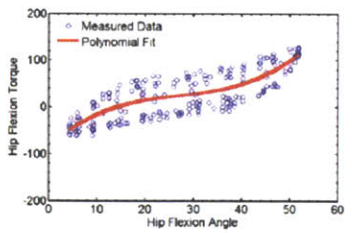
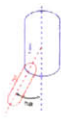
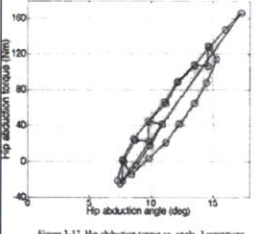
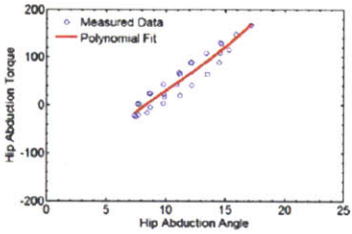
	Visual Depiction*	Abbreviation	Unsuited Human Data [5]		S3 Specifications	
			Minimum (deg)	Maximum (deg)	Min	Max
Shoulder	<p><i>Shoulder Flexion</i></p> 	sf	-75	190	-87.9	217
	<p><i>Shoulder Abduction</i></p> 	sa			-25	110
	<p><i>Humeral Rotation</i></p> 	hr	-119	47	-130.9	96.7
	<p><i>Shoulder Interior/Exterior Transverse Rotation</i></p> 	si	-151	57	-151	57


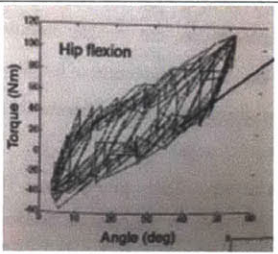

### References

- [3] NASA-STD-3000 Handbook. Man-Systems Integration Standards. Volume III. National Aeronautics and Space Administration, August 1994.
- [4] Openshaw, S., & E. Taylor. Ergonomics and Design: A Reference Guide. Allsteel Inc. (2006).
- [5] Department of Defense Handbook: Human Engineering Design Guidelines (MIL-HDBK-759C) (1995).
- [6] Joint Motion: Clinical Measurement and Evaluations, Roger Soames, Elsevier, 2003
- [7] Ripps, T.B., Garcia, J.M, Macleod, S.R., & S. Jacobs. The Demonstrator Suit: Evaluating a Full Pressure Suit through Manned and Unmanned Testing. 41st International Conference on Environmental Systems, Portland, OR (2011).


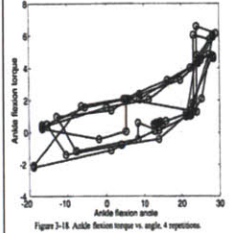
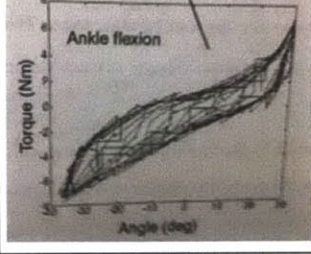
## A.2 Joint Torque

### A.2.1 Hip

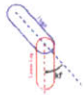
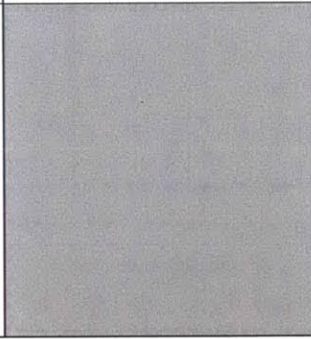
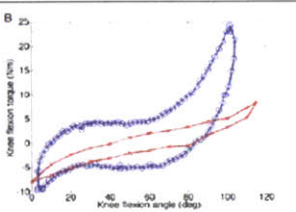

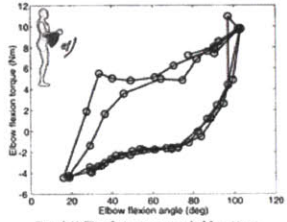
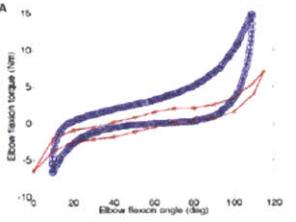
		Human Suited [1]		EMU Robot Suited [1] (Nm)	EMU Robot Suited [5] (Nm)
Visual Depiction*	Abbreviation	Minimum (Nm)	Maximum (Nm)		
<p>HIP</p> <p><i>Hip flexion</i></p> 	hf				
<p><i>Hip abduction</i></p> 	ha	-25	165	 <p>Figure 3-17 Hip abduction torque vs. angle, 3 repetitions.</p>	

		Torque Limitations		S3 Specifications	
Visual Depiction*	Abbreviation	EMU Robot Suited [6] (Nm)	Polynomial Fit Torque Eqns [5]	Min	Max
<p>HIP</p> <p><i>Hip flexion</i></p> 	hf		$\tau = 4.2 \times 10^{-38} \theta^3 - 0.35 \theta^2 + 10.4 \theta - 87.5$	-55	115
<p><i>Hip abduction</i></p> 	ha		$\tau = 4.8 \times 10^{-28} \theta^3 - 1.5 \theta^2 + 33.1 \theta - 198.3$	-25	165


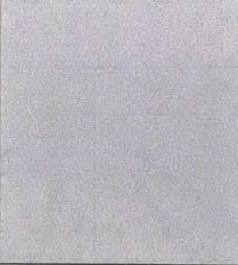
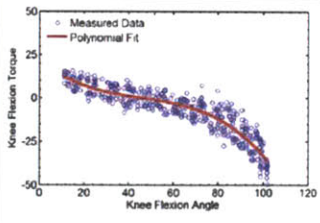
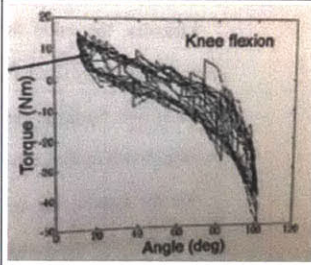

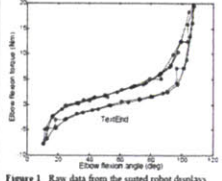
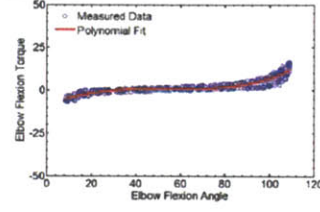
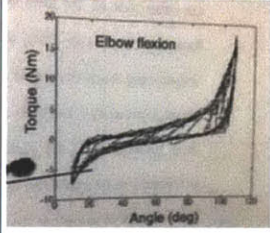
### A.2.2 Ankle

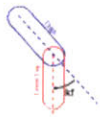

	Visual Depiction*	Abbreviation	Torque Limitations				S3 Specifications	
			Human Suited [1]		EMU Robot Suited [1] (Nm)	EMU Robot Suited [6] (Nm)	Min	Max
			Minimum (Nm)	Maximum (Nm)				
ANKLE		af	-2	7			-2	7

### A.2.3 Knee & Elbow


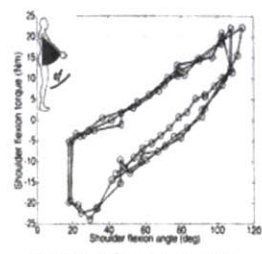
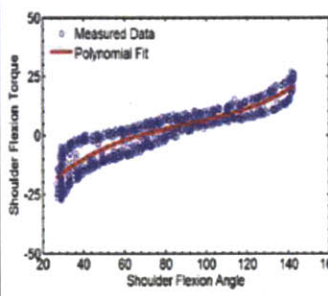
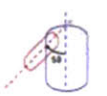
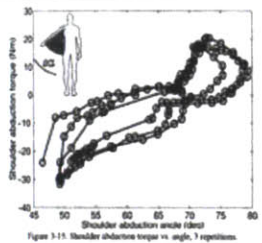
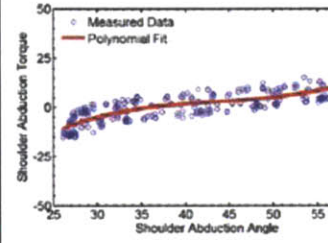
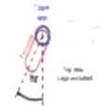
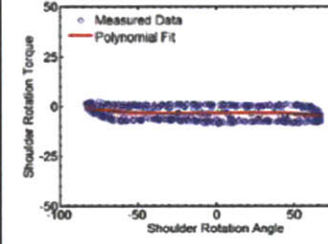
	Visual Depiction*	Abbreviation	Human Suited [1]		EMU Robot Suited [1] (Nm)	EMU Robot Suited [3] (Nm)
			Minimum (Nm)	Maximum (Nm)		
KNEE		kf	-10	25		
ELBOW		ef	-7	15		

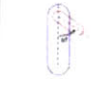
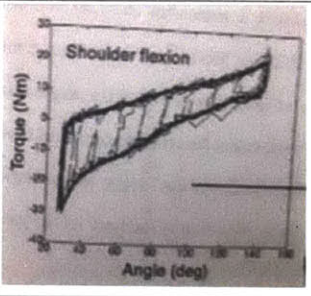

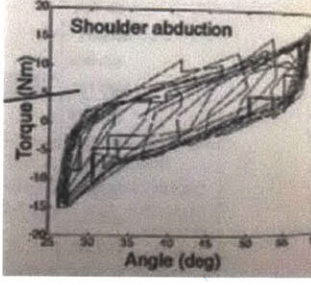

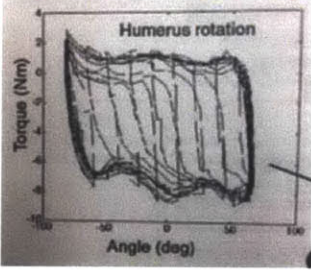


	Visual Depiction*	Abbreviation	EMU Robot Suited [4] (Nm)	EMU Robot Suited [5] (Nm)	EMU Robot Suited [6] (Nm)
KNEE	<i>Knee Flexion</i> 	kf			
ELBOW	<i>Elbow Flexion</i> 	ef	 <small>Figure 1 Raw data from the suited robot displays the vectorial sum of the spicinal joint torques</small>		

	Visual Depiction*	Abbreviation	Polynomial Fit Torque Eqns [5]	S3 Specifications	
				Min	Max
KNEE	<i>Knee Flexion</i> 	kf	$\tau = -1.5 \times 10^{-4}\theta^3 + 0.02\theta^2 - 1.1\theta + 22.4$	-40	32
ELBOW	<i>Elbow Flexion</i> 	ef	$\tau = 6.8 \times 10^{-5}\theta^3 - 0.01\theta^2 + 0.59\theta - 9.5$	-18	15

## A.2.4 Shoulder

	Visual Depiction*	Abbreviation	Human Suited [1]		EMU Robot Suited [1] (Nm)	EMU Robot Suited [5] (Nm)
			Minimum (Nm)	Maximum (Nm)		
Shoulder	<p><b>Shoulder Flexion</b></p> 	sf	-25	23	 <p>Figure 3-14 Shoulder flexion torque vs. angle, 1 repetition.</p>	
	<p><b>Shoulder Abduction</b></p> 	sa	-32	22	 <p>Figure 3-15 Shoulder abduction torque vs. angle, 1 repetition.</p>	
	<p><b>Humeral Rotation</b></p> 	hr				

	Visual Depiction*	Abbreviation	EMU Robot Suited [6] (Nm)	Polynomial Fit Torque Eqns [5]	S3 Specifications	
					Min	Max
Shoulder	Shoulder Flexion 	sf		$\tau = 4.4 \times 10^{-5}\theta^3 - 0.01\theta^2 + 1.26\theta - 44.0$	-25	32
	Shoulder Abduction 	sa		$\tau = 1.8 \times 10^{-3}\theta^3 - 0.24\theta^2 + 10.5\theta - 156.5$	-32	36
	Humeral Rotation 	hr		$\tau = -6.1 \times 10^{-6}\theta^3 - 6.3 \times 10^{-6}\theta^2 + 9.1 \times 10^{-3}\theta - 3.3$	-15	24

## References

- [1] Schmidt, P.B. "An investigation of space suit mobility with applications to EVA operations." PhD Thesis, MIT 2001.
- [3] Schmidt, P., Newman, D.J., & E. Hodgson. "Modeling Space Suit Mobility: Applications to Design and Operations." International Conference on Environmental Systems, 2001.
- [4] Frazer, A.L., Pitts, B.M., Schmidt, P.B., Hoffman, J.A., & D.J. Newman. "Astronaut Performance: Implications for Future Spacesuit Design." IAC 2002
- [5] Stirling, L.A. "Development of Astronaut Reorientation Methods: A Computational and Experimental Study." PhD Thesis, MIT 2008.
- [6] Frazer, A.L. "Modeling Human-Spacesuit Interactions." S.M. Thesis. MIT 2003.



## Appendix B: S3 Designs Implemented in Computer Simulator

For all of the following designs, the knee point of rotation is located at  $(x, y, z) = (0, 0, 0)$ . The X, Y, and Z of the actuators are the locations of the upper and lower endpoints of the actuators when the leg is straight (0 degree knee flexion). The X, Y, and Z of the spools are the locations of the center of the circles representing the spools when the leg is straight (0 degree knee flexion). These designs are expected to fit a 95% male leg, unless indicated otherwise.

**Table B.1 Example simulation design to accommodate 50% female anthropometry**

Example Simulation (50% female anthropometry)						
		X (mm)	Y (mm)	Z (mm)	Actuator Geometry	
Back Actuator	Upper	-82	124	0	200 mm nominal length	10 mm diameter
	Lower	-55	-75	0		
Front Actuator	Upper	82	100	0	295 mm nominal length	20 mm diameter
	Lower	55	-100	0		
Back Spool		-29	0	0	50 mm radius	
Front Spool		10	0	0	50 mm radius	

**Table B.2 Baseline design 1 to accommodate 95% male anthropometry**

Design 1						
		X (mm)	Y (mm)	Z (mm)	Actuator Geometry	
Back Actuator	Upper	-108	183	0	280 mm nominal length	10 mm diameter
	Lower	-65	-100	0		
Front Actuator	Upper	108	183	0	513 mm nominal length	20 mm diameter
	Lower	65	-184	0		
Greave		22	0	0	68 mm radius	

**Table B.3 Design 2 with a longer back actuator than baseline design 1**

Design 2						
		X (mm)	Y (mm)	Z (mm)	Actuator Geometry	
Back Actuator	Upper	-110	200	0	350 mm nominal length	20 mm diameter
	Lower	-65	-150	0		
Front Actuator	Upper	108	183	0	513 mm nominal length	20 mm diameter
	Lower	65	-184	0		
Greave		22	0	0	68 mm radius	

**Table B.4 Design 3 with shorter front and back actuators than baseline design 1**

Design 3						
		X (mm)	Y (mm)	Z (mm)	Actuator Geometry	
Back Actuator	Upper	-110	95	0	150 mm nominal length	10 mm diameter
	Lower	-65	-51	0		
Front Actuator	Upper	87	41	0	250 mm nominal length	20 mm diameter
	Lower	65	-54	0		
Greave		22	0	0	68 mm radius	

**Table B.5 Design 4 with a small back actuator diameter and a short front actuator nominal length**

Design 4						
		X (mm)	Y (mm)	Z (mm)	Actuator Geometry	
Back Actuator	Upper	-108	150	0	200 mm nominal length	10 mm diameter
	Lower	-65	-49	0		
Front Actuator	Upper	108	60	0	300 mm nominal length	20 mm diameter
	Lower	65	-75	0		
Greave		22	0	0	68 mm radius	

**Table B.6 Design 5 with a large back actuator diameter and a short front actuator nominal length**

Design 5						
		X (mm)	Y (mm)	Z (mm)	Actuator Geometry	
Back Actuator	Upper	-108	150	0	200 mm nominal length	20 mm diameter
	Lower	-65	-47	0		
Front Actuator	Upper	108	60	0	300 mm nominal length	20 mm diameter
	Lower	65	-75	0		
Greave		22	0	0	68 mm radius	

**Table B.7 Design 6 with a small back actuator diameter and a long front actuator nominal length**

Design 6						
		X (mm)	Y (mm)	Z (mm)	Actuator Geometry	
Back Actuator	Upper	-108	150	0	200 mm nominal length	10 mm diameter
	Lower	-65	-49	0		
Front Actuator	Upper	108	175	0	487 mm nominal length	20 mm diameter
	Lower	65	-168	0		
Greave		22	0	0	68 mm radius	

**Table B.8 Design 7 with a large back actuator diameter and a long front actuator nominal length**

Design 7						
		X (mm)	Y (mm)	Z (mm)	Actuator Geometry	
Back Actuator	Upper	-108	150	0	200 mm nominal length	20 mm diameter
	Lower	-65	-47	0		
Front Actuator	Upper	108	175	0	487 mm nominal length	20 mm diameter
	Lower	65	-168	0		
Greave		22	0	0	68 mm radius	

**Table B.9 Combo 1 with a short back actuator nominal length and a short front actuator nominal length**

Combo 1						
		X (mm)	Y (mm)	Z (mm)	Actuator Geometry	
Back Actuator	Upper	-108	150	0	200 mm nominal length	10 mm diameter
	Lower	-65	-49	0		
Front Actuator	Upper	108	60	0	300 mm nominal length	20 mm diameter
	Lower	65	-75	0		
Greave		22	0	0	68 mm radius	

**Table B.10 Combo 2 with a short back actuator nominal length and a medium front actuator nominal length**

Combo 2						
		X (mm)	Y (mm)	Z (mm)	Actuator Geometry	
Back Actuator	Upper	-108	150	0	200 mm nominal length	10 mm diameter
	Lower	-65	-49	0		
Front Actuator	Upper	108	99	0	350 mm nominal Length	20 mm diameter
	Lower	65	-98	0		
Greave		22	0	0	68 mm radius	

**Table B.11 Combo 3 with a short back actuator nominal length and a long front actuator nominal length**

Combo 3						
		X (mm)	Y (mm)	Z (mm)	Actuator Geometry	
Back Actuator	Upper	-108	150	0	200 mm nominal length	10 mm diameter
	Lower	-65	-49	0		
Front Actuator	Upper	108	175	0	495 nominal Length	20 mm diameter
	Lower	65	-177	0		
Greave		22	0	0	68 mm radius	



**Table B.12 Combo 4 with a long back actuator nominal length and a short front actuator nominal length**

Combo 4						
		X (mm)	Y (mm)	Z (mm)	Actuator Geometry	
Back Actuator	Upper	-108	250	0	495 mm nominal Length	10 mm diameter
	Lower	-65	-250	0		
Front Actuator	Upper	108	60	0	300 mm nominal length	20 mm diameter
	Lower	65	-75	0		
Greave		22	0	0	68 mm radius	

**Table B.13 Combo 5 with a long back actuator nominal length and a medium front actuator nominal length**

Combo 5						
		X (mm)	Y (mm)	Z (mm)	Actuator Geometry	
Back Actuator	Upper	-108	250	0	495 mm nominal Length	10 mm diameter
	Lower	-65	-250	0		
Front Actuator	Upper	108	99	0	350 mm nominal Length	20 mm diameter
	Lower	65	-98	0		
Greave		22	0	0	68 mm radius	

**Table B.14 Combo 6 with a long back actuator nominal length and a long front actuator nominal length**

Combo 6						
		X (mm)	Y (mm)	Z (mm)	Actuator Geometry	
Back Actuator	Upper	-108	250	0	495 mm nominal Length	10 mm diameter
	Lower	-65	-250	0		
Front Actuator	Upper	108	175	0	495 nominal Length	20 mm diameter
	Lower	65	-177	0		
Greave		22	0	0	68 mm radius	